報　文

地調月報 Bull. Geol. Surv. Japan, vol. 30, p. 71–130, 1979　　551.243 : 551.782 (521.52)

Folds of Miocene Formations in Higashi-Chikuma District, Nagano Prefecture, Central Japan

Hirokazu KATO

1. Introduction

Many geologists have been attracted by the geology and tectonics in the Fossa Magna Region for many years (HOMMA, 1931; MORISHITA, *et al.*, 1957; TANAKA, 1958; SAITO, 1961, 1968; TAKESHITA, 1969, etc.). Various types of sedimentary, volcanic or intrusive rocks of Neogene to Quaternary Age distribute in this region, and many geological structures, in particular folds and faults whose orientation and forms are characteristic develope there.

Though studies on the geological history of this region have greatly advanced in recent years, they were not always enough to explain the structural and tectonic development quantitatively. The analytical study of their structural development is expected to be a good key for throwing light on the geological history of Greentuff Movement in this Fossa Magna Region.

The purposes of this study are to define deformations in the northern part of the Fossa Magna Region, to explain the folding mechanism analytically and to discuss the dynamic folding history. In order to get answers of these subjects, some detailed field survey, experimental and theoretical study have been done as described in the followeing sections.

2. Geological Setting

The studied area is shown in Figure 1. Many students of Tokyo University of Education surveyed this area as shown in Figure 1. The stratigraphic sequence and the correlation are shown in Table 1 and 2.

Neither the base rocks nor the lowest Tertiary formation are found in the area (Fig. 2).

The Neogene strata are divided lithologically into six formations in ascending order (Table 1).

1. The Uchimura Formation (Middle Miocene) is composed of andesite lava, tuff breccia, and tuffaceous sandstone and shale with fossils, for example, Balanus sp., Chlamys sp., and so on. The formation distributes only in the crest part of the Nishikibe Anticline, that is, Miyanoiri, Hofukuji-cho in the studied area.

2. The Bessho Formation (Middle Miocene) which overlay the Uchimura Formation with conformity, is mainly composed of massive black shale with many fossils. However, the uppermost part of the formation consists of medium and coarse grained sandstone, conglomerate and alternation of sandstone and mudstone. Its type locality is the Yu River near Bessho Spa in Shioda-cho. The

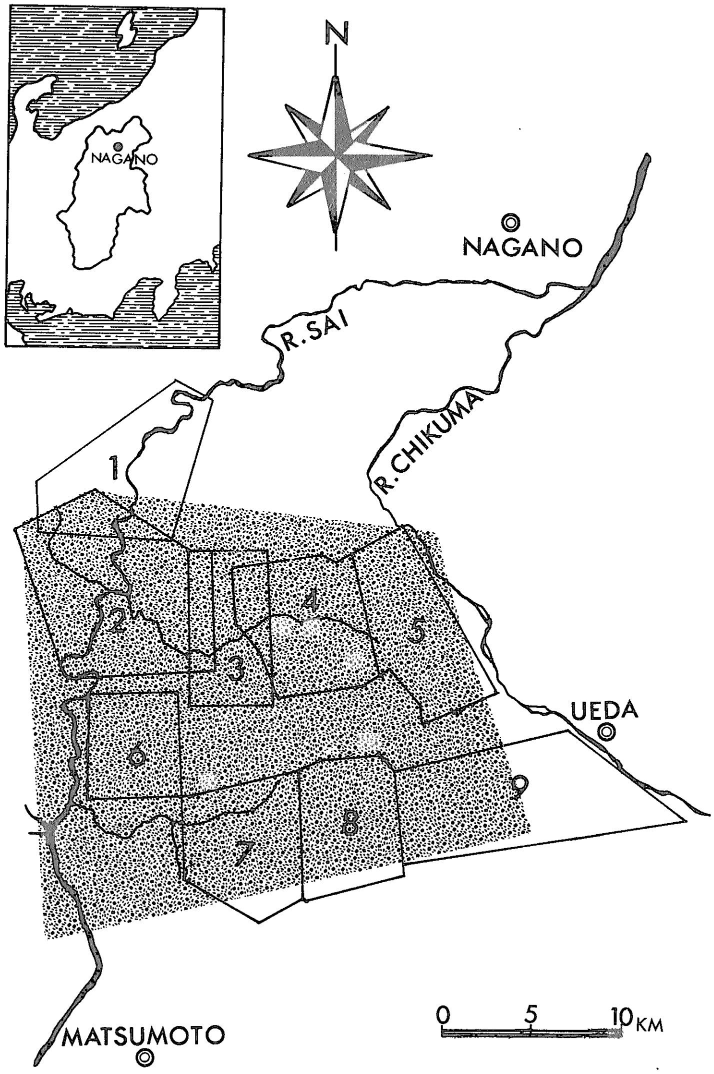

1 SHIMIZU 1970; 2 KATO 1969; 3 KAWAUCHI 1974;
4 FUKAZAWA 1972; 5 TAKEUCHI 1971; 6 KASAHARA 1974;
7 MARUI 1972; 8 KIKUCHI 1972; 9 ITOI 1972;

Fig. 1 Index map of the studied area.

thickness of the formation is changeable as shown in Figure 4; 1500 m–2000 m near Matsumoto City, 1,350 m in the northeast part of Matsumoto City, 1,000 m+in Anazawa, 500 m at Bessho Spa, and 350 m near Chikuma River. This formation is intruded with dikes of porphyrite, quartz-diorite and andesite. It contains many fossils, for example, *Dosinia kaneharai*, *Cultellus otsukai*, *Anadara minoensis* and so on.

3. The Aoki Formation comprieses grey massive sandy shale mainly in the lower part and the

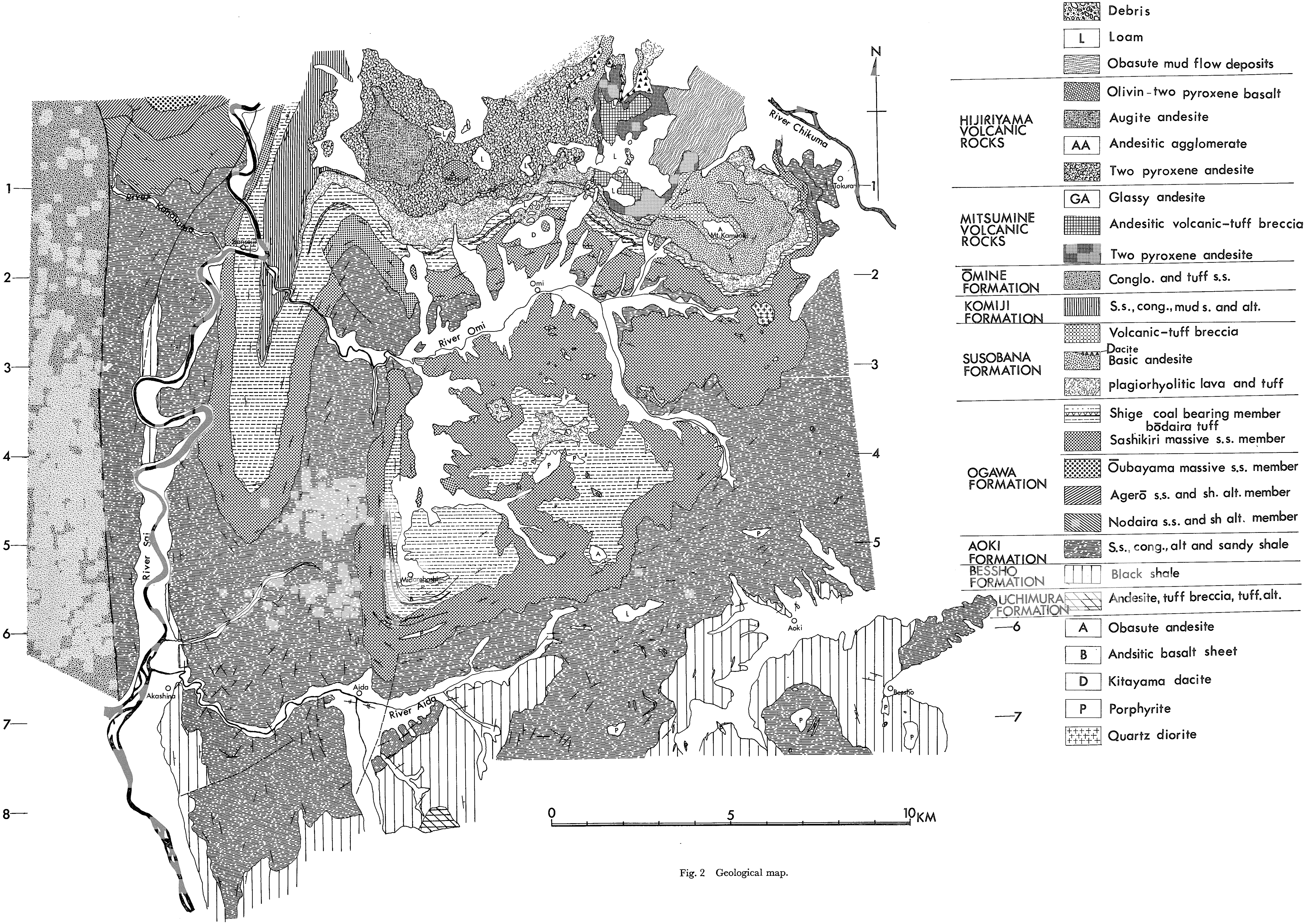

Fig. 2 Geological map.

Table 1.

Age		Formation	Member	(m)	Columnar Section	Lithofacies
QUAT.		Hijriyama volc.				andesite lava, basalt agglomerate
NEOGENE	UPPER MIOCENE	Komiji Form.				sandstone, conglomerate alternation
		Susobana Form.	up. / mid. / low	900+	welded tuff	volcanic-tuff breccia andesite lava plagiorhyolitic lava and tuff
		Ogawa Formation	Shige Member	700	Bōdaira Tuff	tuffaceous sandstone massive sandstone, sandy shale and conglomerate
			Sashikiri Member	600		massive sandstone and conglomerate with coal seams
	MIDDLE MIOCENE	Aoki Formation		1300	Haraji Cong. Kido Cong.	alternation of shale and sandstone sandy shale massive sandstone and conglomerate
		Bessho Formation		1500		alternation of sandstone and shale black shale
		Uchimura Formation				andesite tuff breccia tuffaceous sandstone and shale

alternation of sandstone and sandy shale in the upper part. Particularly, the basal part of this formation have two members composed of conglomerate and sandstone; the upper one is named the Haraji Member, and the lower one is named the Kido Member. In the alternating sedimentary rocks, minor structures, such as minor folds, minor faults and boundins are found. It is very difficult to correlate the members of the Aoki Formation each other, because the lithology of that formation is changeable in the horizontal direction as shown in Figure 3 and Figure 5. This formation bears some fossils and they are reported by TANAKA (1962). The conglomerate comprises mainly pebble to cobble-sized gravels of chert and hard sandstone of Palaeozoic, andesitic-basaltic breccia brought from the Uchimura Formation as reported by YAMAGISHI *et al.* (1963) and SAITŌ and IIJIMA (1972) only in Ueda City,

Table 2.

GEOLOGIC AGE		FOSSA MAGNA	middle part of Sinshu F. HONMA 1931	Omi River I. KOBAYASHI & H. ISOMI 1950	southern foot of Mt. Hijiri A. MORISHITA et al. 1957	SAKAI Village M. FUKAZAWA 1971	northern area of Matumoto K. TANAKA & H. SEKI 1966	Nagno Oil Field H. FUJIMOTO et al. 1946	Shiga Village S. MARUI 1972	Higashi-chikuma Area H. KATO 1977
Quater-nary	HOLO-CENE									
Quater-nary	PLEISTO-CENE	Toyono Stage								
NEOGENE	PLIOCENE	Saruma-ru Stage Sigara-mi Stage			Hijiriyama A.	Hijiriyama A.	Shigarami G.: Komiji F.			Hijiriyama A.
NEOGENE	UPPER MIOCENE (upper)	Ogawa Stage	Hokushin Group, Ogawa Formation: upper	Komiji F. Shige F.	Komiji? F. Kōsō Tuff Shige F.	Susobana Group: Kamuriki F., Koso Tuff Omi G.: Shige F.	Nakagomi F. Omi Group: Shige F.	Iwadonoyama F.: upper	Omi Group: massive sandstone	Susobana: Komiji F., upper, middle, lower Ogawa F.: Shige F.
NEOGENE	UPPER MIOCENE (lower)	Ogawa Stage	Hokushin Group, Ogawa Formation: lower	Sashikiri F.	Sashikiri F.	Omi G.: Sashikiri F.	Omi Group: Iwadonoyama F., Maruki F.	Iwadonoyama F.: lower	Omi Group: massive sandstone	Ogawa F.: Sashikiri F.
NEOGENE	MIDDLE MIOCENE	Aoki Stage	Hokushin Group, Aoki Formation: upper, lower	Akamatsu F.	Akamatsu F.	Aoki G.: Akamatsu F.	Aoki Group: Kodachino-iri F., Ikezawa F., Hosoda F., Horidaira F., Kitayama F., Hakuba F.	Kodachinoiri Formation: upper, lower	Aoki Group: upper, lower	Aoki Formation: upper, middle, lower, Kido Member
NEOGENE	MIDDLE MIOCENE	Bessho Stage	Bessho Formation				Bessho G.: Tazawa F.	Akashina F.: upper, lower	Bessho Group: Anazawa F.	Bessho F.
NEOGENE	LOWER MIOCENE	Uchimura Stage	Chūshin Group, Uchimura Formation: upper, lower				Uchimura G.: Kariyahara F., Inakuratōge F., Shiokura F., Ibuka F.		Uchimura G.: tufface ous mud, green pyro. r.	Uchimura F.
NEOGENE	LOWER MIOCENE	Moriya Stage	Chūshin Group, Moriya Formation							

quartz-diorite and diorite distributed in Uchimura region, and black shale breccia (10–40 cm in size) brought from the Bessho Formation in the lower part of the formation as shown in Figure 12. The type locality of the formation is located along the roadcut from Kido in Aoki Village to Shunara Pass. The largest thickness (1,300 m) is found in the west limb of the Komiji Syncline, and becomes thinner toward the east. The remarkable change in the thickness is found at the Matsumoto—Nagano Line. The Aoki Formation overlies the Bessho Formation conformably as a whole.

4. The Ogawa Formation in the western area of the Saigawa Crushed Zone is much different in the lithofacies from that in the eastern area of the Saigawa Crushed Zone.

That is, in the western area it is divided into the Nodaira Member (the alternation of sandy shale and sandstone, 700 m in thickness), the Agero Member (the alternation of sandstone and sandy shale, 1,000 m in thickness), and the Oubayama Member (massive sandstone, more than 50 m in thickness) in ascending order. These are reported by the author in 1970. In the east of the Saigawa Crushed Zone, the Ogawa Formation is divided into two members, that is, the Sashikiri Member in the lower and the Shige Member in the upper, respectively. They are typically distributed along Omi River. The Sashikiri Member is composed of light grey-light blue, massive, coarse to fine-grained sandstone

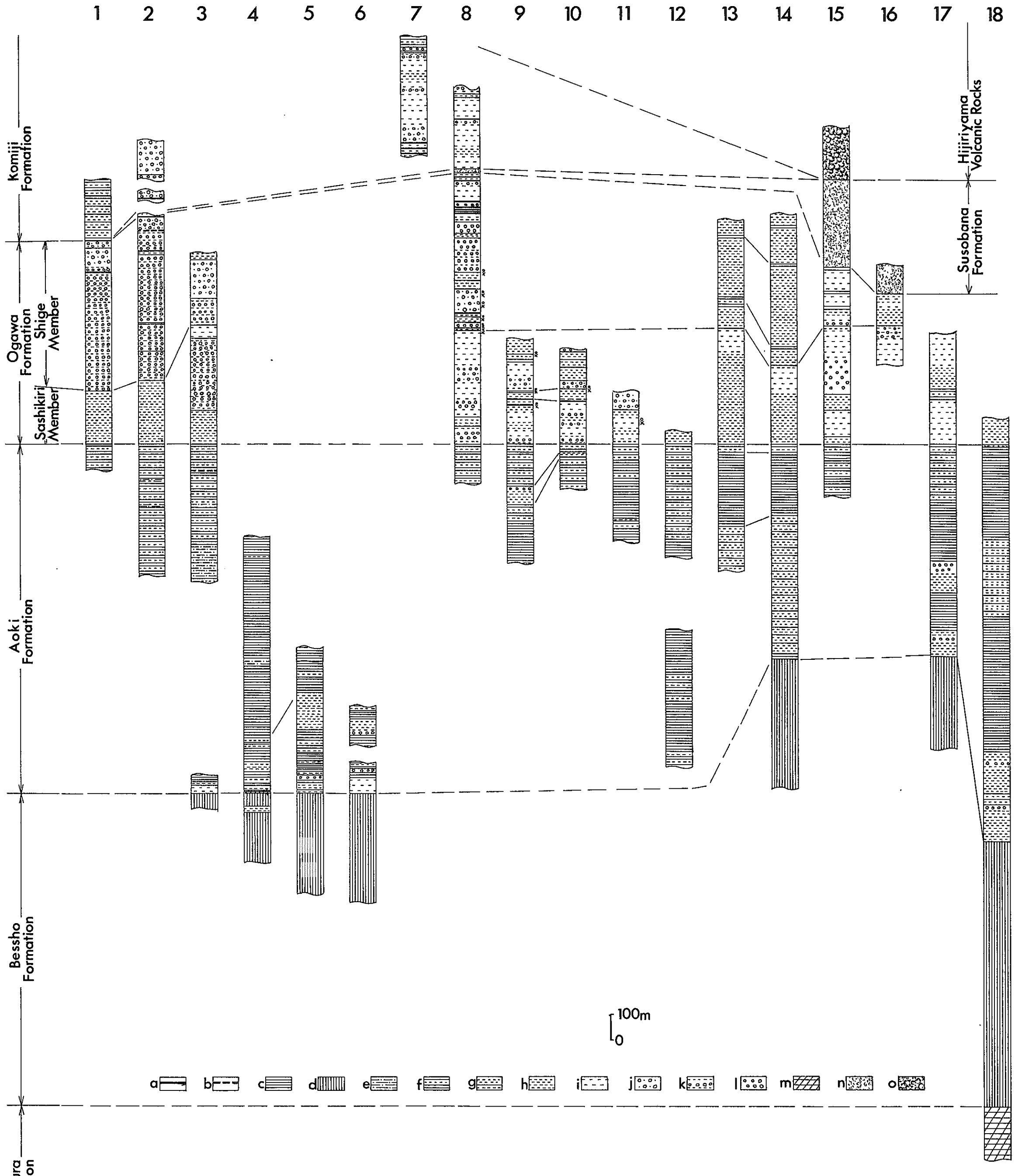

1. Sai River-Tsukudami, 2. Kanakuma River-Omi River, 3. Ikezawa route, 4. Amada route, 5. Hakuba route, 6. Ōguchizawa route, 7. Nagaiwa, 8. Omi River, 9. Katsura-Macchi, 10. Bessho-Nakazato, 11. Yagoshi, 12. Matsutome, 13. Hanagawara Pass, 14. Kazakoshi Pass, 15. Kajiura-Omi, 16. Mt. Azumaya, 17. Shunara Pass, 18. Anazawa route.

a. coal seam, b. coal seam(intermittenly), c. sandy shale, d. shale, e. alternation of sandstone and shale, f. shale rich alternation, g. sandstone rich alternation, h. medium grained sandstone, i. coarse grained sandstone, j. very coarse grained sandstone, k. sandstone and comglomerate, l. conglomerate, m. andesite(of the Uchimura Formation), n. rhyolitic tuff and lava, o. andesite(of the Hijiri Volcanic Rocks).

Fig. 3 Columner sections.

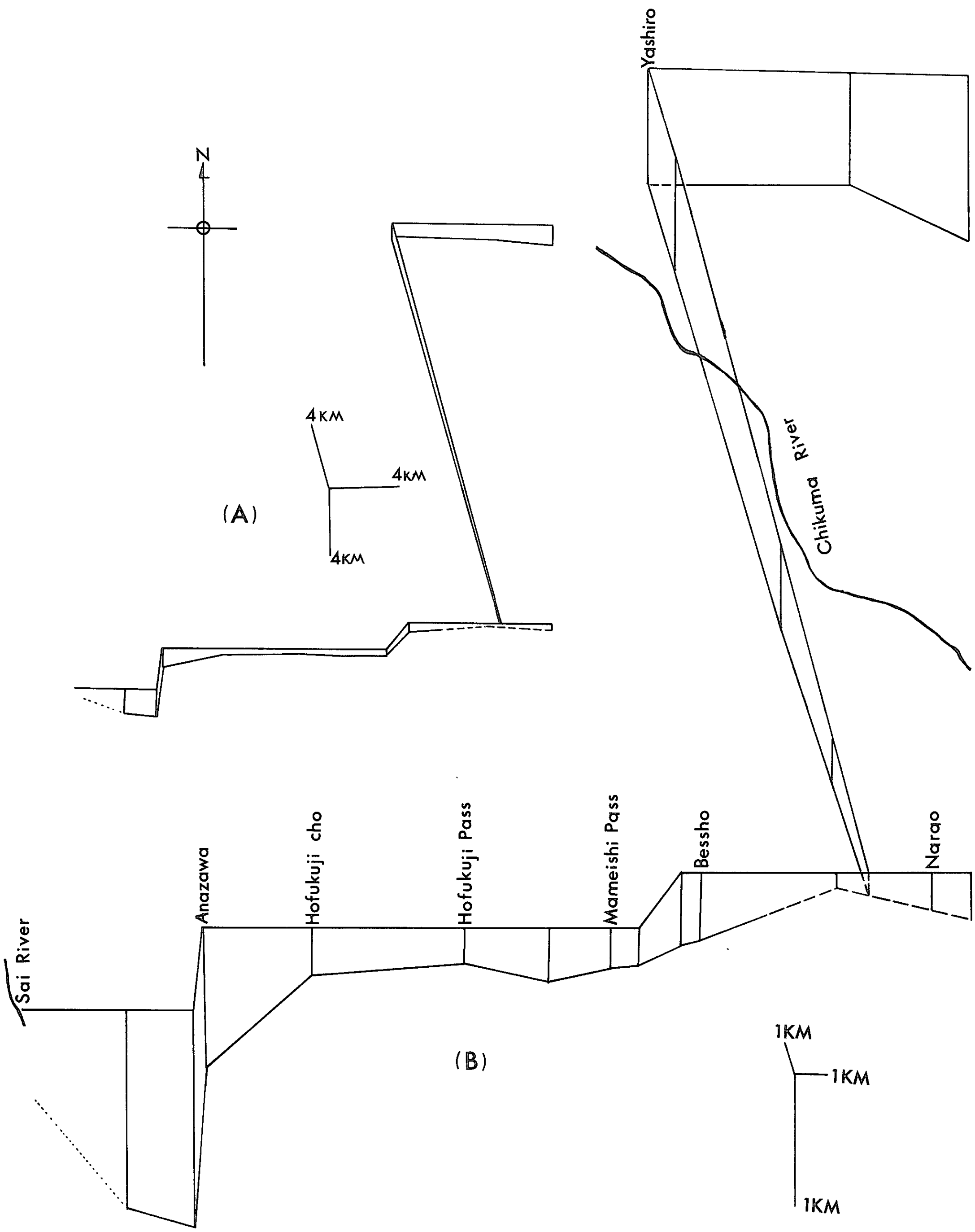

Fig. 4 The thickness of the Bessho Formation.
(A) shows natural thickness of the Bessho Formation.
(B) shows exaggerated thickness of the Bessho Formation.

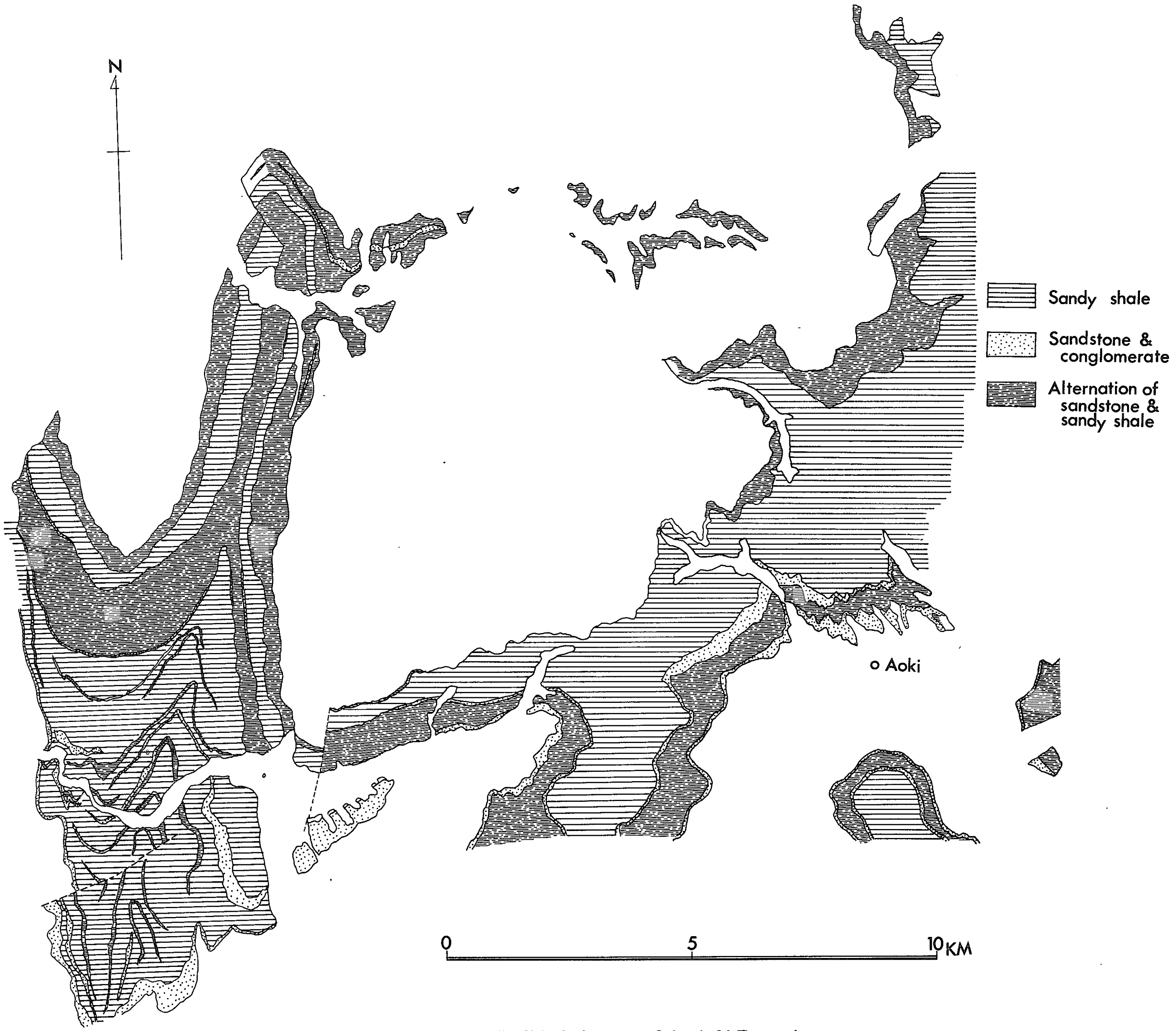

Fig. 5 The lithofacies map of the Aoki Formation.

and conglomerate. Coal seams, thin mudstone and several layers of *Ostrea*-bearing sandstone are intercalated in the middle and uppermost parts of the formation. Conglomerate compries not only chert and sandstone gravels of Pre-Tertiary but Greentuff ones of Tertiary. The thickness of this formation are 120 m near Sanseiji, 520 m at Sashikiri, 400 m at Kamibori, and at Ōgawa–Koniuma, 350 m near Ōnoda and less than 100 m at Tokura. The Shige Member is composed of massive arkose medium grained and coarse grained sandstone, conglomerate and conglometric sandstone.

Sandy mudstone, thin alternation of sandstone and sandy shale and coal seams are frequently intercaleted in this member. It becomes tuffaceous toward the upper part. Many ripple marks, laminations and plant fossils can be found in these sandstone layers. The Shige Member is intruded with many volcanic rocks (porphyrite dikes, basalt sheet and so on) in the area of the east of the Matsumoto—Nagano Line (Figs. 2 and 6). The Bōdaira Tuff is intercalated in the uppermost part of the Shige Member and is distributed intermittenly at the southern foot of Mt. Hijiri. The tuff is white in color and contains quartz grains, pumice grains, carbonaceous matter and pebbles. The thickness of this tuff member ranges from 10 m to 30 m. It bears fossil flora called "Bōdaira Flora" and some molluscan fossils in fresh water (SAITŌ and IIJIMA, 1972).

The thickness of the Shige Member is 490 m at Tsukudami, 620 m in the area along Omi River, 570 m at the crest area of Noma Anticline, 400 m at Shunara Pass, 250 m at Ichinokawa and Ōnoda and less than 100 m to the east of Ōnoda.

5. The Susobana Formation (upper Miocene) is mainly composed of rhyolitic lava, tuff and

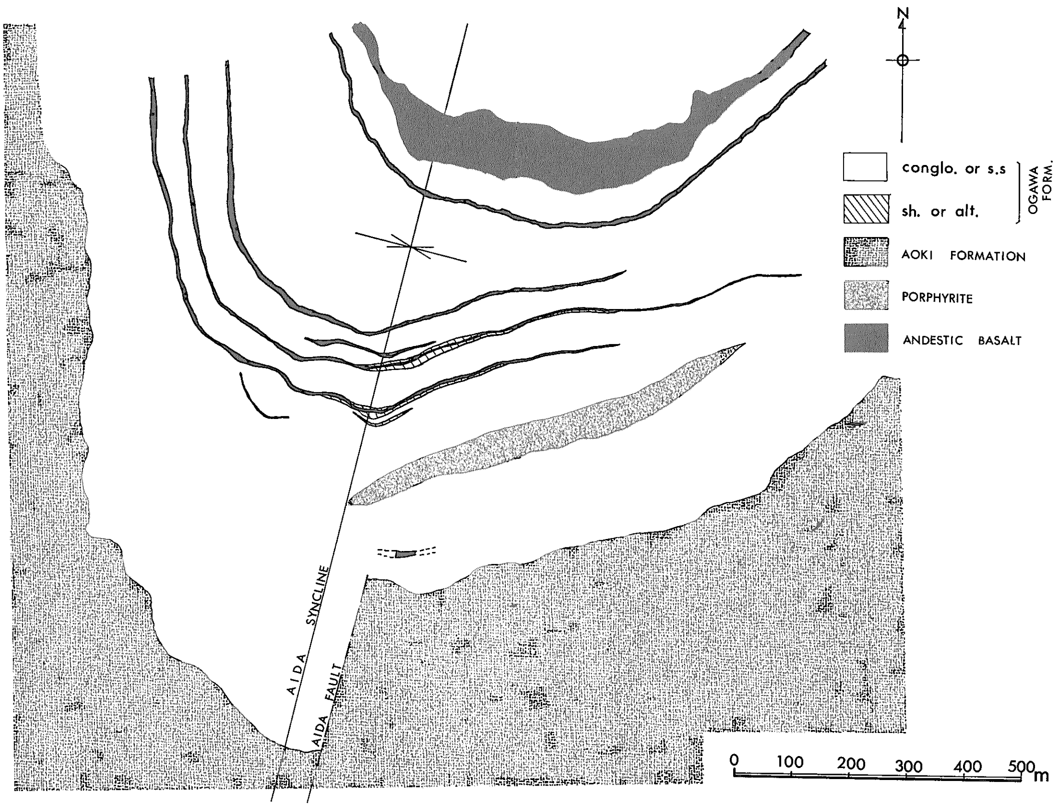

Fig. 6 Basaltic andesite sheets in the Ogawa Formation.

andesite lava. To the south of Hijiri Heights and around Mt. Kamuriki, this formation is divided into three members. The lowest member mainly comprises of plagio-rhyolitic tuff and lava and partly dacite lava with large quartz grains of which diameters are 1–7 mm, plagioclase, biotite, amphibole, and augite. This is partly altered, and bears chlorite and sericite. This member comprises small fragments of shale, which is smaller than 3 cm in size, and fragments are brought from the lower formations. Many porphyritic dikes intrude into this formation. The Kōsō Tuff (Kato, 1970) along Omi River is interfingered with this member. The middle member is dominantly composed of grey-bluish grey andesitic lava, partly of tuff-breccia and lithic tuff. The upper member is mainly composed of andesitic tuff-breccia and partly of andesitic lava and tuff. Around Mt. Kamuriki, this member comrises welded tuff. Blocks in the tuff-breccia are mainly of andesite, partly of green tuff and mudstone, especially cobble sized gravels of quartz-diorite are dominant in the lowest part of the member. To the north of Hijiri Heights, the lowest member is composed of altered rhyoritic lava with quartz grains, pyrite but no biotite. Intercalations of some white tuff layers are in this member. The middle member is composed of altered amphibole andesitic lava, partly andesitic tuff-breccia. The upper member comprises silicificated dacitic tuff, tuff-breccia and lava with quartz grains of which diameters are 1–3 mm, and its thickness is variable. The type locality of the Susobana Formation is the cutting along the road from Mt. Kamuriki to Shijūhachimagari Pass. The thickness of this formation reaches more than 900 m. As a whole, it superposes the Oagawa Formation with conformity, but the upper member superposes the middle member with partial unconformity around Mt. Kamuriki.

6. The Komiji Formation consists of sandstone, sandy shale, conglomerate and their alternation. The lower part of this formation is tuffaceous and intercalated with coal seams, and bears plant fossils. The uppermost part is cut by the Komiji Fault and covered with unconformity by the Hijiri Volcanic Rocks (Fig. 3). This formation superposes the Susobana Formation. The type locality of this formation is the roadcut from Ashinoshiri in Ōoka Village to Nagaiwa. The thickness of the formation attains more than 690 m at the axis of the Komiji Syncline.

7. The Oomine Formation (Plio-Pleistocene) distributes in the west of the Nakayama Fault. In the studied area this formation consists of tuffaceous medium grained sandstone, coarse-very coarse grained sandstone.

8. The Hijiriyama Volcanic Rocks are divided into two members, namely the Hijiriyama Volcanic Rocks (in the narrow sense) and the Mitsumine Volcanic Rocks. The former is mainly composed of bluish black pyroxene andesitic lava and basaltic andesitic lava. In the lower part of the member, basalt-andestite volcanic breccia and intermittent agglomerate layers are intercalated. The size of those breccia is from 5 to 10 cm on an average and the maximum is about 60 cm. The matrix is lithic tuff. The black two pyroxene basalt is distributed at Mt. Hijiri, and andesitic lava and volcanic breccia with large augite crystals (5–10 mm in size) are recognized at Mt. Tarara which is located in the west of Mt. Hijiri. The latter member covers the Susobana Formation with unconformity, and contacts with the Hijiri Volcanic Rocks at Lake Hijiri. The lower part of this member is basaltic andesitic lava, and the middle part is composed of andesitic volcanic breccia with tuff or tuffaceous sandstone layers. The size of breccia ranges from 5 to 50 cm in diameter, and the kinds of it are andesite, dacite and sandstone originated from the Ogawa Formation. The upper part of this member is of black glassy andesite lava which occupies the summit portion of Mt. Mitsumine. The Hijiri Volcanic Rocks (in a broad sense) unconformably superposes the Komiji Formation and the Susobana

Formation.

9. Intrusive rocks Many intrusive rocks are distributed in the eastern area to the Matsumoto—Nagano Line. For example, the Kitayama Dacite of the Ogawa Formation distributes at Mt. Kitayama, and andesitic basalt sheets in the south of Midarebashi Village (Figs. 2 and 6). Many porphyrite dikes with NE–SW trend intruded the Bessho, the Aoki, the Ogawa and the Susobana Formations are of remarkable ones.

3. Geological Structures

3.1 Major folds

3.1.1 Takafu Syncline

This syncline is one of the biggest folds in the northern Fossa Magna Region. In the studied area, only its southern end part can be observed and deformation of the syncline extends from the Aoki Formation to the Ogawa Formation (Fig. 7).

The axis trends NNE–SSW and plunges to the north and the plunging angle is less than 30 degrees. Limb dips are from 30 to 40 degrees and this syncline is nearly symmetric. Minor folds develope in the west limb of this syncline.

3.1.2 Nodaira Anticline

From the Bessho Formation to the Ogawa Formation are strongly participated to the deformation of the Nodaira Anticline. The east limb is overturned with high angles (60–80 degrees) in the Aoki Formation but it shows gentle dips (30 degrees) in the superposed formation. The axial plane dip towards the east, so that this fold is asymmetric. Because of lacking in effective key bed, the feature of this anticline is still unknown in detail to us. The northern end of this anticline is cut by the Saigawa Crushed Zone.

3.1.3 Komiji Syncline

The length of the axis of the Komiji Syncline is about 23 km, and the axial line strikes to N 5° W in the southern part of Aida River, the N–S in the northern part of Aida River and to N 10°W–20°E in the northern part of Omi River. This syncline is cut by the Komiji Fault. The west limb is steeper than the east one, and is partly overturned, that is, this syncline is intensively asymmetric. The axial plane dips toward the west. It plunges to the north about 10–20 degrees. Its deformation extends from the Bessho Formation to the Komiji Formation, but not to the Hijiriyama Volcanic Rocks. Many minor folds develope in the southern area of this fold (Figs. 7 and 8).

3.1.4 Noma Anticline

This anticline is named by KOBAYASHI and ISOMI (1950) for the first time. The length of the axis is about 22 km and strike of it is N 15°E between Aida River and the Noma Fault and N 20°W in the north of the Noma Fault. The axial trend is essentially N–S, but it seems to be changed by the block rotation which had happened during the time when the Noma and the Hakuba faults were formed. The axial distance between the Komiji Syncline and the Noma Anticline becomes narrower in the south. The both west limbs are steeper than the east ones, but the Noma Anticline is less intense in the deformation rate, and more asymmetrical than the Komiji Syncline. This anticline plunges to the north about 30–40 degrees. The axial plane dips toward the west in the northern area, but the east in the southern area (Figs. 7 and 8). Its deformation extends from the Bessho Formation to the Ogawa Formation. Many minor folds develope in the east limb and the southern area of the crest (Figs. 9 and 10).

3.1.5 Nanatsumatsu Syncline

This fold is named by KAWAUCHI (1973) for the first time. This locates on the east of the Noma Anticline. The axis of the syncline is 7 km in length and the strikes about N–S direction. The axial plane is generally vertical but partly dips toward the east in the north end. It plunges to the north about 20–30 degrees. In the southern area, the Nanatsumatsu Fault developes on the east of this syncline in parallel. This syncline is asymmetric strongly and the east limb is nearly horizontal while the west one is steep. It seems to be warped shape in the end part. Some minor folds develope in axial part of the syncline.

Its deformation extends from the Aoki Formation to the Ogawa Formation.

3.1.6 Aida Syncline

The length of this axis is about 8 km, and the general strikes of the axis is about N 15 °E. It plunges to the north less than 20 degrees and extends gradually to the north end. The axial plane is almost vertical and partly dips westwards. This is open fold and its dips less than 30 degrees, and the west one 20–30 degrees in the Ogawa Formation (near the axis of this fold), but is more than 60 degrees in the Aoki Formation. From the Bessho Formation to the Ogawa Formation are involved in this syncline.

3.1.7 Nishikibe Anticline

This is named firstly by TANAKA (1958). The length of this axis is about 6.5 km within the studied area, but whole length is about 13 km reported by Uchimura Research Group (1953). The general trend of the axis is NE–SW in Aiyoshi, Minakami, Yakyu, and Anazawa area, and is changed to N–S or N 5 °W–S 5 °E in the southern part of the studied area. Its deformation extends from the Uchimura Formation to the lower Aoki Formation. As it plunges to the north about 30–45 degrees abruptly, it deforms little to the northern area. The west limb dips between 30 and 60 degrees whereas the east one dips between 10 and 30 degrees, that is, this anticline is strongly asymmetrical. At the Minakami Route which is located in the northern part of this anticline, the thickness of the Aoki Formation changes little between both limbs. At Yakyu Route which is located in the middle part of this anticline, the thickness of the Aoki Formation also changes little. However, their lithofacies are very different from each limb. That is, in the west limb, sandstone and sandstone rich alternation are dominant, whereas in the east one, sandy shale rich alternation is dominant.

It is the important fact that the former is more competent than the latter. In the Anazawa Route which is located in the southern part of this anticline, the Kido sandstone and conglomerate Member, which is the lowest one in the Aoki Formation, of the west limb is much thicker than that of the east one, and the change in thickness of the Bessho Formation is much the same as that of the Kido Member.

3.1.8 Kinokoyadani Syncline

The axis of this syncline is about 6.5 km in length and strikes to NE–SW in the northern part, but changes to N–S in the southern part. The axial plane is almost vertical and the axis plunges to the north less than 20 degrees. The deformation extends from the Bessho Formation to the lowest part of the Aoki Formation. Both limbs dip in 10–20 degrees, and this syncline is symmetrical. The thickness of the lower part of the Aoki Formation attains largest in the crest part.

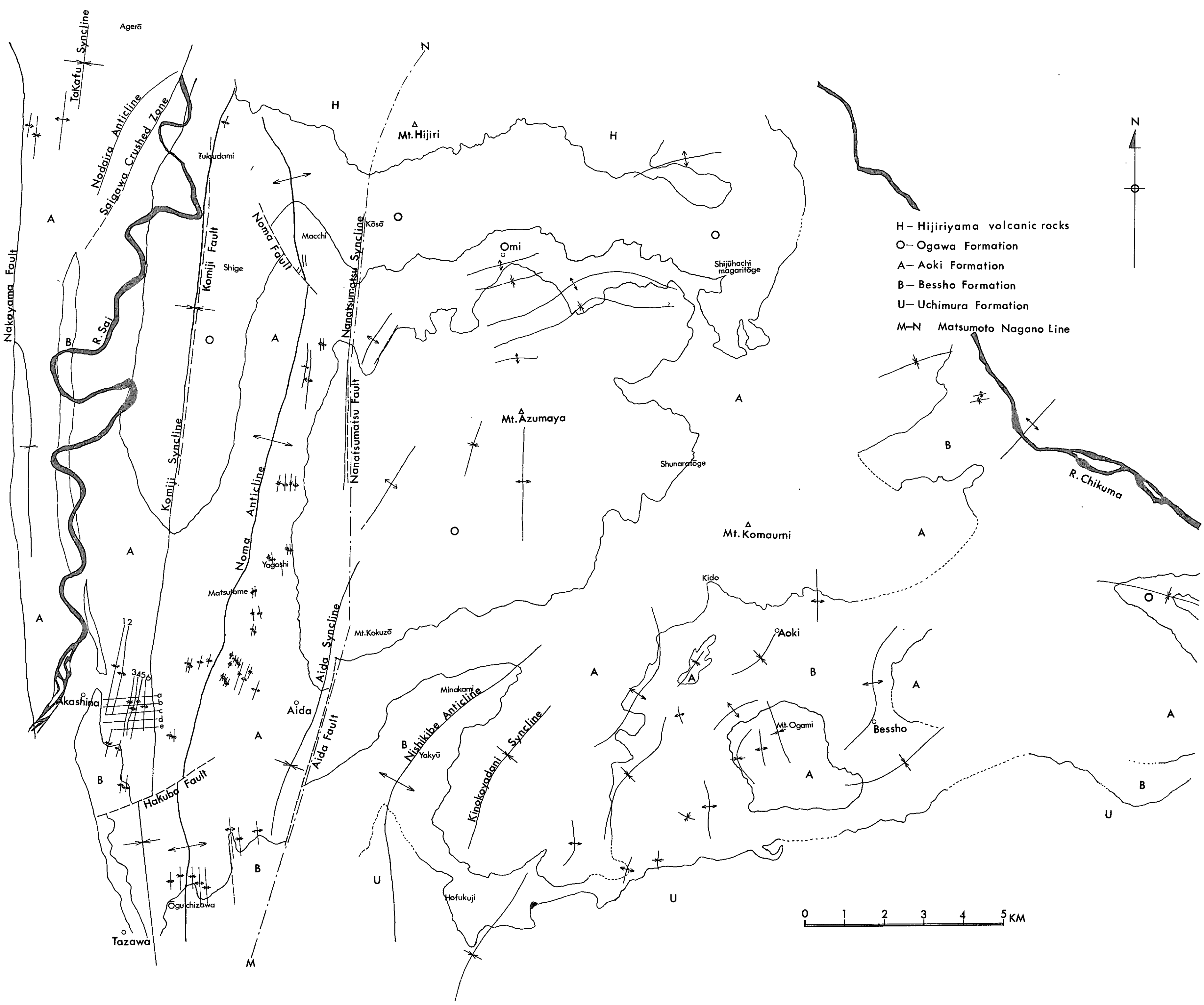

Fig. 7 General tectonic map.

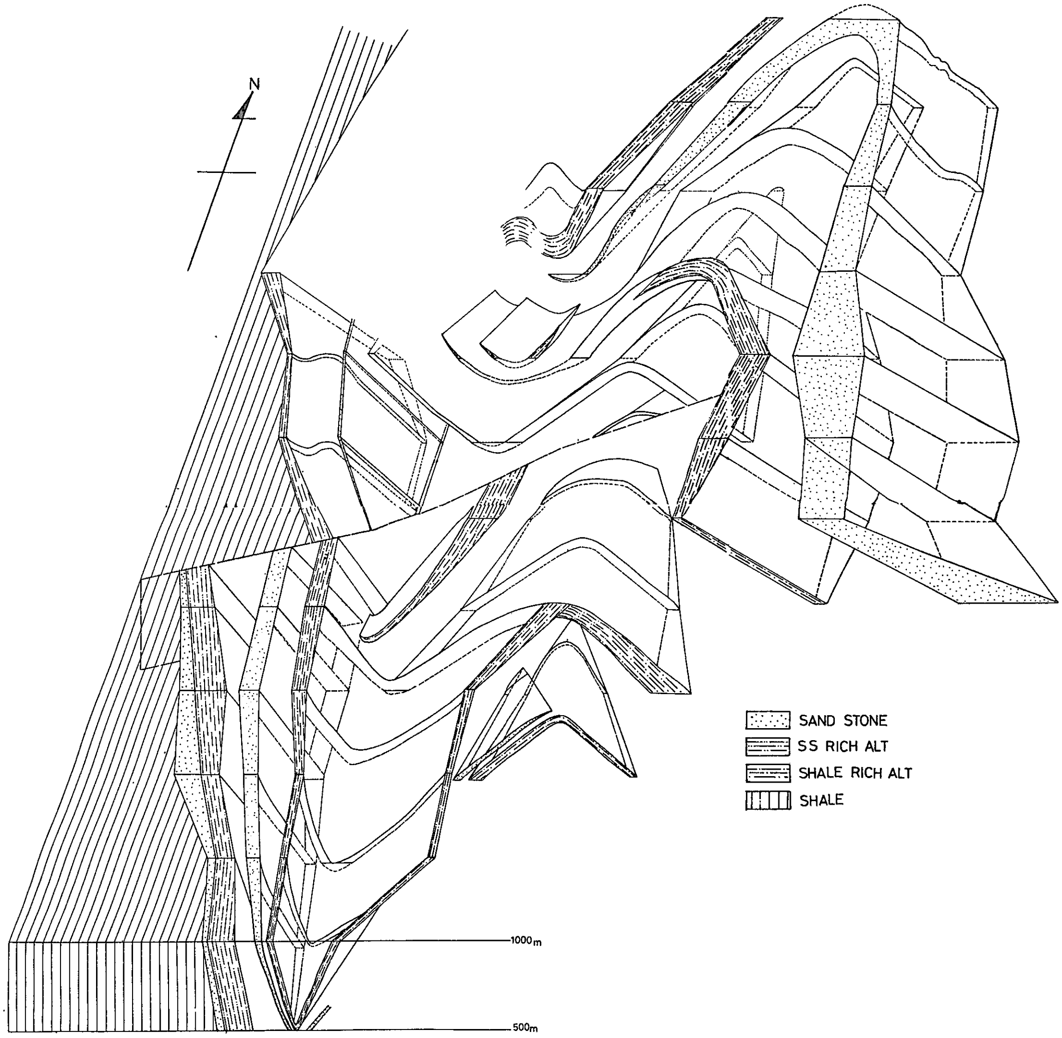

Fig. 8 The block diagram of the Komiji Syncline and the Noma Anticline in the nothern part of the studied area.

3.2 Major Faults

3.2.1 Saigawa Crushed Zone

This fault zone trends to N–S in the studied area, and to NE–SW in the northern area. This zone is showing a pivot type fault, that is, the normal fault is found in the southern area (the east side is up), but the reverse fault is found in the morthern area (the west side is up). The crushed zone is from 50 m to 100 m in width, and many minor faults and joints develope within the crushed zone. The layers in this zone are very steep and partly overturned.

3.2.2 Komiji Fault

This fault trends to N–S or N 10°E–S 10°W and cut the axis of the Komiji Syncline with acute angle. In the southern area, the west side is generally down and its maximum slip reaches 150 m. In

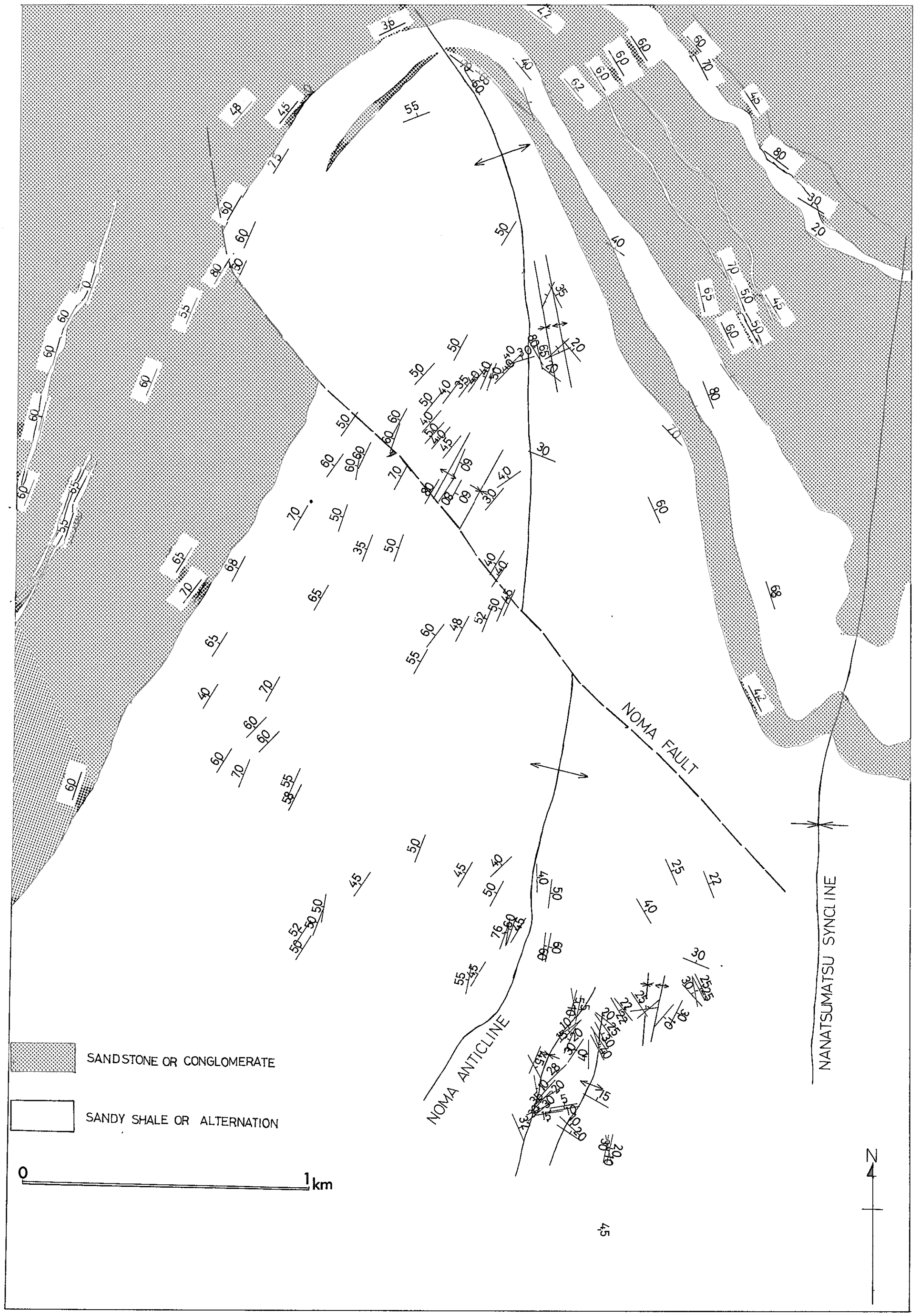

Fig. 9 Tectonic map near the crest of the Noma Anticline along Omi River.

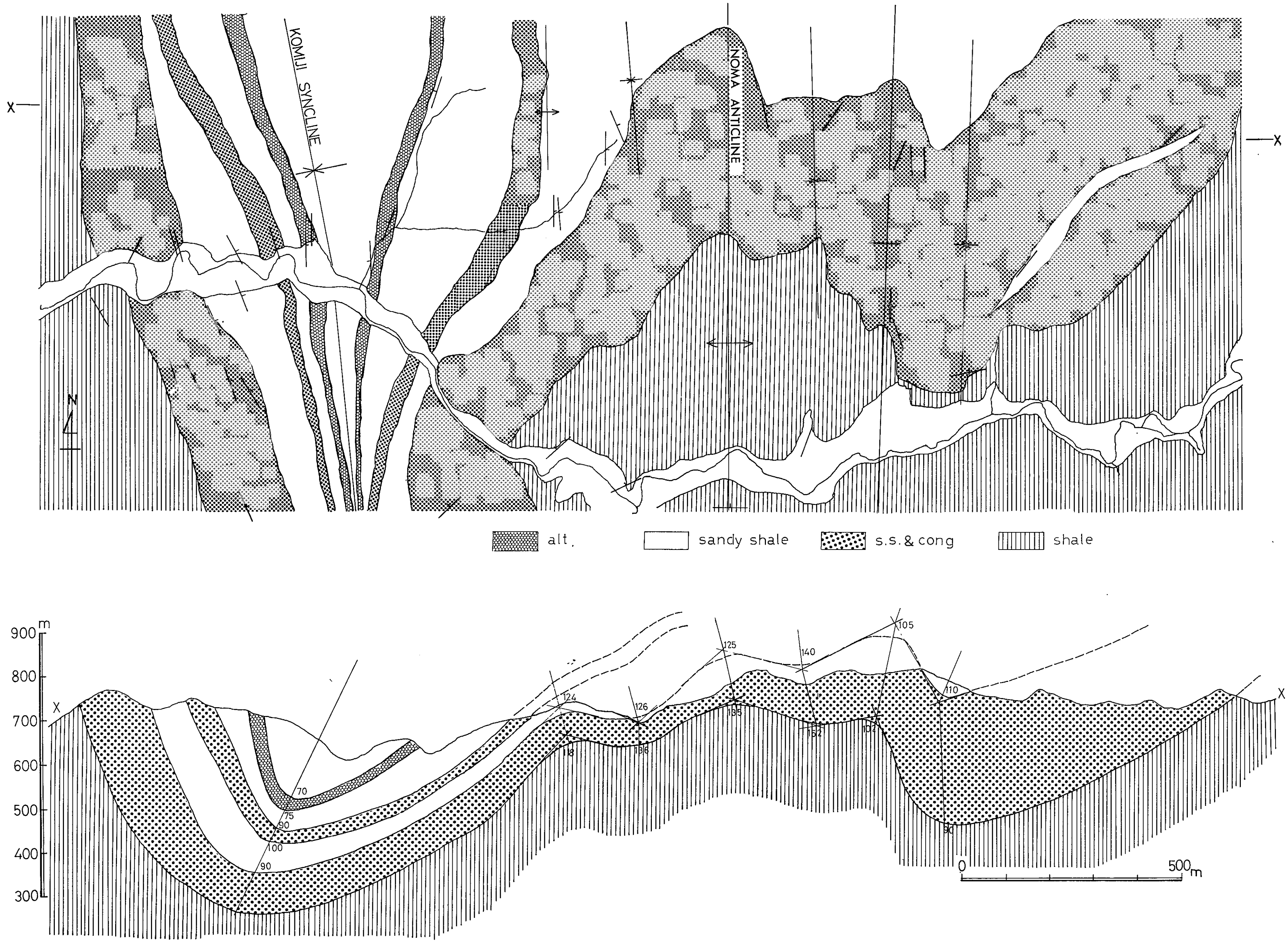

Fig. 10 The features of the Komiji Syncline and the Noma Anticline in the southern part of the studied area.

the northern area, the east side is down and its maximum slip attains more than 1 km. This is, therefore, believed to be a pivot type fault. The dislocation comes to be bigger towards the north. At the entrance of the Maruyama Route, its open fault plane which cuts the conglomerate of the Komiji Formation, and slickensides on the plane are observed as shown in Figure 11 (A).

3.2.3 Noma Fault

This fault trends to NW–SE and belongs to a kind of wrench fault. Though the heave of the northern east block can be estimated to be 700 m, the throw of fault is only less than 50 m (the south western block is down).

3.2.4 Nanatsumatsu Fault

This is named by KAWAUCHI (1973) for the first time. The fault trends to N–S along the axis of the

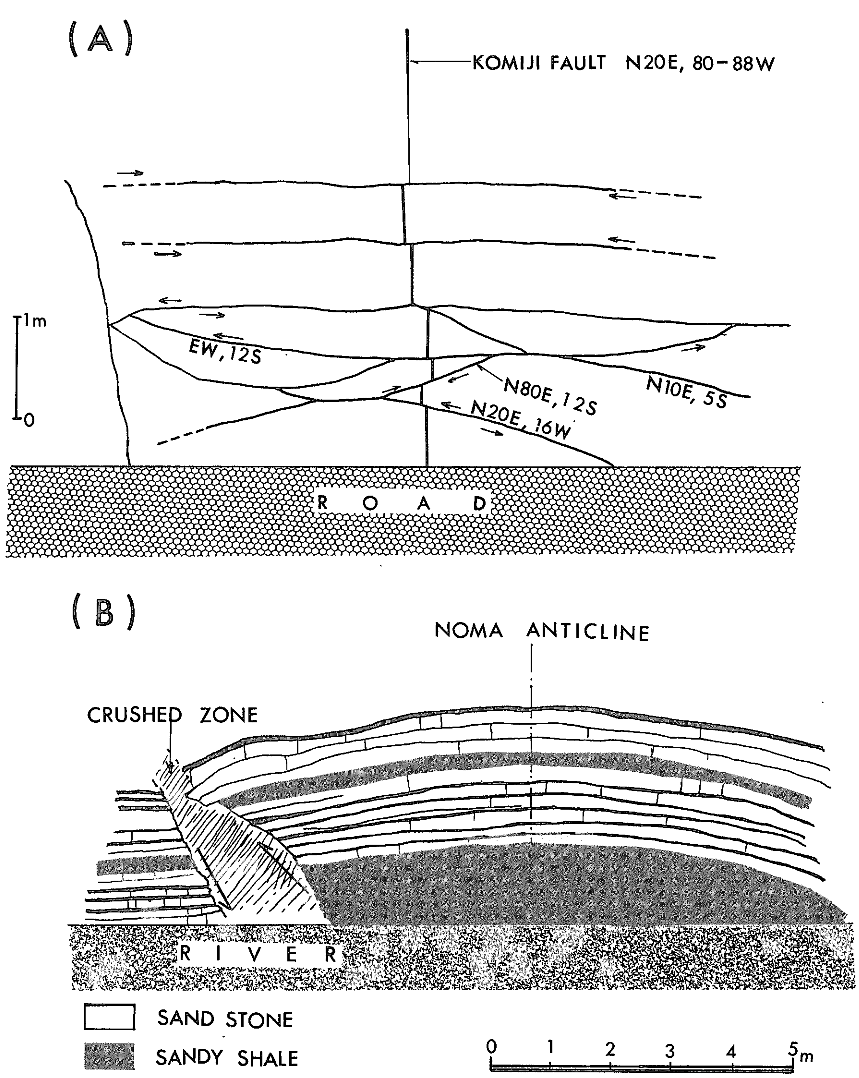

Fig. 11 Some profiles of minor faults.

(A) shows minor tectonic faults which cut the Komiji Fault on the Maruyama route.

(B) shows a minor reverse fault with crushed zone near the crest of the Noma Anticline.

Nanatsumatsu Syncline.

The west side is down and the net slip appears to be larger (100 m) to the south. The sense of this fault is the same as the Aida Fault.

3.2.5 Aida Fault

This fault runs in NNE–SSW direction along the Aida Syncline cutting the Bessho Formation. The slip of westside down comes to be larger to the south and the maximum value of 200 m is observed in the west. The south end of it is not clear because of being covered with alluvial sediments. The north end of this fault is not also clear and this fault does not give any disruption to the basaltic sheet of Mt. Kokuzo. The thickness of formations, especially in the lower Ogawa Formation and the Aoki Formation changes abruptly at each side of this fault, that is, in the east side of this fault the thickness of it is thinner than that of the west one.

3.2.6 Hakuba Fault

This fault is inferred from the dislocation of the sandstone and conglomerate of the lowest part of the Aoki Formation, and also that of the fold axis of the Komiji Syncline and the Noma Anticline. The trend of this fault strikes to ENE–WSW, and the slip comes to be larger in the west. The northern block is dislocated to the east. The maximum slip is 700 m.

3.3 Minor structures

3.3.1 Sedimentary Structures

Deformations during the time of sedimentation are formed by currents and gravitational force caused by the movements of the basement. In the studied area, the initiation and final features of major structures may be affected by the initial features of the nepton. Therefore, it is necessary to describe and analyze the sedimentary structures in order to get more knowledge about initial conditions which caused the tectonic folding. In this sense, the author intended to study such facts as the mechanics of slumping structures, clastic dikes and boundinage. The outline of sedimentary structures of the studied area was reported by Tanaka *et al.* (1973). The author could add some additional data to their work as shown in Figure 12. Tanaka *et al.* pointed out that when the Bessho Formation and the Aoki Formation were depositing, currents were from south to north in its direction. The author strongly supports their opinion (Fig. 13).

The distribution of cross beddings and water currents restored from them are very interesting as shown in Figure 14. Cross beddings in the studied area are planer type according to Nagahama (1963), and the maximum inclinations of the forset beds are very concordant with the dips of limb of the Noma Anticline, but also neighbouring minor folds, and the inclinations of axial planes of slumping folds. Furthermore, the distribution of cross beddings are the same as those of minor folds. Minor folds whose wave lengths are less than a few meters in the studied area are assumed to be mostly slumping folds. The reasons why the author judged the origin of minor folds are given as follows:

(1) Those minor folds develope in specified alternations of sandstone and sandy shale of the Aoki Formation and the Bessho Formation.

(2) Some of the minor folds are truncated by the superposed strata as shown in Figure 15.

(3) Their features are mostly similar type (Fig. 16).

(4) They frequently exist together with other slumping structures (Fig. 17).

(5) They have a large curvature without fracturing.

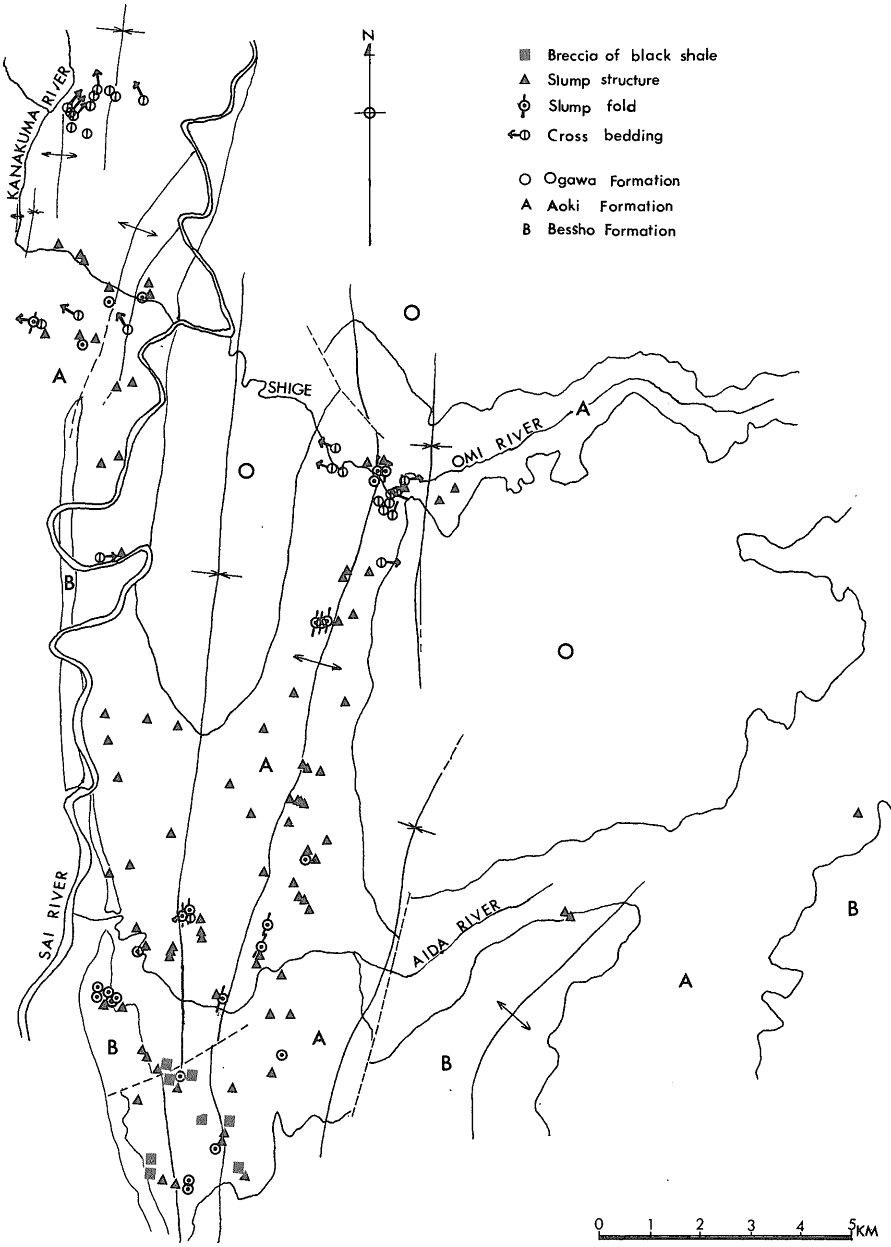

Fig. 12 The distribution of sedimentary structures.

(6) They have no bedding slip.

Some minor folds may be tectonic ones as shown in Figure 18 from their features. Their distribution is shown in Figure 12, and it is interesting that axial trends of slumping folds are pallel to that of large tectonic ones such as the Noma Anticline and the Komiji Syncline.

Clastic dikes are observed within stratigraphic horizon from the upper part of the Bessho Formation to the lower part of the Ogawa Formation, and those tends to be formed near the tectonic boundaries

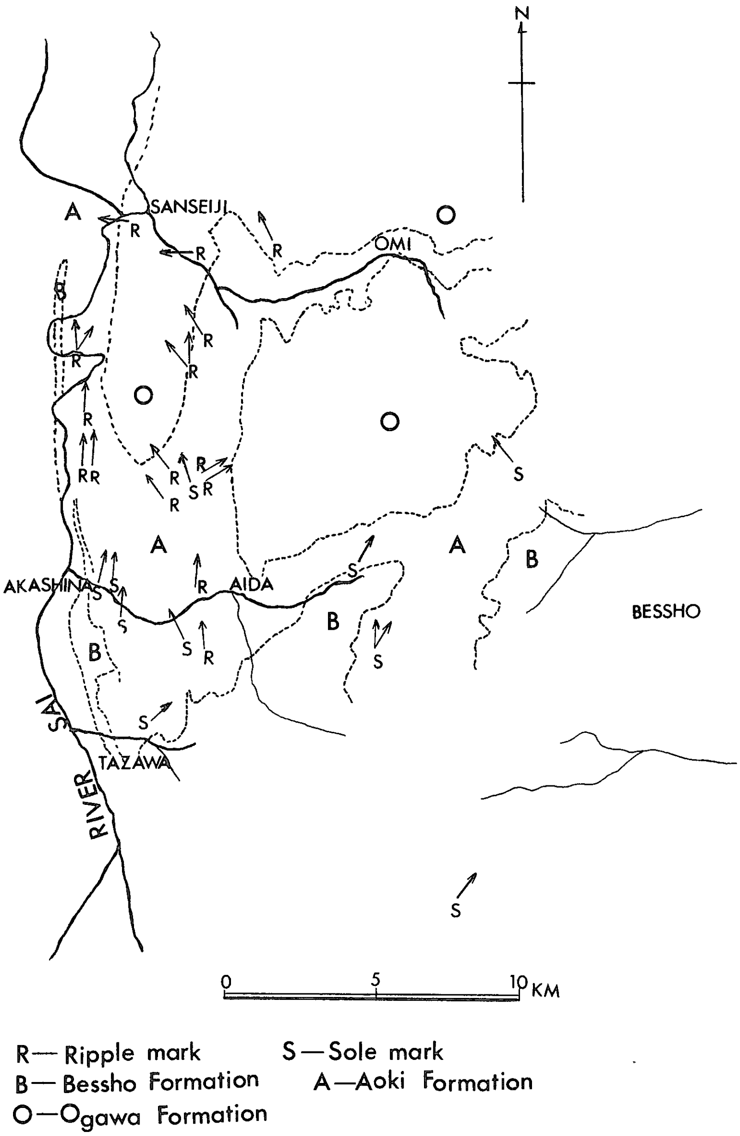

Fig. 13 Palaeo-current directions estimated from ripple marks and some kinds of sole marks in the Aoki Formation and the Bessho Formation.

of the basement, that is, the Saigawa Crushed Zone and the Chūō Uplifting Zone (Figs 12 and 21). The materials of dikes are mostly fine grained and coarse grained sandstone, partly conglomerate, and the alternation of sandstone and shale. The widths of dikes are mostly less than 20 cm as shown in Figure 19, but their lengths are unknown yet. Many joints develope in clastic dikes, and some minor faults cut dikes. Clastic dikes are mostly planner in shape and cut the layers with right angle or high angle. Major clastic dikes are shown in Table 3. They are divided into the two types as shown in Figure 20. Type 1 is found in many places in the studied area, and developes in the uppermost part of the Bessho Formation and in the lower part of the Aoki Formation. Type 2 is observed at locality 9 in

Table 3 Data of clastic dikes.

Locality No.	Trend	Width (cm)	Feature	Dike material	Intruded formation	Structure
1–1	N5W, 30N	30	planer	med.s.s.	u.m.B.F.	fractured, partly faulting
1–2	NS, 70W	10	planer	med.s.s.	u.m.B.F.	
2–1	N80E, 75N	20	wavy	med.s.s.	u.m.B.F.	
2–2	N30W, 80W	40	planer	med.s.s.	u.m.B.F.	fractured
2–3	N10W, 70W	2	planer	med.s.s.	u.m.B.F.	
2–4	NS, 60E	5	planer	med.s.s.	u.m.B.F.	
3–1	N20W, 70E	100		med.s.s.	l.A.F.	load casted
4–1	N5W, 60W	10	wavy	med.s.s.	u.m.B.F.	
4–2	N5W, 75E	10	partly w.	med.s.s.	u.m.B.F.	
4–3	NS, 80W	25	planer	med.s.s.	u.m.B.F.	partly laminated
4–4	?	10–30	irregular	med.s.s.	u.m.B.F.	
4–5	N20W, v.	3–5	partly w.	c.s.s.	u.m.B.F.	
4–6	N22W, v.	10	partly w.	c.s.s.	u.m.B.F.	
4–7	EW, 75S	5	wavy	med.s.s.	u.m.B.F.	
4–8	N80E, 80S	10	planer	med.s.s.	u.m.B.F.	
4–9	?	20	irregular	med.s.s.	u.m.B.F.	
4–10	N30E, 80S	10	wedge	med.s.s.	u.m.B.F.	well faulted
4–11	N80E, 60W	12	planer	med.s.s.	u.m.B.F.	
4–12	N70W, 65N	15	planer	med.s.s.	u.m.B.F.	
4–13	N80E, 50N	25	planer	med.s.s.	u.m.B.F.	This dike cuts slump fold.
4–14	N80W, 60N	20	planer	med.s.s.	u.m.B.F.	
4–15	N80E, 55N	15	wavy	med.s.s.	u.m.B.F.	
4–16	EW, 65N	5	wavy	med.s.s.	u.m.B.F.	
4–17	N70E, 70N	10	planer	med.s.s.	u.m.B.F.	
4–18	N80W, 72S	20	wavy	hard m.s.s.	u.m.B.F.	faulted
4–19	N20E, v.	3	planer	med.s.s.	u.m.B.F.	
4–20	?	10	irregular	med.s.s.	u.m.B.F.	
4–21	N70E, 80S	10	planer	med.s.s.	u.m.B.F.	
4–22	EW, 80S	20	planer	hard m.s.s.	u.m.B.F.	faulted
4–23	N65E, 75S	5	planer	med.s.s.	u.m.B.F.	partly faulted
4–24	N60E, 55S	20	planer	med.s.s.	u.m.B.F.	
4–25	NS, 80W	25	planer	med.s.s.	u.m.B.F.	
4–26	N65E, 50S	20	planer	med.s.s.	u.m.B.F.	
4–27	?	?	irregular	med.s.s.	u.m.B.F.	
4–28	N10E, 80W	10	wavy	hard s.s.	u.m.B.F.	fractured
4–29	N50E, 85W	10	planer	med.s.s.	u.m.B.F.	
4–30	N45E, v.	30	planer	med.s.s.	u.m.B.F.	
4–31	N30E, 85W	7	planer	med.s.s.	u.m.B.F.	
4–32	?	?	irregular	med.s.s.	u.m.B.F.	slumped
4–33	N40W, 85W	20	partly w.	med.s.s.	u.m.B.F.	partly faulted
4–44	N40W, 60W	20	planer	med.s.s.	u.m.B.F.	
4–45	N60E, 80S	15	planer	med.s.s.	u.m.B.F.	faulted
4–46	N10E, v.	20	planer	med.s.s.	u.m.B.F.	
4–47	N30E, 65N	3	partly w.	med.s.s.	u.m.B.F.	
4–48	N40W, 65W	5	partly w.	med.s.s.	u.m.B.F.	
4–48	N50W, 50N	10	planer	med.s.s.	u.m.B.F.	
4–49	EW, 80N	20	planer	med.s.s.	u.m.B.F.	
4–50	N30W, 40E	10	planer	med.s.s.	u.m.B.F.	

Table 3 (Continued).

Locality No.	Trend	Width (cm)	Feature	Dike material	Intruded formation	Structure
4–51	N70W, 60S	10	planer	med.s.s.	u.m.B.F.	
5–1	N80E, 45S	10	planer	med.s.s.	l.A.F.	
6–1	N5W, 70E	15	planer	c.s.s.	u.m.B.F.	
7–1	N20W, v.	12	sheet	c.s.s.	u.m.B.F.	
8–1	N50W, 50N	10	planer	med.s.s.	l.A.F.	
8–2	N30W, 80E	10	planer	med.s.s.	l.A.F.	
9–1	N40W, 80E	5	wavy	med.s.s.	m.A.F.	
9–2	N30W, 70W	5	wedge	med.s.s.	m.A.F.	
9–3	N30W, 70W	20	lense	med.s.s.	m.A.F.	partly faulted
9–4	N40W, 58W	20	planer partly w.	med.s.s.	m.A.F.	including coal fragments
9–5	N30W, 55W	15	partly w.	med.s.s.	m.A.F.	
9–6	N15W, 85W	20	wedge	med.s.s.	m.A.F.	
9–7	N35W, 65W	40	planer	med.s.s.	m.A.F.	grading
10–1	?	?	planer	med.s.s.	l.A.F.	
11–1	?	?	planer	med.s.s.	u.A.F.	
12–1	N40W, 82S	2	planer	med.s.s.	u.m.B.F.	
12–2	N42W, 72S	100	planer	med.s.s.	u.m.B.F.	
13–1	?	?	irregular	?	u.B.F.	
14–1	NS, v.	20–35	planer	med.s.s. and c.s.s.	u.m.B.F.	partly slipped
15–1	N20E, 72E	10	planer	med.s.s.	u.B.F.	
15–2	N40E, 72E	50	planer	med.s.s.	u.B.F.	

* Locality No. is shown in Fig. 21.
* u. m. B. F. means the uppermost part of the Bessho Formation.
* u. B. F. means the upper part of the Bessho Formation.
* l. A. F. means the lower part of the Aoki Formation.
* m. A. F. means the middle part of the Aoki Formation.

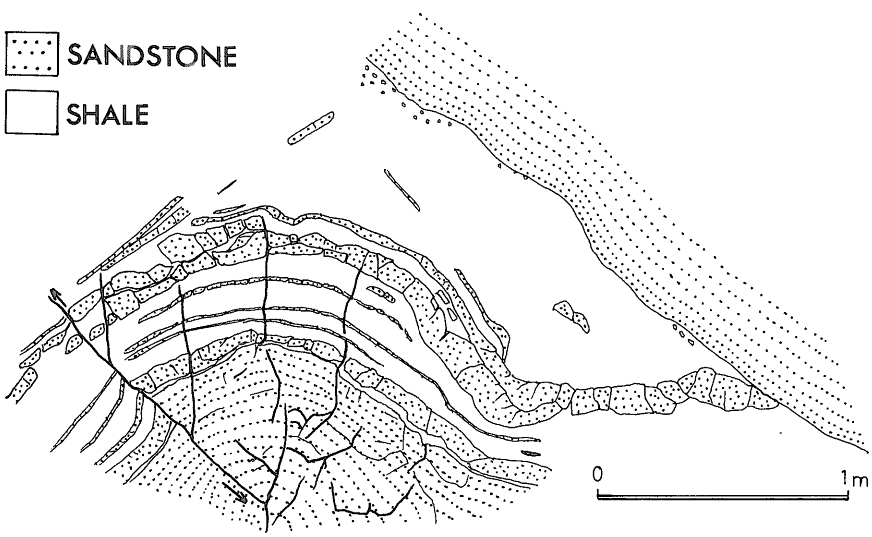

Fig. 15 An example of the truncated slumping fold in the Aoki Formation near Asō.

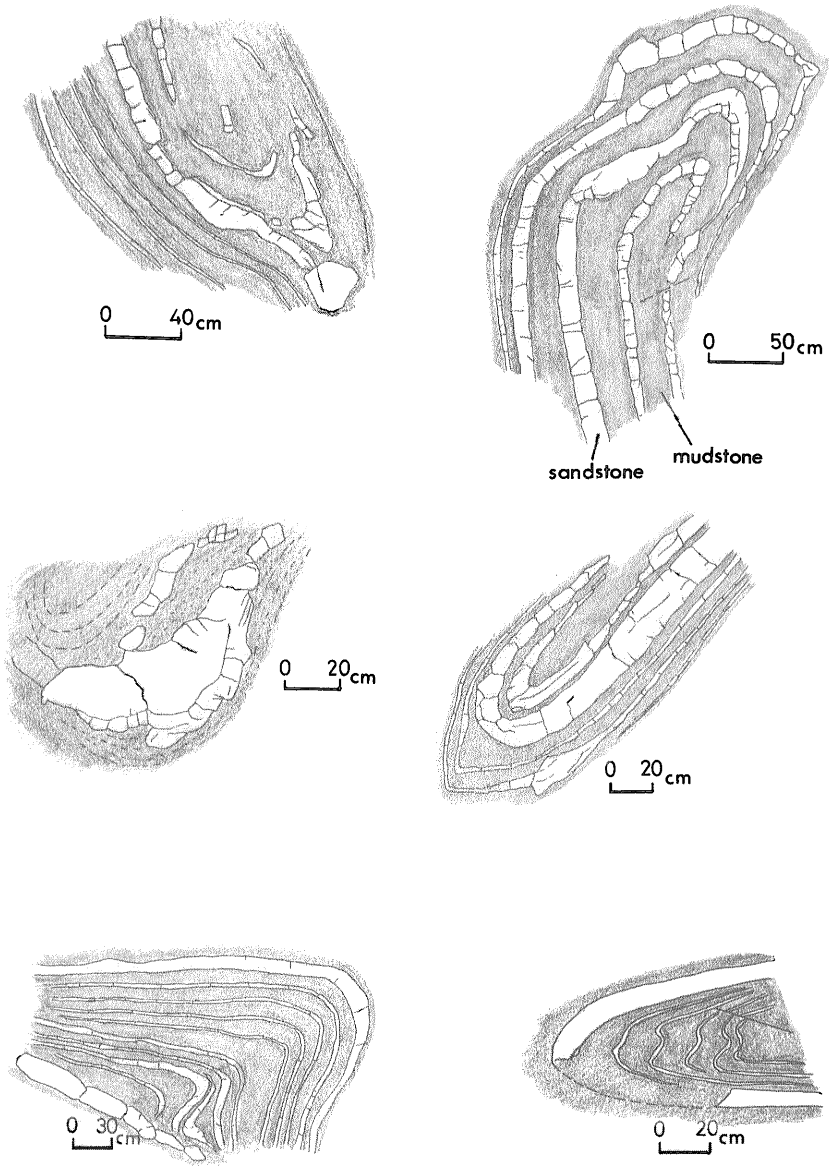

Fig. 16 Some profiles of slumping folds in the Aoki Formation.

Figure 21. It becomes to be thinner downward, and is wavy where it meets with the lower end layer. It developes in the middle part of the Aoki Formation and its materials are composed of sandstone, pebbles of pre-Tertiary rocks and blocks of sandstone. The distribution of various slump structures described above is shown in Figure 12. Their distribution is restricted in the Bessho Formation and the Aoki Formation, and in the west of Matsumoto—Nagano Line. It is interesting that their distribution are continuous along the axis of the Noma Anticline from the south to the north regardless stratigraphic horizon.

The Saigawa Research Group (1966) pointed out that a disturbed zone, named "Saigawa Disturbed

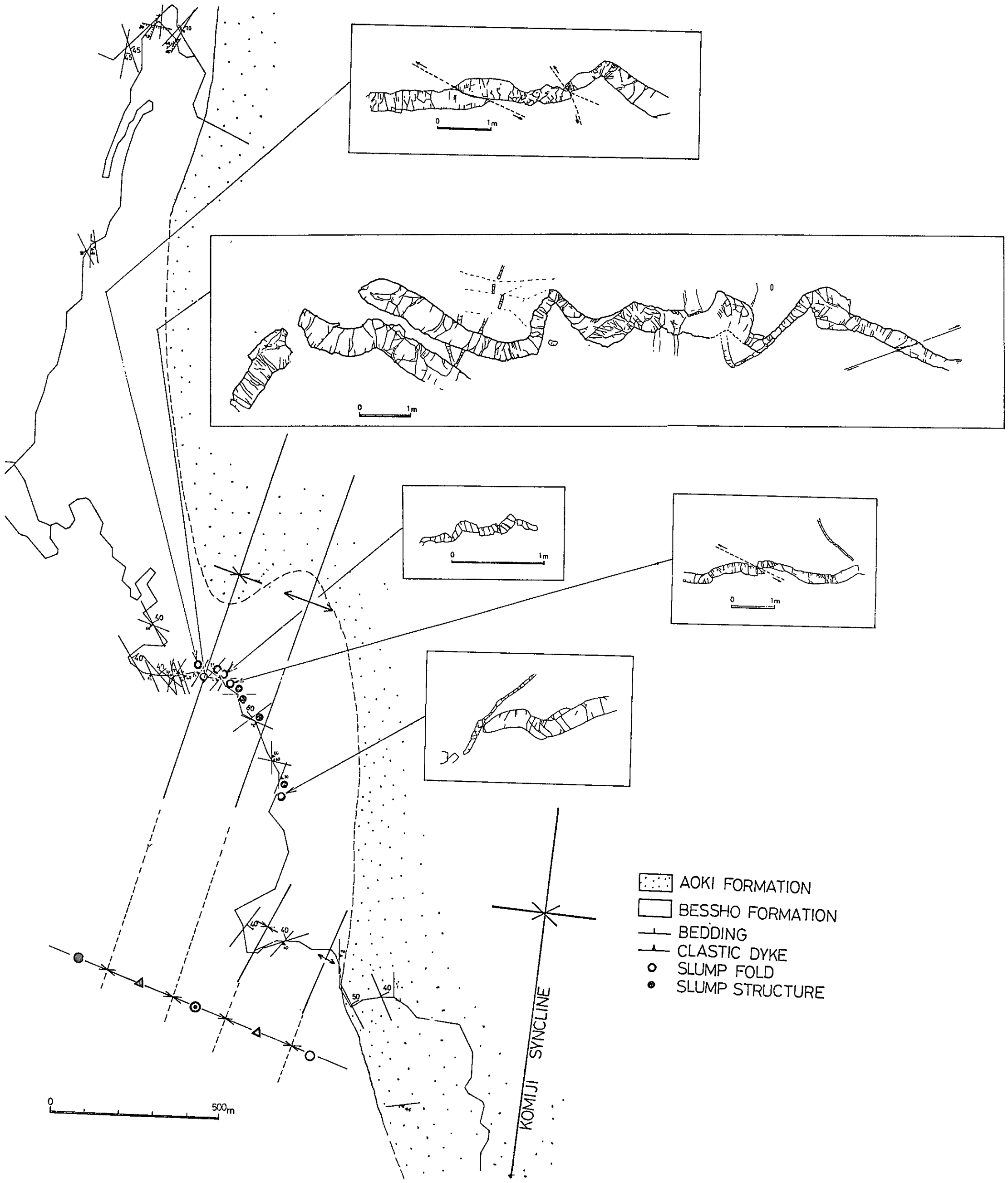

Fig. 17 The route map of Nagamine Drag Road.

Many clastic dikes, slumping folds and other slump structures are observed.
●, ▲, ◎, △ and ○ are symbols of clastic dikes in each area (See Fig. 20 (B)).

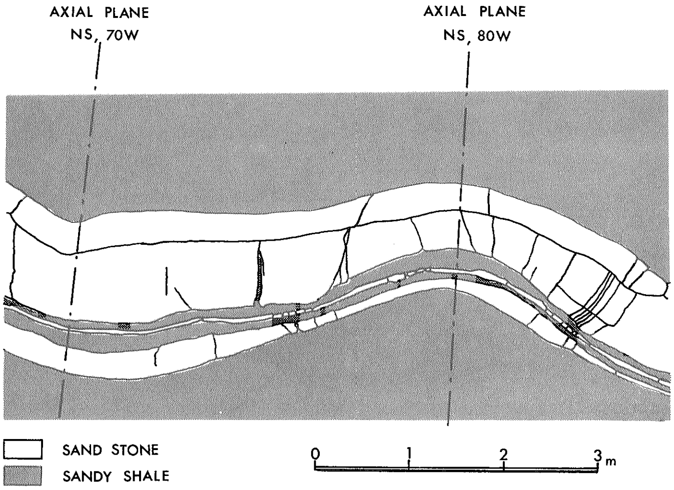

Fig. 18 An example of the minor tectonic fold in the Aoki Formation.

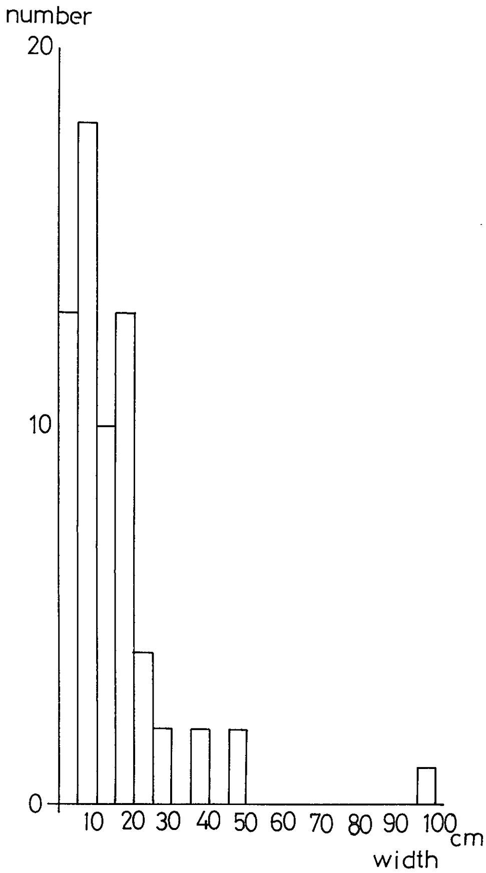

Fig. 19 The frequency histogram of the width of the clastic dikes in the Aoki Formation and the Bessho Formation.

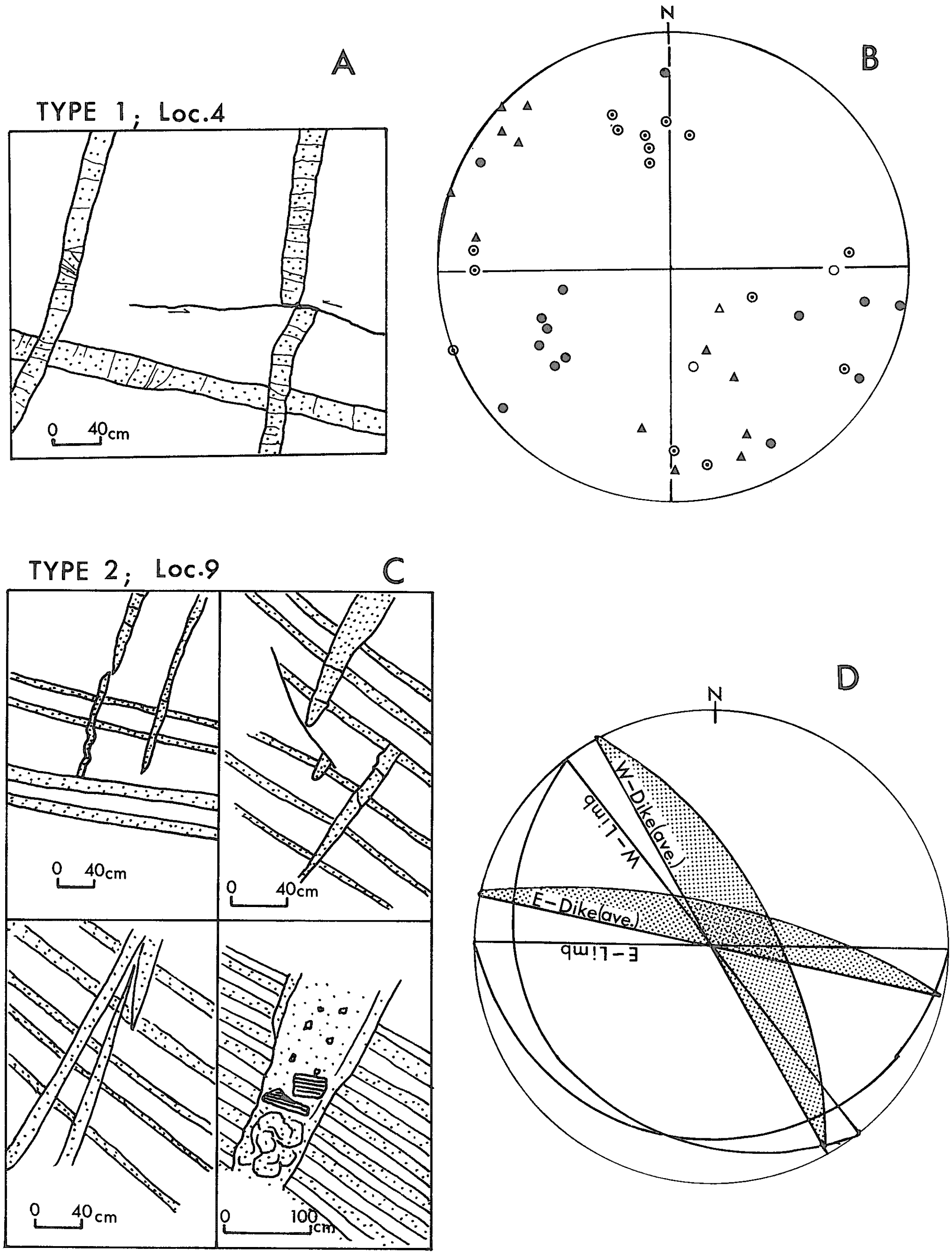

Fig. 20 Two types of clastic dikes.

(A) shows examples of Type 1 clastic dikes of which dike materials emplaced from the lower part.
(B) shows stereo projection of clastic dikes.
(C) shows examples of Type 2 clastic dikes of which dike materials emplaced from the upper part.
(D) shows stereo projections of average clastic dikes and limbs of minor folds.

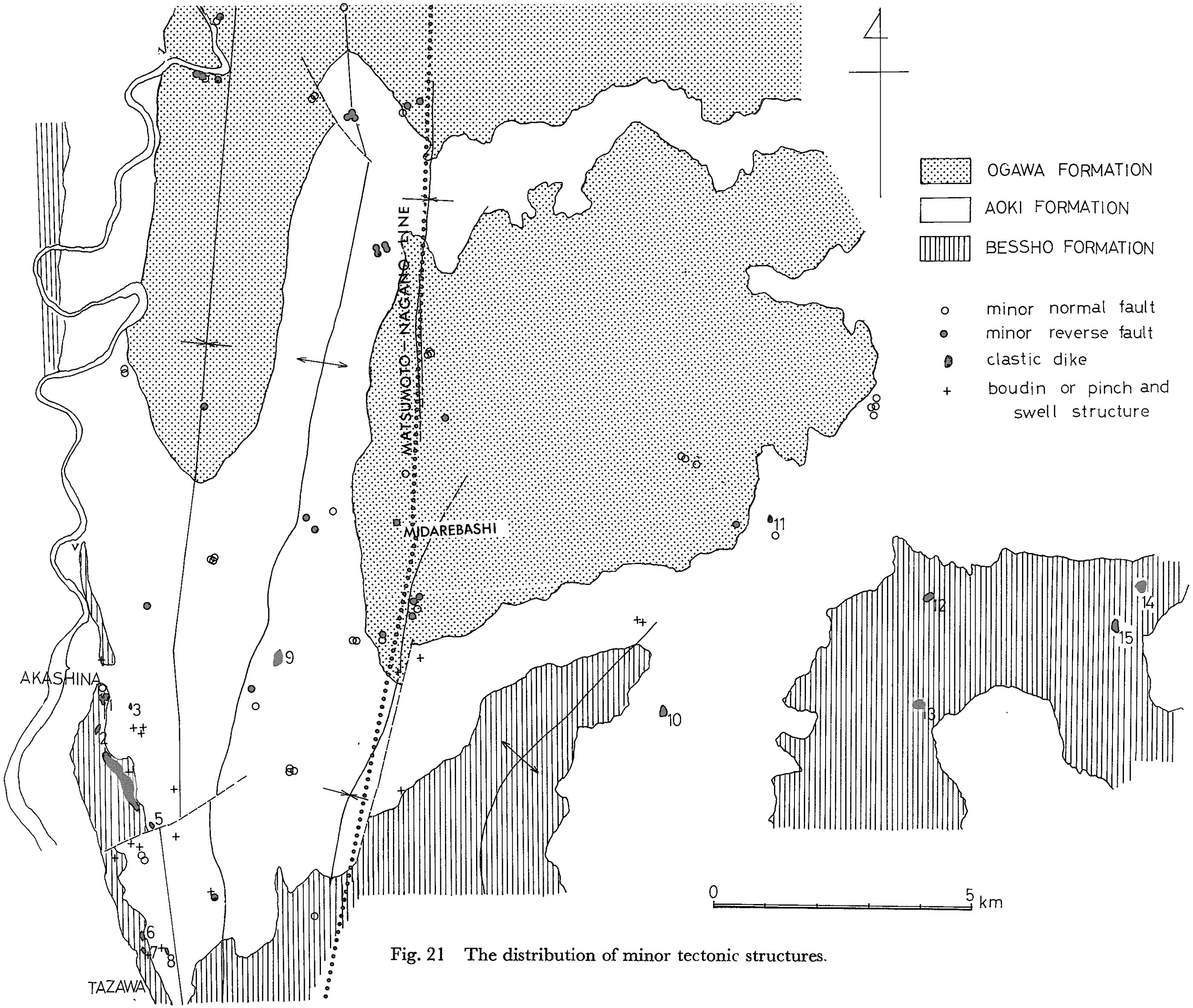

Fig. 21 The distribution of minor tectonic structures.

Zone" of which length is about 30 km and width is 1.5–2.0 km with the trend of SSW–NNE developes in the west part of the studied area. In this zone high dips (partly overturned) of starta, various types of sedimentary structures and faults are observed. The most remarkable change in lithofacies and geological structures can be found at this zone (KATO, 1970). Saigawa Disturbed Zone is artificially defined because the disturbed zone comprises not only initial high dip area during the period of deposition but high dip area by later tectonic movements. But the distribution of slump structures extends along the Saigawa Crushed Zone, and also the axis of the Nodaira Anticline. In the southern part, for example, in Akashina, their distribution comes to be indistinct, and the similar tendency is also recognized in the distribution of slumping structures along the Noma Anticline.

It is noteworthy that these concentrations of sedimentary structures correspond with the zone changing in lithofacies and thickness remarkably. A part of this fact reported by KAWAUCHI (1973) and KASAHARA (1973). The author will discuss about this zone later.

Boudins and pinch-and-swell structures are observed in the alternation of sandstone and sandy shale near tectonic boundary of the basement blocks as the same as clastic dikes. Their distribution concentrates in the boundary of the Ogawa and the Aoki Formations, and of the Aoki and the Bessho Formations.

Boudins are classified into four types from their features as follows:

Type 1 is rectangular body and its fracture planes are very clear without plastic necking down.

Type 2 is lenticular body. Some surrounding materials show considerable plastic flowage, and some boudins have many fractures without any dislocation.

Type 3 is rhombic body with linear fracture plane whose lengths are about 50 cm. Boudins of this type are observed only at Nagamine Drag Road.

Type 4 is pinch and swell structure. In this type, plastic flowage is dominant, and each fragments are not separated.

In the studied area, this type of boudin is often observed.

Directions of elongation of each boudin is parallel to the layering.

3.3.2 Minor folds

It is generally said that various folds whose types and scales are different to each others coexist in the same folding area. Some geologists (TSUNODA, 1973 and KATO, 1970) have tried to get more understanding about major folds from analysis of minor folds, but they seem to be failed. The one reason is that it is difficult to estimate the origin of these minor folds whose wavelengths are between a few meters and a few tens of meters as already described above. The another reason is that it is also difficult to describe the folds whose wavelengths are between a few tens of meters and a few hundred meters as the strain images of major folds. As a fact, it was not sufficient to describe the three dimensional deformation of minor folds. The author described and analyzed the distance between axes (that is, half wavelength), the length of axes and the maximum amplitude because of the difficulty of constructing the exact profiles of minor folds.

(1) Classification and distribution of tectonic minor folds: The distribution and type of minor folds is closely connected with the tectonic provinces (Fig. 22) of this studied area. The minor folds are classified as follows from their shapes and axis trends.

Type 1: Minor folds of this type are distributed in the area III of Figure 22. They develope in the uppermost part of the Bessho Formation and in the Aoki Formation. The axis trends to N–S and

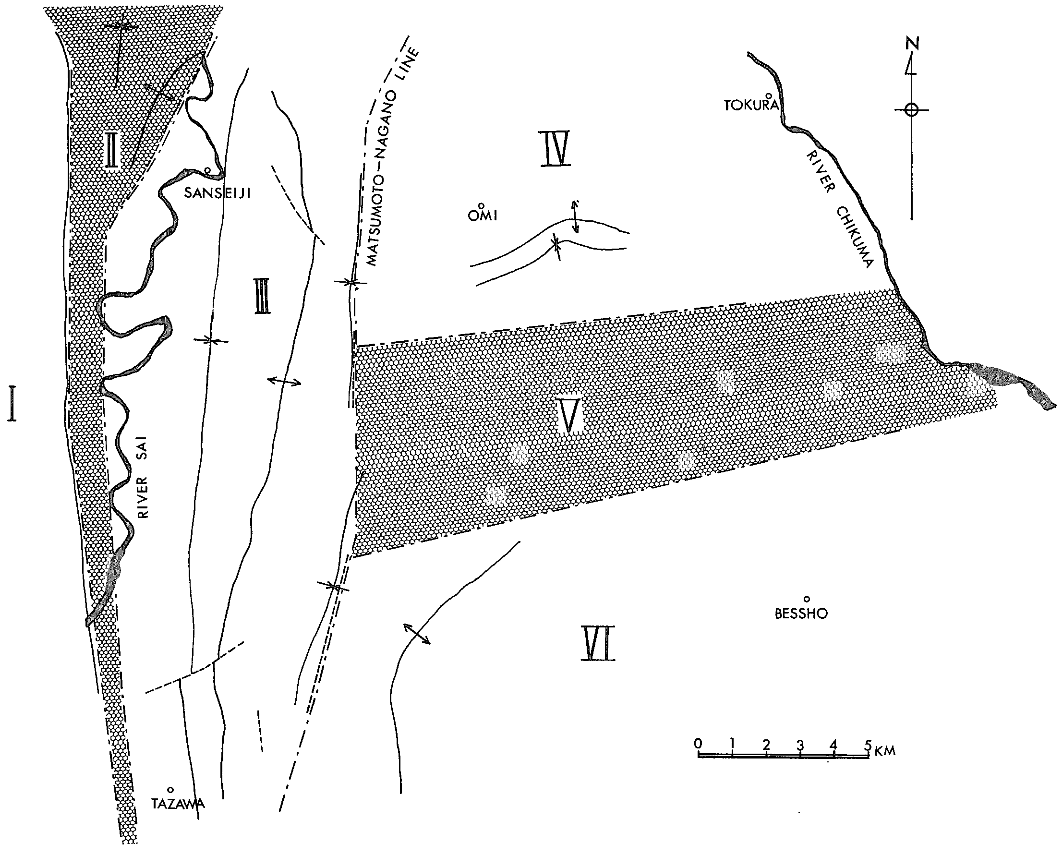

Fig. 22 Tectonic provinces in the studied area.

are concordant with those of major folds. Their distribution is not universal exactly. That is, they develope closely in the southern part of the Komiji Syncline and in the east limb of the Noma Anticline.

Type 2: These minor folds are distributed in the area IV of Figure 22. They develope between the upper part of the Aoki Formation and the Susobana Formation. The inclinations of limbs are less than 20 degrees. The axis trends to E–W.

Type 3: These minor folds are distributed in the area V.

They develope between the upper part of the Aoki Formation and the Ogawa Formation. The inclinations of limbs are less than 20 degrees. The axis trends to N–S.

Type 4: These minor folds are distributed in the area VI of Figure 22. They develope between the middle part of the Bessho Formation and the lower part of the Aoki Formation.

The axis trends remarkably wavy and indistinct. They mainly plunge to the north but some plunge to the south. They deform little and strongly asymmetrical.

(2) (Half) Wavelength, namely the distance between axes: The frequency diagram of wavelengths of Type 1 minor folds is shown in Figure 23 (A). These wavelengths are mostly less than 500 m. The average value is 334 m. The wavelengths of major folds, that is, those between the Komiji Syncline and the Noma Anticline are from 2 km to 6 km. Therefore, wavelengths of major folds are about ten times

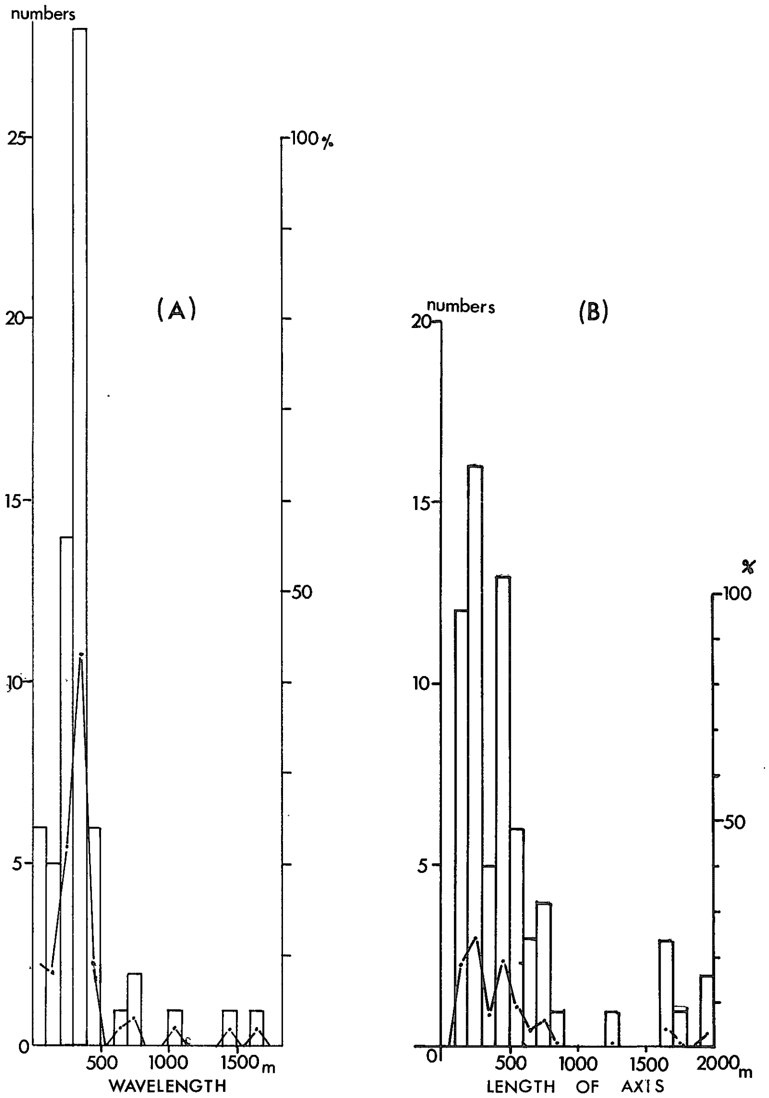

Fig. 23 The frequency diagrams of wavelengths and lengths of axis of minor folds in Area III.

as long as those of minor folds. As minor folds of Type 2, 3 and 4 are mostly irregular, their wavelengths are changable. They will be described later.

(3) Length of axis (Z):

The frequency diagram of the lengths of the Type 1 minor folds' axis is shown in Figure 23(B). They occupied 77% between 200 m and 500 m as the same case of the wavelengths.

It is noted that the lengths of axes which are between 1,000 m and 1,500 m are little in this studied area.

(4) The length of axis versus the half wavelength ratio:

In order to investigate the horizontal features of minor folds, the length of the axis versus the half wavelength ratio is shown in Figure 24. The frequency of the ratio of Type 1 minor folds is shown in

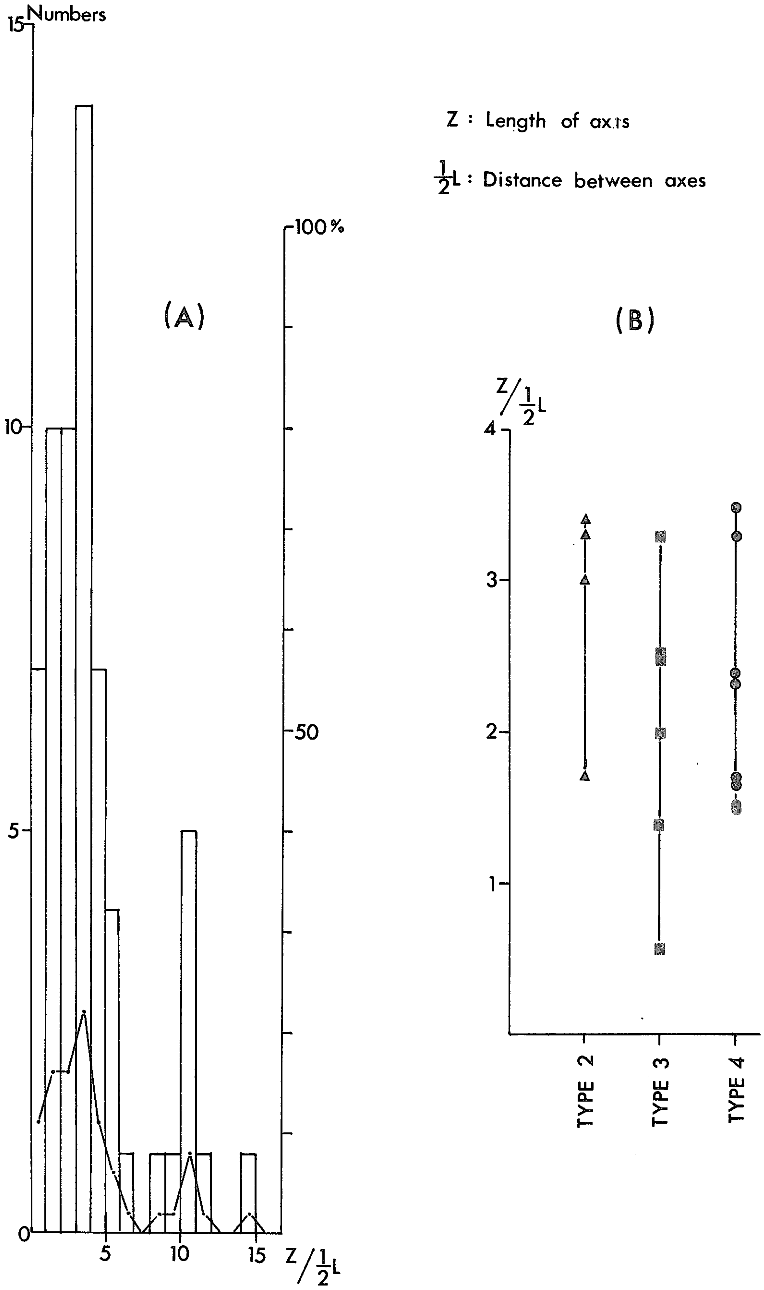

Fig. 24 The ranges of length of axis-half wavelength ratio of minor tectonic folds.
(A) shows the frequency diagram of axis length-half wavelength ratio of minor folds in Area III.
(B) shows the range of axis lengths-half wavelength ratio of minor folds in Area IV, V and VI.

Figure 24 (A). If the horizontal features of minor folds can be represented by ellipsoid, general horizontal features of these minor folds are pallel to the major folds.

The ratios of Type 2, 3 and 4 minor folds are shown in Figure 24 (B). They are mostly less than 3.5 but more than 1. Minor folds of these types develope weakly. Furthermore, in order to study the relation between lengths of axes and wavelengths, their values are plotted in Figure 25. It is noted that the ratio of Type 1 of minor folds are different from those of Type 2, 3 and 4, that is, the distribution of the ratio are classified by the line whose value is 1. It is noticeable that the lengths of axes are less ten times as long as distances between axes of the whole minor folds in the studied area.

Furthermore, the lengths of axis are roughly proportional to the wavelengths, especially minor folds of Type 1 have this tendency strongly. But this is not always right in individual cases showing as follows. For example, the values of minor folds in the west limb of the Komiji Syncline (markO), and in the axial part of the Noma Anticline near Ōguchizawa (mark ◉) are shown in Figure 26. The distance between axes seems to be constant and independent of the length of axis. Thus, these two values have not close but rough connection.

(5) (Maximum) Amplitude and the distance between axes:

Figure 27 shows the relation of maximum amplitude and the distance between axes of minor folds in Type 1. In minor folds of the west limb in the Komiji Syncline, which are deformed strongly, the

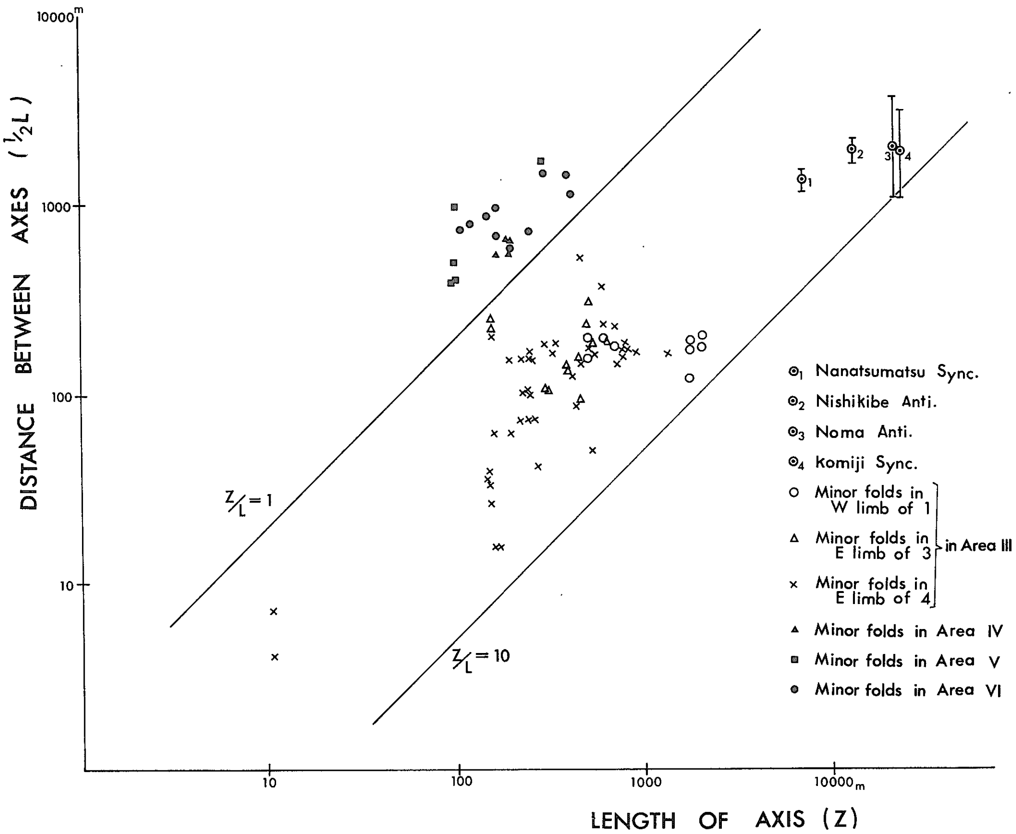

Fig. 25 The relation between axes lengths and half wavelengths of major folds and minor folds.

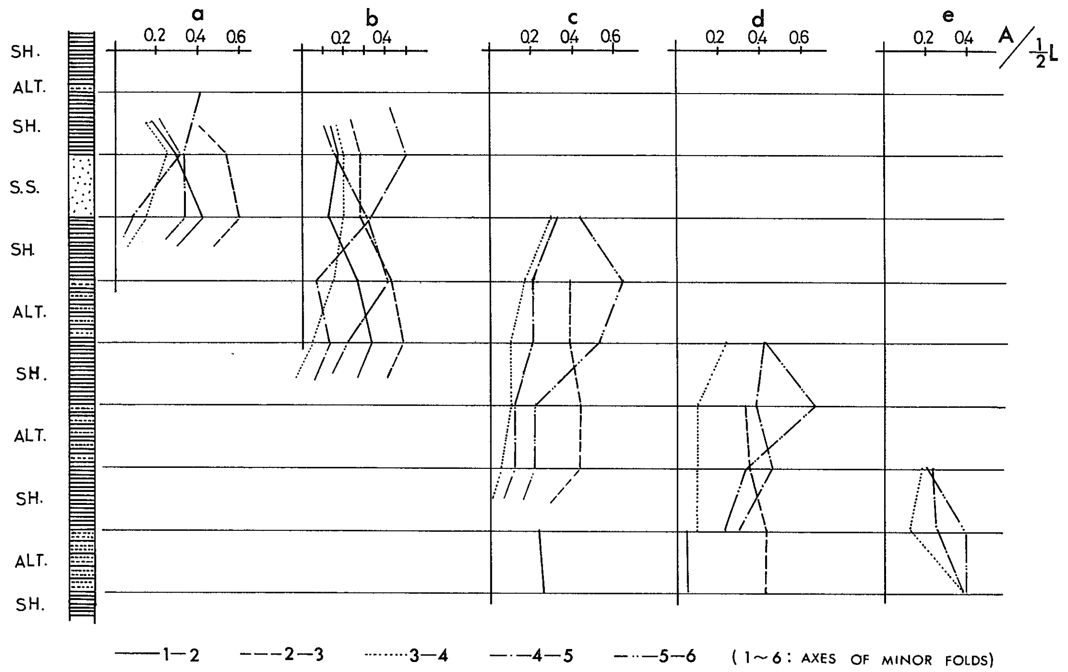

Fig. 28 The amplitude-half wavelength ratio of minor folds in the west limb of the Komiji Syncline.
1–6 shows axes of minor folds shown in Fig. 7.

larger maximum amplitude becomes to be, the larger the distance between axes also becomes to be. Furthermore, the ratio of maximum amplitude versus half-wavelength is larger as shown in Figure 27 (mark ○). On the contrary, in minor folds of the west in the Noma Anticline, the larger the distance between axes become to be, the smaller the ratio becomes to be as shown in Figure 27 (mark △). In minor folds in the axial part of the Noma Anticline, their relation is unclear because of little change of the distances between axes. Figure 28 shows the ratio of amplitude to half-wavelength of minor folds of the west limb in the Komiji Syncline at each stratigraphic horizon. As the minor folds plunge to the north and the strongest deformation of each fold are not always represented in the same cross section, the result comes to be indistinct.

But the ratio increases at the boundary from sandy mudstone to the alternation of sandstone and sandy shale, and the ratio decrease at the boundary from the alternation to the sandy mudstone. Minor folds reach the maximum amplitude-wavelength ratio at sandstone or alternation in mudstone.

3.3.3 Minor faults

Though many minor faults develope in the studied area, the mutual relations between folds and minor faults have not been clear yet, since it has been difficult to make clear whether the origin of the minor folds are sedimentary or tectonic.

In order to get more complete knowledge about folding mechanism the author tried to analyze minor faults. For the purpose, the author made an assumption that the fault having displacement of more than 20 cm and fault clay or crushed zone are considered to be of tectonic origin. Some examples of minor faults are shown in Figure 11. Minor faults shown in Figure 11(A) are observed in the cutting of the Maruyama Route near the axis of the Komiji Syncline in the conglomerate of the Komiji Formation.

Though their displacements are between 10 and 20 cm, they cut the Komiji Fault and they have slickenside and fault clay.

Therefore, they are tectonic origin. Some of them cut pebbles in the Ogawa Formation. Minor reverse faults with crushed zone shown in Figure 11(B), are observed in the alternation of sandstone and sandy shale of the Aoki Formation in the south of Macchi Village near the axis of the Noma Anticline. They seem to be a kind of the kink band. Many minor faults of the same sense develope near this outcrop. Because tectonic minor faults mostly cut the strata which dip stteply, the displacement after the formation of minor fault is unknown and their orders of the formation are not distinguished. But some interesting facts are noted as follows. Minor reverse faults are restricted in the west of the Matsumoto-Nagano Line as shown in Figure 21. They seem to concentrate to the axial parts of folds. In contract, minor normal faults develope in the whole studied area.

3.4 Matsumoto—Nagano Line

Hirabayashi (1969) pointed out from the analysis of geological structures that the remarkable changes in tectonic and geologic conditions exist between areas both sides of this line, which runs from Matsumoto-Aida-the west of Mt. Hijiri-Mt. Chausu to Nagano. Thus he named this line "Matsumoto—Nagano Line". This line accords with the "fault line" named by Honma (1931). In the studied area, this line trends to N–S, namely from Matsumoto-Aida Fault-the axis of the Nanatsumatsu Syncline to the westward of Mt. Hijiri as shown in Figure 7.

Tectonic and igneous activities in the eastern area are very different from those of the western area as follows.

(1) Minor reverse faults are limited in the western area as described above.

(2) Major folds and minor faults with strong deformations are restricted in the western area and none in the eastern area.

(3) The axis trends, plunges and the features of minor folds are regular in the western area but they are very irregular in the eastern area. The length of axis versus the distance between axes ratio of minor folds in the western area is different from that in the eastern area.

(4) Volcanic rocks (porphyrite, andesite and so on) are restricted in the eastern area.

(5) Slumping structures are distributed mostly in the western area.

4. Structural Analysis

4.1 Fundamental characters of folds

In order to investigate the mechanism of folds, it should be known the characters and distribution of stresses and strains affecting the tectonic system which includes the folding. The mechanism of folding may be classified into two categories, they are buckling and bending. The buckling folds are formed by the horizontal compression essentially, and the bending folds are formed by the vertical movement. Natural folds are formed by the compression which has various angles to the layers as Uemura and Takahashi (1974) points out. Therefore, it is needed to clarify the fundamental characters of these two types of fold in order to distinguish folds in nature. The fundamental characters of these folds may be limited to forms, thickness and stress-strain relations showing as follows:

4.1.1 Characters of forms

The control factors forming folds are the movement of basements, ductility contrast, thickness ratio of competent and incompetent layers and so on. Among these factors, the most important and observable one in nature is only the movement of the basements. If the basement blocks uplift differentially each other, the cover layers are deformed like box shaped folds. If the lower boundary is deformed to be sinusoidal, the bending folds show the sinusoidal shape. As described above, the forms of this bending type folds are controlled by the displacement of the basement. As the deformation comes to be weaker in the direction of upper level, it should be examined the amplitude-wavelength ratio comes to be smaller, and the interlimb angle comes to be larger in the direction of upper level as shown in Figure 29.

The control factors forming buckling folds are ductility contrast, thickness ratio of competent and incompetent layers, mean shortening and so on. The shape of this type have been shown to be sinusoidal by many experiments (BIOT, 1961; CURRIE *et al.*, 1962; RAMBERG and STEPHANSSON, 1964; HUDLESTON, 1973; KATO, 1975). Buckling folds are more periodical than bending folds. But according to WILLIS (1894) and JOHNSON (1969), buckling folds can show the non-periodical shape if the initial deflections exist. This fact explains that minor folds which seem to be buckled are not always continuous. In multi-layered buckling folds, the whole layers harmonically fold together in some

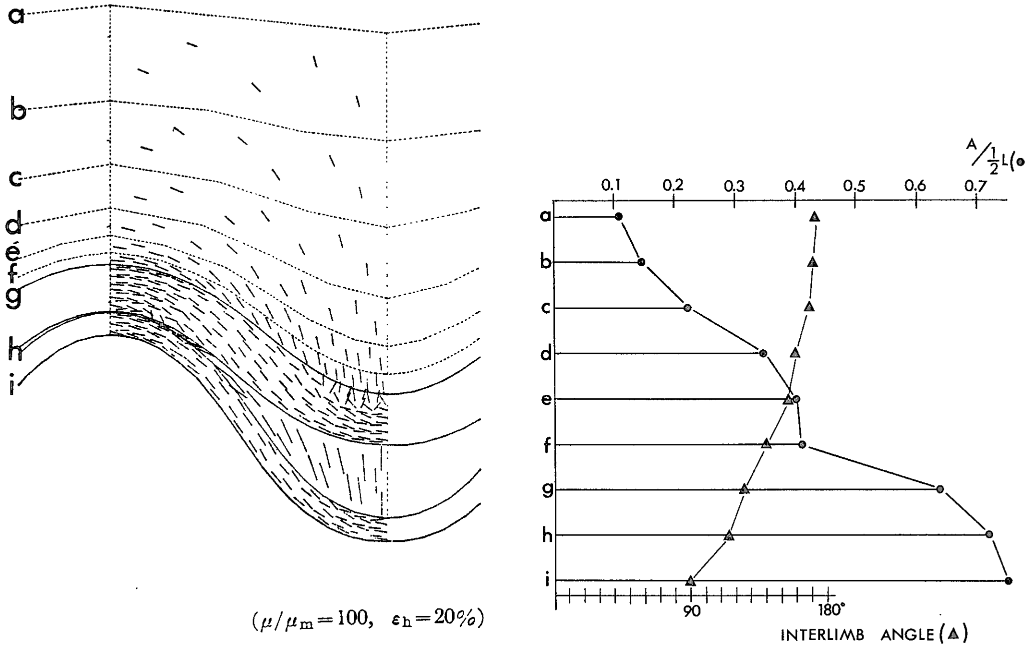

After IKEDA, Y. and SIMAMOTO, T. (1974)

Fig. 29 The idealized distribution of the amplitude-half wavelength ratio, and interlimb angle of the bending fold.

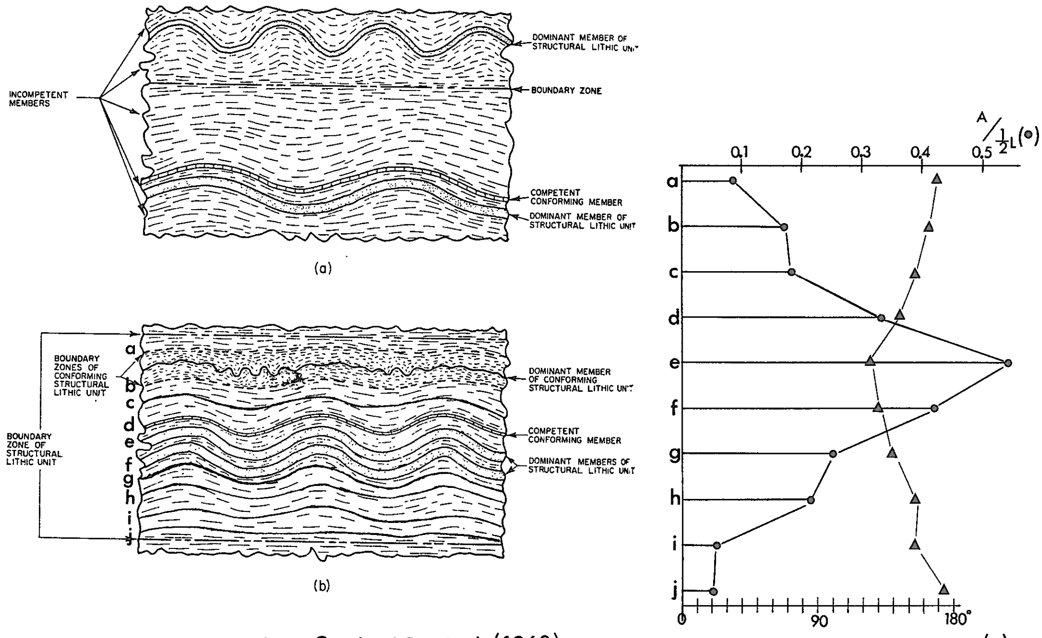

After Currie J.B. et al. (1962)

Fig. 30 The idealized distribution of the amplitude-half wavelength ratio, and interlimb angle of the buckling fold.

cases, but in other cases, various folds whose wavelengths are different develope (Ramberg and Stephansson, 1964; Hara, 1967; Kato, 1975). In buckling folds, it should be examined that the amplitude-wavelength ratio is maximum at the competent layer or competent unit, and the interlimb angle is minimum at the competent layer as shown in Figure 30.

4.1.2 Characters of thickness

In bending folds, the incompetent layer is the thinnest at the crest of anticline, and it is the thickest at the bottom of syncline. The thickness of the competent layer changes little except in much deformed folds (Ikeda and Shimamoto, 1974).

In buckling folds, the thickness of the competent layer is a little large in the hinge except at the case which the competency contrast is high. Because the initial thickness is not known to us, it is very difficult to estimate to change of thickness caused by tectonic movement. As a matter of fact, thicknesses of each limbs are often different each other in nature, therefore, the axis of fold locates in the place where the thickness changes remarkably at the time of deposition, which is affected by the movement of the basement.

4.1.3 Characters of stress-strain image

Stress-strain images will be discussed in this section from the natural deformed layers and the experimental results.

First, the buckling fold is considered. The stress distribution of the free-layer-fold-model is analyzed by Sanford (1959).

According to his paper, the tangential stress is tension stress in the crest, and it shows the maximum value in the core part. But the shear stress parallel to the layer shows the maximum value at the inflection points. DIETERICH and CARTER (1969), and SHIMAMOTO and HARA (1976) analyzed the single layer fold model by using finite element method. It is interesting in their works that the pattern of the minimum principal stress near the crest of anticline shows concave, though the external force is horizontal and that the minimum principal stress is mostly compressive.

Second, the stress and strain pattern of the bending fold is considered. IKEDA and SHIMAMOTO (1974) described the stress pattern for bending experiments. They concluded that the maximum compressive stress is the vertical to the layer in the crest of the anticline, but not true in the inner arc. That is, the maximum principal stress is horizontal to the layer in the inner arc and it disappear as the layer shortening increases. In the following sentenses, we consider the expected minor structures from these facts described above. For the buckling fold, normal faults and tension joints are formed in the crest of anticline and reverse faults and minor folds develope in the core and/or in inflection points when the competency contrast is high.

Minor structures formed by compressive stress generally develope in the whole area but a little in the crest of anticline when the competency contrast is low, because the compressive stress parallel to the layer is dominant only in the initial stage of major folding, the formation of minor folds are restricted in the initial stage. This fact is also supported by Hudleston's experiments (1973).

On the other hand, in the bending folds, some minor folds develope in the core of syncline as the deformation comes weaker in the outer arc.

4.2 Analysis of major folds

The morphological parameters of folds are important, because they show the deformation rate of folds. They are amplitude and distance between fold axes. Because of showing the mechanism of folding, they have characteristic spatial distributions. Therefore, it may be possible to discuss the mechanism of folding from these parameters.

4.2.1 The ratio of (maximum) amplitude to the distance between axes (half wavelength)

The vertical changes of this ratio of the Komiji Syncline and the Noma Anticline are shown in Figure 31. It is clear that the ratio is maximum at the boundary between the Aoki and the Bessho Formations (at the Kido Member which is composed of sandstone and conglomerate), and at the Ogawa and the Susobana Formations. The horizontal change of this ratio of the Aoki and the Bessho Formations in cross sections 6, 7 and 8 are shown in Figure 32. The ratio is larger from the east to the west. And the ratio is larger distinctly to the west of the Aida Syncline.

This fact suggests that the origin of folds located in the west of the Matsumoto—Nagano Line is different from that in the east of the line.

4.2.2 Mean shortening

It is difficult to draw the exact profile for major folds, therefore, mean shortening can not be shown exactly. But the limbs of folds in the studied area are comperatively straight and mean shortening values can be got roughly. Mean shortening of the Komiji Syncline and the Noma Anticline is shown in Figure 31. This value reaches the maximum at the Kido Member which is the lowest member in the Aoki Formation and at the Ogawa and the Susobana Formations as same as the case of the amplitude-half wavelength ratio.

4.2.3 Dips of limbs

Dip variations on the route which is perpendicular to the fold axes are shown in Figures 33, 34, 35

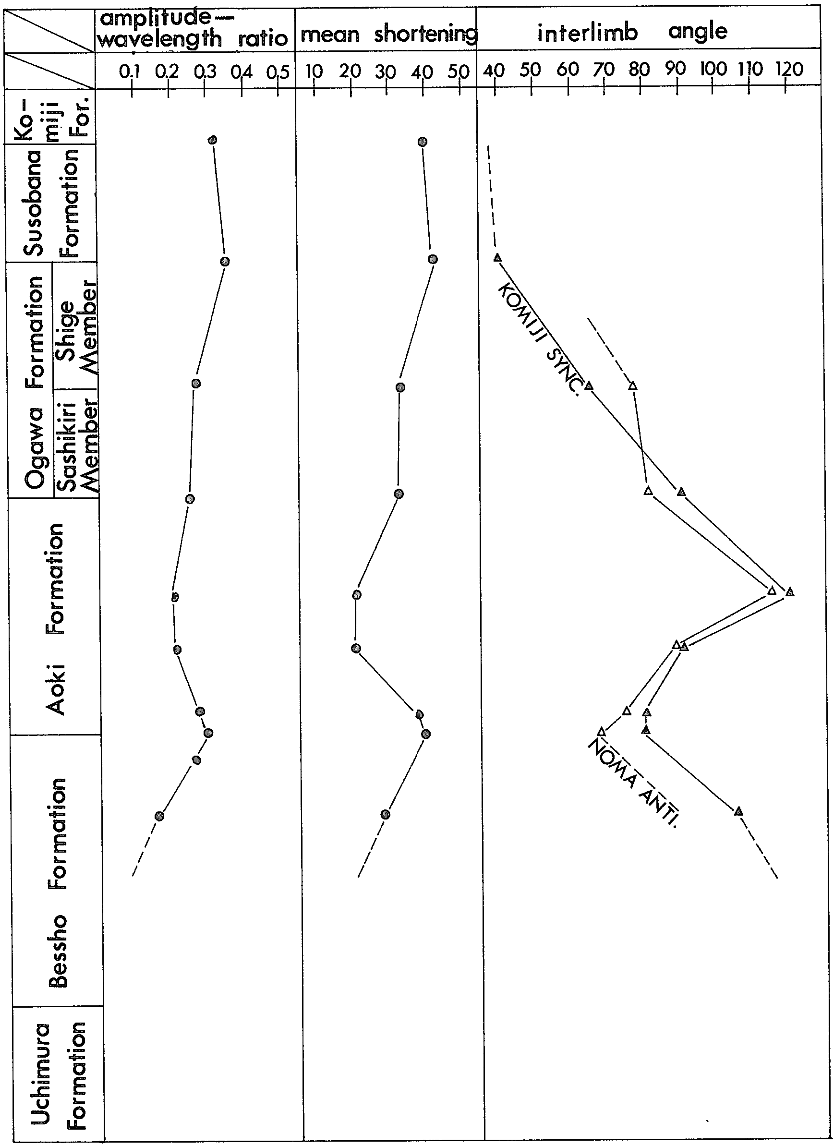

Fig. 31 The distribution of the amplitude-half wavelength ratio, mean shortening and interlimb angle of the Komiji Syncline and the Noma Anticline.

and 36. Though dips on the same tectonic level are not always plotted, the difference of heights along the route is as little as ignored. Dips of limbs of the Komiji Syncline are shown in Figure 33. Dip variation of the Komiji Syncline along Omi River is shown in Figure 33(A). Dips of the west limb are very steep or near vertical and partly overturned. Dips of the east limb are more gentle than those of the west limb, but more than 50 degrees. Dips of limbs of the Komiji Syncline in Ikezawa Route are shown in Figure 33(B).

The east limb is more gentle than the west limb in the case of (A) of Figure 33, and comes to be gentle rapidly. Figure 33(C) shows dips in Hakuba Route and it shows the same tendency as the

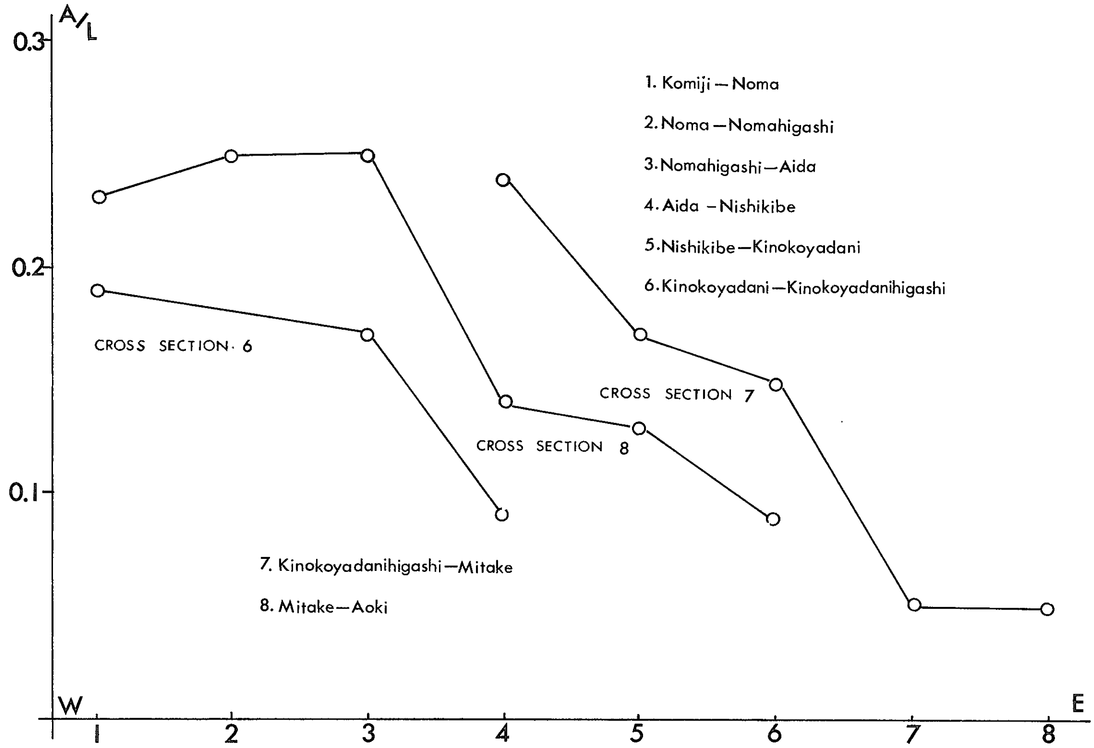

Fig. 32 The horizontal change of the amplitude-half wavelength ratio in the cross section 6, 7 and 8 shown in Fig. 40.

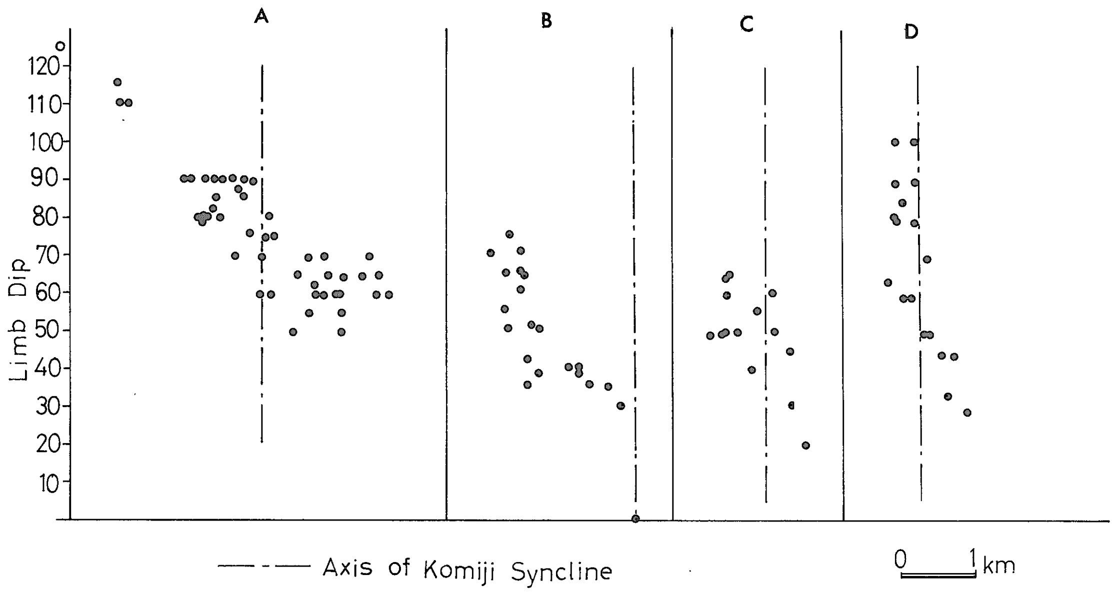

A: dips along Omi River, B: dips on the Ikezawa route, C: dips on the Hakuba route, D: dips on the Ōguchizawa route.

Fig. 33 Dip variation of the Komiji Syncline.

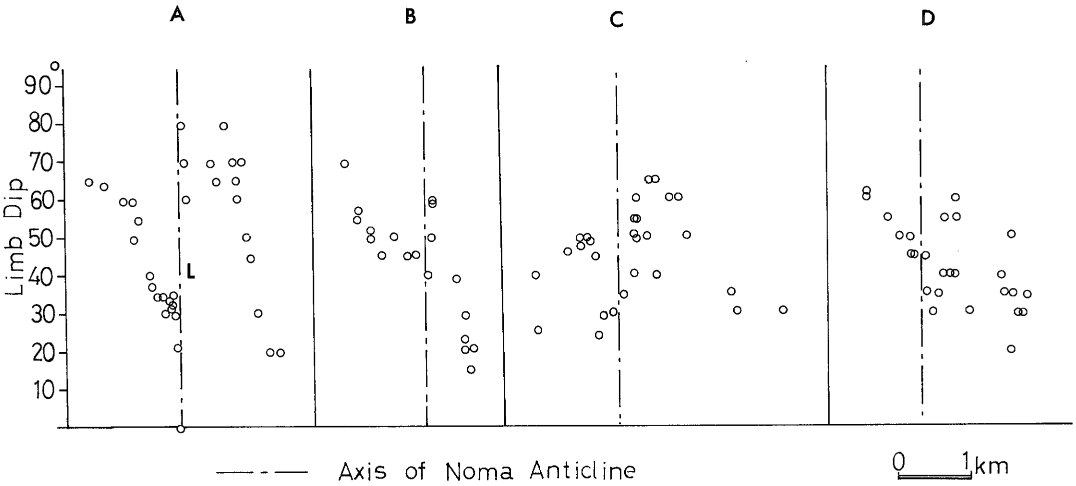

A: dips on the Noma Village Road, B: dips along Omi River, C: dips on the route across Yagoshi and Matsutome, D: dips along Aida River.

Fig. 34 Dip variation of the Noma Anticline.

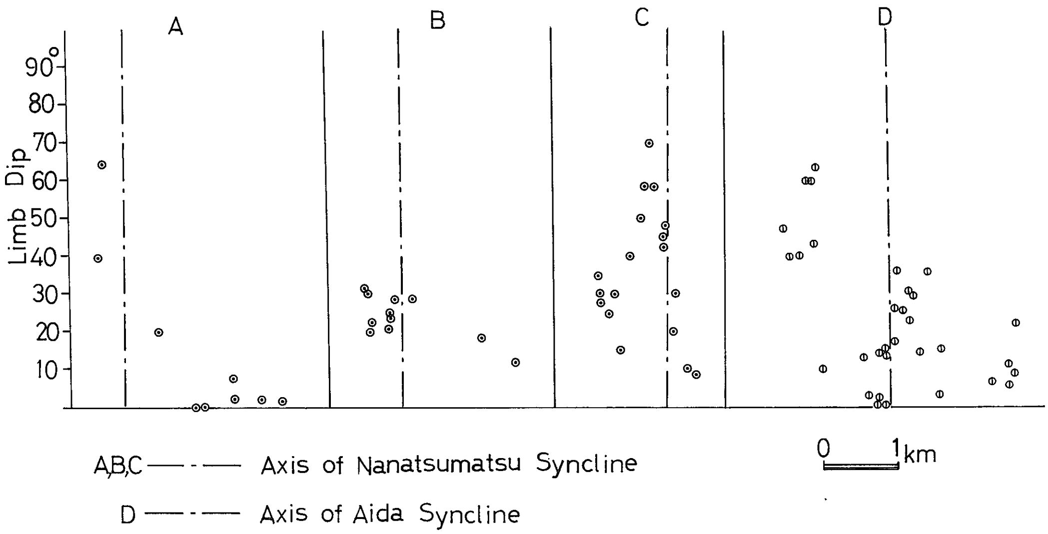

A: dips at Katsura, B: dips along Omi River, C: dips on the route from Nishijō to Bessho, D: dips on the route across Iwaidō.

Fig. 35 Dip variation of the Nanatsumatsu Syncline and/or the Aida Syncline.

case of (B). Figure 33(D) shows dips in Ōguchizawa Route. The west limb dips steeply and is partly overturned but the east limb is more gentle than the west one. Figure 33(A) and (D) show dips in sandstone and conglomerate rocks. Figure 33(B) and (C) show dips in sandy shale and alternation of sandstone and sandy shale. Dips of limbs of the Noma Anticline are shown in Figure 34. Figure 34(A) shows the variation of dips in the route across Noma Village. Dips of the west limb come to be gentle toward the axis and to be horizontal in the axial part. The east limb dips steeply near the axial part but comes to be gentle rapidly toward the east. Figure 34(B) shows dips along Omi

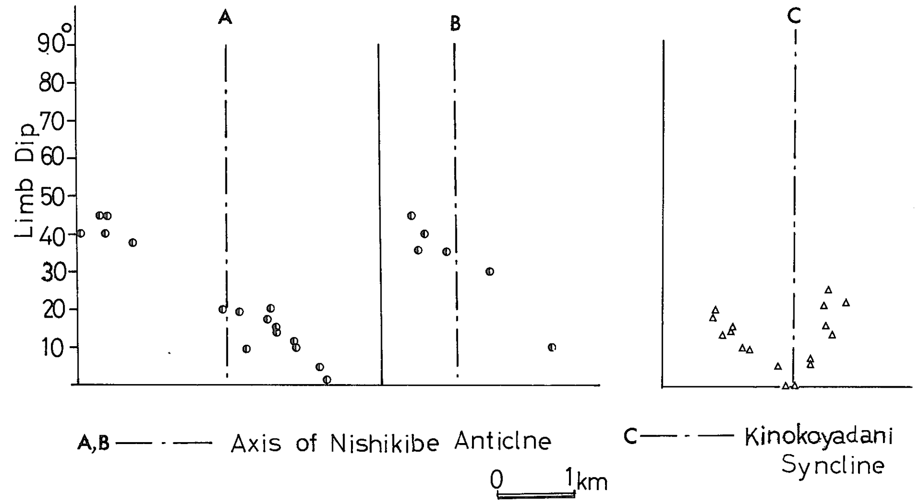

A: dips on the route across Yakyū, B: dips on the route across Minakami,
C: dips on the route to the east of Yakyū.

Fig. 36 Dip variation of the Nishikibe Anticline and/or the Kinokoyadani Syncline.

River. Dips of the east and west limbs come to be gentle to the east. Figure 34(C) shows dips in the route across Yagoshi and Matsutome. The west limb does not show the uniform change in dips and either limb is gentle toward the east. Figure 34(D) shows dips along Aida River. The west limb comes to be gentle to the axis but the east limb is not clear because of development of minor folds. Figure 35(A), (B) and (C) show dips in the Nanatsumatsu Syncline and (D) shows dips in the Aida Syncline.

Figure 35(A) shows dips near Katsura in the Ogawa Formation and the west limb is steeper than the east limb and comes to be steeper to the axis of the Nanatsumatsu Syncline. Figure 35(B) shows dips in the Aoki Formation along Omi River, and the west limb is steeper a little than the east one. Figure 35(C) shows dips in the Ogawa Formation in the route from Nishijō to Bessho and their variation of dips is similar to the case of (A) of Figure 35. Figure 35(D) shows dips in the route across Iwaido in the Aida Syncline. The west limb comes to be gentle to the axis, and the east limb comes to be gentle to the east. Figure 36(A) shows dips in the route across Yakyu, and Figure 36(B) shows dips in the route across Minakami in the Nishikibe Anticline. The west limb is steeper than the east one, and comes to be gentle to the axis. The east limb comes to be gentle to the east. It may be summarized about dips as follows.

The west limb of each folds comes to be gentle to the axis except the west limb of the Komiji Syncline and the Nanatsumatsu Syncline which are located on the changing parts of lithofacies, thickness and various minor structures. Dips of the west limb come to be the steepest in competent layers like sandstone and conglomerate rocks as shown in Figure 33(A), (D), and Figure 35(A), (C). The east limb comes to be gentle to the east.

4.2.4 Interlimb angle

Interlimb angles which are calculated from dip variations described above of the Komiji Syncline and the Noma Anticline are shown in Figure 31. It is remarkable that the interlimb angle shows the maximum value in the Aoki Formation and the Bessho Formation which are thought to be in-

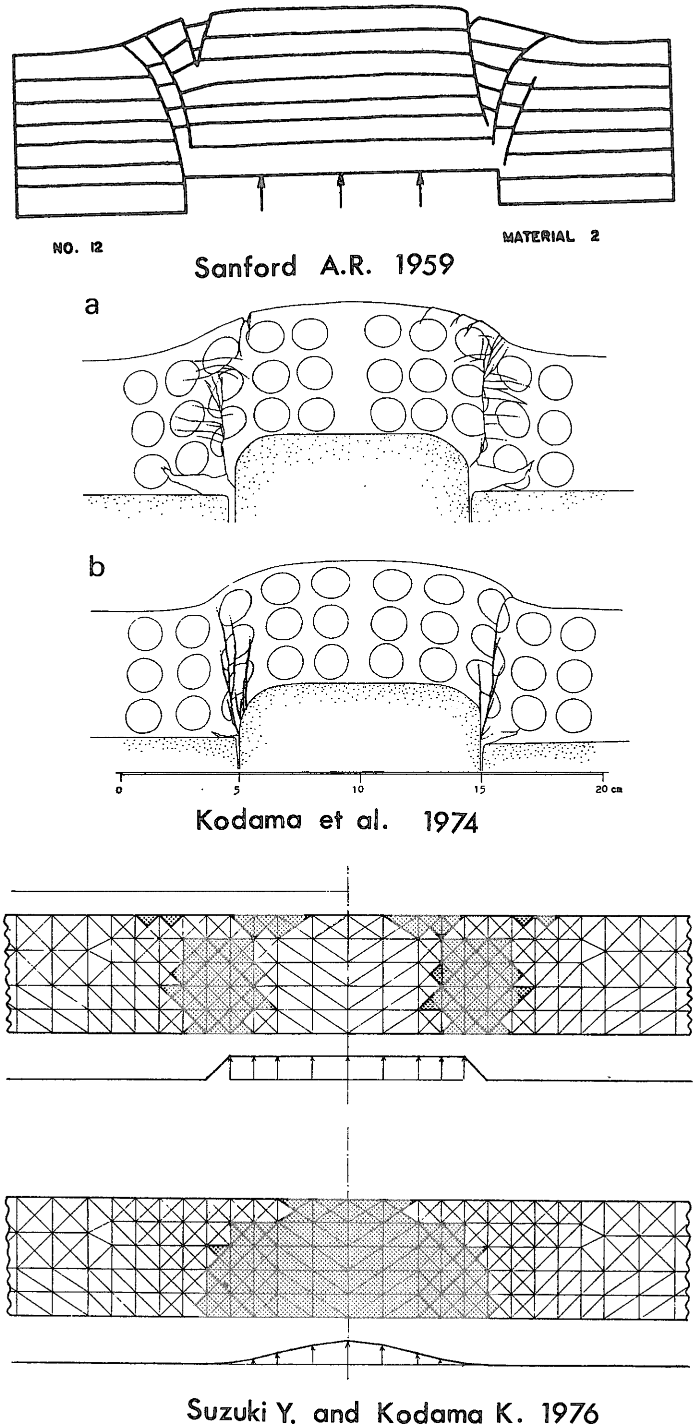

Fig. 37 Some experiments of bending by SANFORD (1959), KODAMA *et al.* (1974), and SUZUKI and KODAMA (1976).

competent from their lithofacies. But interlimb angle shows the minimum value in the Ogawa Formation and the Susobana Formation, and the Kido Member of the lowest member of the Aoki Formation. All of them are thought to be competent.

4.3 Analysis of minor structures

4.3.1 Analysis of clastic dikes

The formation of clastic dikes developing in the studied area is affected by the movement of the basement, and is not always related to the major folding, judging from its mechanism of the formation, and their distribution as described later. But the formation of them are important on the estimation of initial conditions of the tectonic system including major folding. The author wants to explain the following three facts about clastic dikes. First, the origin (or the mechanism) of the fractures of clastic dikes. Second, the mechanism of emplacement of the dike material (source of the dike material). Third, the age of the formation of the dikes. KUTSUZAWA and FUJITA (1967) analyzed clastic dikes developed in the upper Miocene Formation which are distributed in the westward of Sendai City in Miyagi Prefecture. They proposed that clastic dikes are classified into two types, they are tension clastic dikes and shear clastic dikes. Clastic dikes in the studied area are also classified into two types. Type 1 is nearly vertical to the layer, and trends in mostly one direction or partly two directions which are perpendicular to each other. The layers of both sides of clastic dikes do not show any dislocation. Therefore, these clastic dikes are inferred to be made as the tension fractures, that is, they are tension clastic dikes. These clastic dikes develope in the upper part of the Bessho Formation and in the lower part of the Aoki Formation. They distribute in the horizontal direction in the area where dips of surrounding layers change remarkably, in other words, in the shoulder of uplifting blocks such as the Saigawa Crushed Zone and the Chūō Uplifting Zone (Fig. 21). Such distribution of tension clastic dikes as described above provides the features of uplifting basal blocks which are the causes of their formation. According to many experimental works such as HAFNER (1951), SANFORD (1950), KINUGASA (1974), KODAMA (1974), and SUZUKI and KODAMA (1976) as shown in Figure 37, tension fractures and normal faults occur on the crest of the surface and enlarge their distribution to the surrounding area when the sinusoidal displacement is given at the lower boundary of the layer. On the other hand, tension fractures or plastic area occur at the shoulders

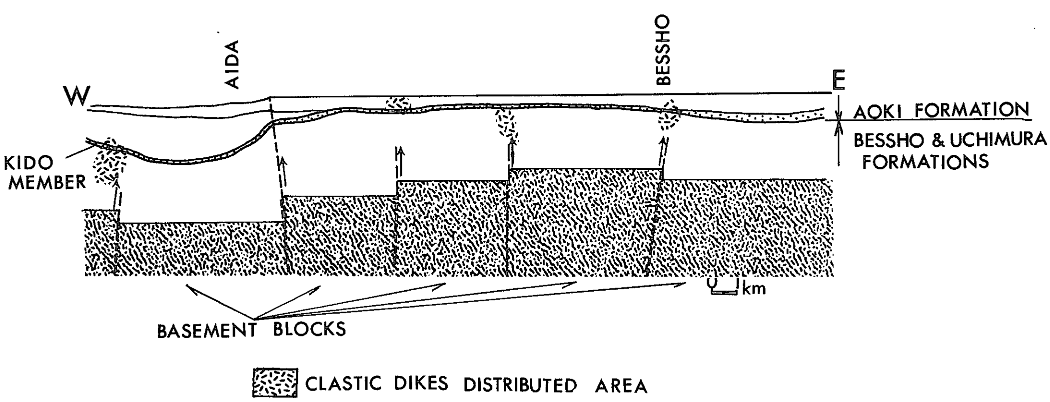

Fig. 38 The idealized distribution of the clastic dikes and basement blocks.

of uplifting blocks and enlarge their distribution to the lower part when the step displacement is given at the lower boundary of the layer. Though the uplifting movement of the basal block was not always one direction and neither one time exactly, they were formed when the Saigawa Crushed Zone and Chūō Uplifting Zone uplifted (Fig. 38). As some clastic dikes of Type 1 are interrupted by the upper sandstone layers and some have laminations being parallel to the walls of dikes, dike material is considered to be injected forcefully from the lower layers. Because some kinds of flow structures are found in clastic dikes, and dikes are formed during the time of sedimentation, and under the conditions of low temperature and of low pressure, clastic materials must contain the water in order to let them flow. The age of the formation of Type 1 clastic dikes are nearly the same as the time of the sedimentation of layers as described above, and furthermore, the coexistence of clastic dikes and various slumping structures supports this idea. Therefore, the age of their formation is from the deposition of the upper part of the Bessho Formation to that of the lower part of the Aoki Formation. Clastic dikes of Type 2 seem to be also tension clastic dikes as they have no dislocation in the both sides of dikes. As some clastic dikes of Type 2 are interrupted by the lower sandstone layers, their dike material is considered to be injected from the upper layers forcefully.

4.3.2 Analysis of minor folds

(1) The mechanism of minor folds

Tectonic minor folds in the studied area are considered to be buckling folds from the following reasons.

Minor folds do not develope in massive, thick, non-bedded, and uniform sandstone, coglomerate and sandy shale, in other words, they exist only in the alternation of sandstone and sandy shale or a single sandstone layer and a single conglomerate layer enclosed in sandy shale, which have the anisotropy in sequences due to layering.

Minor folds come to be indistinct rapidly towards the upper and lower layers as shown in Figure 28.

Wave shapes of minor folds at each layer are not always harmonic.

Minor folds are not drag folds judging from their features and distributions.

(2) The possibility of minor folding associated with major bending fold

The shortening area of the secondary origin which resulted from the uplifting movement of basal blocks develope in the tectonic systems of bending folding. In such shortening area, minor buckling folds may develope, and some minor folds in the studied area may have been formed in this way. Ikeda and Shimamoto (1975) examined some numerical experiments that the Newtonian layer is bended by the sinusoidal displacements affected to the lower boundary. They concluded that the layer shortening do not exceed 20%, and that remarkable buckling folds can not develope.

But only very gentle small folds expected to be formed under this shortening value. The author had some experiments about the minor folding with the rotation of major fold's limbs in order to study the origin of minor folds. Elastic models, which were made from silicon rubber sheets and gelatin-water mixture, were used in order to know the stress-strain distribution and minor deformations. Silicon rubber sheets play the role of the competent layer, and the gelatin-water mixture play that of the incompetent layer, respectively. The weight ratio gelatin to water is 1 : 7, and the thickness of silicon rubber sheets are 0.5 mm and 1.0 mm. The detailed procedure has already been reported (Kato, 1973). The strain character of the bending fold is shown by the orientation of long axes of strain elipsoids in Figure 39.

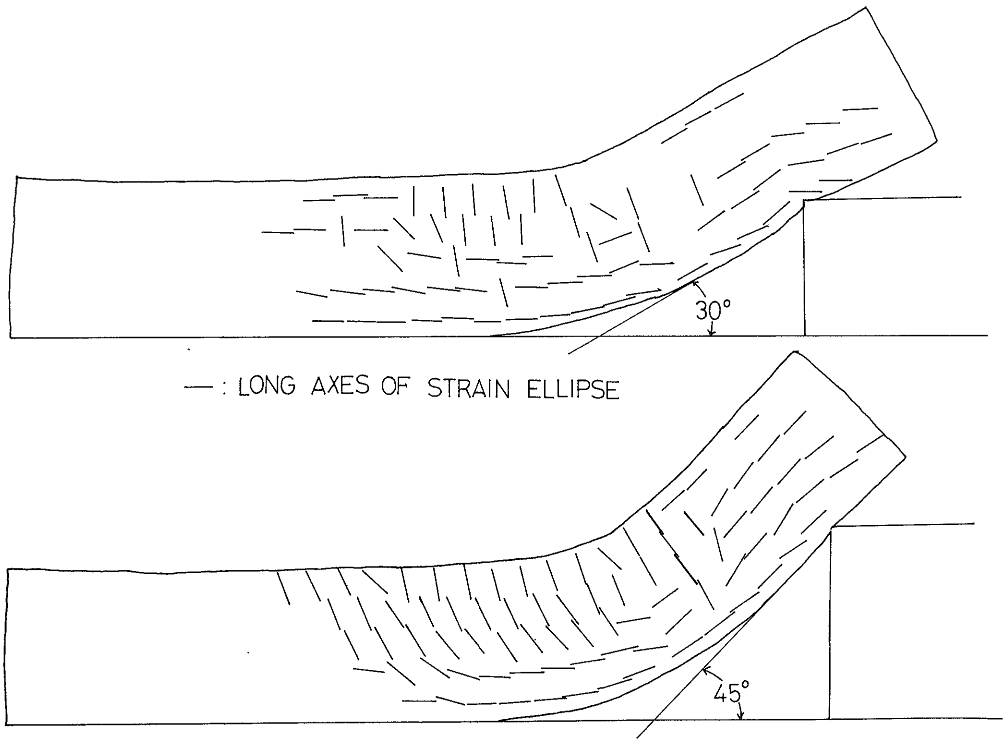

Fig. 39 The strain distribution in the bending layer of gelatin-water mixture.

The long axes of strain elipsoids tend to be perpendicular to the layer toward the inner arc of the layer and their orientation are stronger as the layer is bent progressively. Then the minor folds are expected to develope in the inner arc of the major folds.

In the No. 721 experiment of Figure 40, the thicknesses of two silicon rubber sheets are equal with each other, that is 0.5 mm.

The inner sheet buckles at the central part of the layer, where the curvature is maximum, and those minor buckle folds propagate toward the both ends of the sheet. But outer sheet do not buckle in this experiment. In 701 experiment, the inner sheet is thicker than the outer one, that is, the thickness of the inner sheet is 1.0 mm and that of the outer one is 0.5 mm. The inner sheet is thinner than the outer one in No. 711 experiment, that is the thickness of the inner sheet is 0.5 mm and that of the outer one is 1.0 mm. Though the strain distributions of these two models are very similar, minor folds develope only in the inner sheet of No. 711 experiment. These results of the experiments suggest that minor buckle folds made by these mechanism develope ralely. Even if it is possible to be formed minor folds by this mechanism in nature, such minor folds develope only in the core near the axial part when the limbs of major folds rotated highly. The wide distribution of the minor folds in the studied area as shown in Figure 7 can not be explained by this mechanism, and therefore they should have formed by the buckling process firstly explained in this chapter.

(3) The age of minor folding

JOHNSON and HONEA (1975) examined buckling experiments by using the elastic models which are composed of four photoelastic rubber sheets and gelatin layers. In their models, four sheets are set

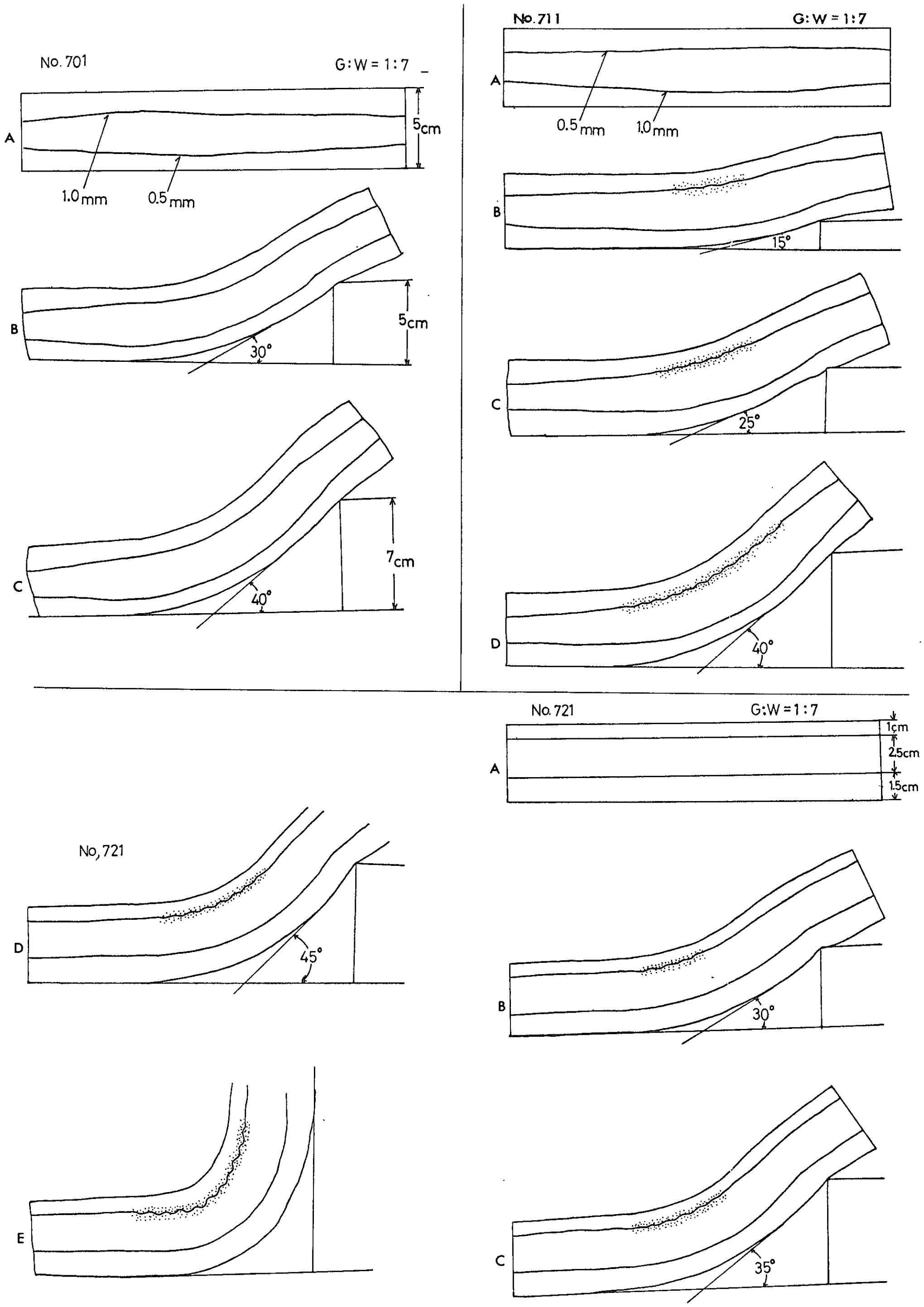

Fig. 40 Some model experiments using silicon rubber sheet and gelatin-water mixture, which show the initiation and propagation of small folds associated to the major bending folding.

to be parallel at intervals of 5 cm. The thickness of the sheets are 5, 2.5, 1.9 and 3.8 cm. When this stack is compressed laterally, the thinnest rubber sheet begins to buckle at first, but the thickest rubber sheet do not buckle even when the layer parallel compression become to be very large. The author tried the similar experiments by using silicon rubber sheets and gelatin-water mixture, and got the same result that the thinner competent layer began to buckle at first (Kato, 1975). After all, in the multi-layered buckling folds, the thinnest layer begins to buckle at first with the smallest wavelength, and the thicker layers begin to buckle later with larger wavelengths. Therefore, minor folds whose competent layers are thinner than those of major folds began to buckle a little faster than major folding. From their experiments, the author believes that minor folds in the studied area are formed in the middle and/or upper Miocene.

5. Discussions

5.1 Effects of initial irregularities of bedding on fold initiation and propagation

It will be considered in this chapter that the initial irregularities control the fold initiation, that is, the location of the anticline and/or syncline, and fold propagation. It is generally assumed in the most of theories and experiments about the buckling that there is infinite dimension horizontally or much larger dimension laterally than the expected wavelengths and that the layer is initially flat. Under the above assumptions, symmetrical and periodical waves develope continuously in the horizontal direction, when the sinusoidal distribution of the stress is given to the lower boundary of the system. But this fact has not always accordance to the field observations. Because the thickness of each layer or each formation is not always constant as shown in Figures 3 and 4, and there are initial deflections which are estimated from the distribution of many slumping structures. And natural folds disappear laterally with one or two wavelengths even if they are not cut by faults.

Johnson (1969) explained this fact with following three reasons.

(1) High angle faults (Hetenyi, 1946; Biot, 1968).

(2) Thrust made by salt dome or intrusive body (Willis, 1894, Henteny, 1946).

(3) The layer is not flat in the beginning of folding.

Willis (1894) found that the initial dips of bedding planes of a sequence being folded can control the position and the relative growths of folds from his experiments. Cobbold (1975) investigated the fold initiation and propagation in his experiments by using paraffin wax which is given bell-shaped initial disturbance. From his experiments, waves become to be regular when the shortening is more than 15% when the viscosity ratio is 10. From Skjernac (1975), regular waves do not develope when the shortening is 17% in her viscous buckle experiments by using patty and plasticene. Such worse periodicity of folds described above is considered to be resulted from the following natural conditions;

5.1.1 Irregularities in sedimentary rocks

Cobbold (1975) pointed out that there are sedimentary lense and nodule as geologic initial deflections. These irregularities are enough to initiate minor folds of which wavelengths are smaller than a few meters. Except such lense and nodule, initial disturbances of layering such as some kinds of slumping structures are also considered.

5.1.2 Non-tectonic depression and/or culmination (raised part) during deposition

The Noma Anticline accompanied with minor folds is the typical example of this as shown in Figure 9. Directions of dips of these folds accord mostly with those of the forset beds of cross beddings.

As direction of the maximum dip of the forset bed shows the current direction at deposition, their direction points out that there are some non-tectonic depression and/or the raised part near the axial parts of these folds. In other words, irregularities of beds as initial deflections at deposition may control the deposition of folds (not only major folds but minor folds). Furthermore, as the distribution of cross beddings accords with that of minor folds, these initial irregularities may control the developement of minor folds (especially their propagation to the axial direction). ITO (1976) reported the same initiation about the Nanakura Anticline near Futatsui in Akita Prefecture. He pointed out that the axis of the anticline accords to the line of the maximum uplifting of the base which is deduced from the distribution of cross beddings and the change of the lithofacies.

5.1.3 The thickness change of layers

The thickness change of limbs of the Nishikibe Anticline in the Bessho Formation is the typical example of this as shown in Figure 4. The similar change of thickness are also observed in the Aoki Formation, especially in the Kido Member, which is the lowest part of the Aoki Formation, as described in the previous section. KAWAUCHI (1973) and KASAHARA (1973) reported that thickness of the Ogawa Formation and the Aoki Formation are the thinnest at the axial part of the Noma Anticline and that the thickness of the west limb is much thicker than that of the east one. The author's study supports their thoughts that the change of the thickness locates near the folding axis. The similar situations exist in many cases, for example, the Aida Syncline and the Komiji Syncline as shown in Figure 41. Furthermore, the lithofacies and the thickness of each strata change near theaxial part, especially in the Aoki Formation.

TAKEUCHI and SAKAMOTO (1976) also reported that the thickness of the Aoki Formation in the west limb of the Saigawa Anticline which was namely the Nodaira Anticline, was five times as thick as that of the east limb. The thickness of the east limb is also different from that of the west one in the Takafu Syncline and in the Hikage Anticline in the northern Fossa Magna. The hinges of major folds distribute in the studied area locate at the place where the thickness and lithofacies of not only formations but each single layer change. This fact means that folds initiate at the boundary of the differential depression, and initial wavelengths are controled by initial irregularities at the beginning of folding. Therefore, under Willis's conditions, much deformed folds can develope even when the mean shortening of the system is a little (less than 10%).

5.2 The mechanism of major folds

Four ideas have been proposed about the folding mechanism in the northern Fossa Magna area, they are;

(1) Simple buckling folds by the lateral compression from the northwest or the west of the Itoigawa—Shizuoka Tectonic Line.

TOMIZAWA (1953) surveyed the Nishikyo-Kamikusugawa Anticline along Susobana River in the westward of Nagano City. He was of the opinion that the fold is caused by the shear stress which points to the southwest from the northeast. He gave evidences that the fold have the asymmetrical and inclinated feature, the east limb is very steep, partly overturned whereas the west one is gentle, and that the vertical fault with crushed zone in the axial part is transformed to the thrust. He also reported the same feature about the Saigawa Anticline in the midstream drainage basin of Sai River. Tomizawa's model is that the horizontal layers in the initial stage of folding by the lateral compression from the northwest. He can not explain, however, that the thicker limb is steeper than the thinner one, and the origin of the external force which caused the large shortening (30–40%) and the compatibility of the strain in this area. Suzuki (1974) denied such lateral compression from the west and from the east as the main cause of folding. He pointed out that the geologic structures of Tertiary formations in the area between Ōmachi City and Lake Aoki are gentle and those trends are perpendicular or oblique to the trend of the northern Fossa Magna, and that half dome and basin structures trend to the north from the south.

(2) The bending folds (or the block folding) of cover layers by the differential block movements of the basement.

SUZUKI (1974) said that folds in this area are combshaped folds belonging to the intermittent fold classified by BELOUSSOV (1954). His explanation about the folding mechanism in this area is that the basement is broken into several blocks and that these blocks moved up or down each other. He considered that the horizontal beds at sedimentation are lengthened when the blocks moved down and they have to be folded when the blocks moved up. He suggested that the mudstone of the Bessho Formation can inject into the stress concentrated parts near the boundaries of these blocks.

He gave evidences that, after the deposition of the Ogawa Formation in the western area of the Saigawa Anticline had to move down more than the eastern area of it, but the present distribution of beds shows the final down movement of the eastern area and that the Saigawa Anticline locates in such hinge parts of differential up or down movement. According to SAKAI *et al.* (1976), numerical experiments by using finite element method shows that folds develope in the boundary between the mobile basement and the fixed one. However, such folds are very gentle and thier features are sinusoidal. Therefore, their results do not agree to the mechanism of natural folds even though each parameters of experiments are changed. Suzuki's idea is geologically weak because the differential movement of basements begins from the deposition at stage of the Aoki Formation at least, and because the correlation of the Ogawa Formation in different basins, that is in Takafu and Komiji Basins is not always sufficient. And all minor folds are not always made by the injection of mudstone resulted from the up or down movements of the basements as Suzuki says. On the contrary, most of minor folds are related to the major folding as described in the previous section. But his suggestion is partly correct, that is, the hinges of folds locate at the changing points of the thickness caused by the differential deposition before folding.

(3) A kind of the drag folds associated with wrench faults.

KOMATSU (1967) showed the geometrical illustration about the pattern of compressional forces which are perpendicular to the fold axes, and he suggested that this pattern accorded with the stress pattern of wrench faults. According FUJITA (1975), along the Itoigawa—Shizuoka Tectonic Line, the folding axes are parallel to this line and they are oblique to it in the Niigata Area. Their axes pattern reflects the axis of sedimentary basins, but tectonic movements. MOODY and HILL (1956) suggest the secondary stress field associated with the major primary fault, and that in such stress field, a kind of drag folds by wrench faults may be possible to be formed. However, even if their idea is correct, only one or two wavelengths folds can be formed by such mechanism.

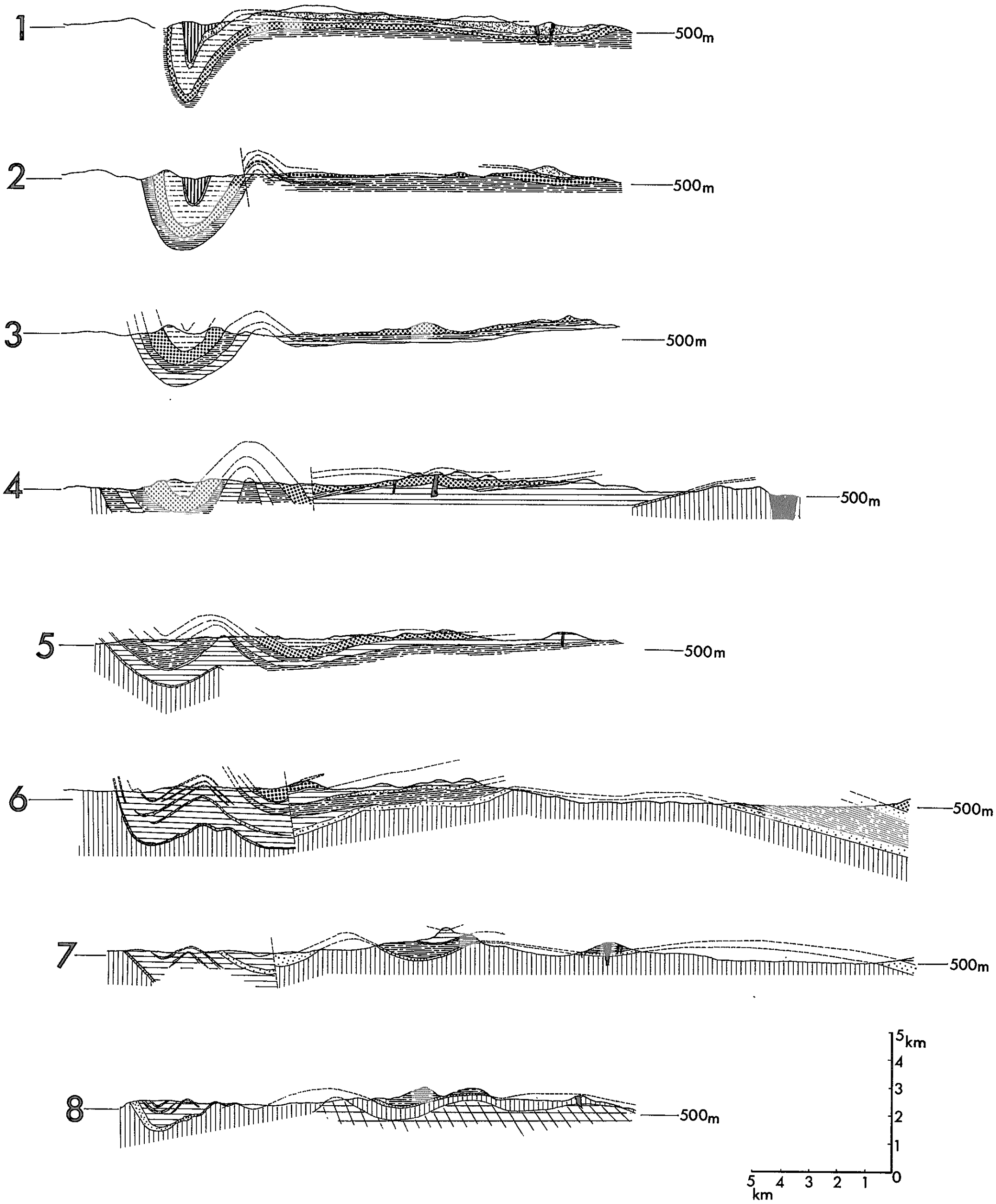

Fig. 41 Cross sections.

Well-developed folds in the northern Fossa Magna can not be explained by such mechanism quantitatively.

(4) A kind of the buckling fold by the compression oblique to the layering which is related for the inclined basement.

Uemura (1971) considered that overturned folds in Mt. Kushigata in the northern Niigata Prefecture were formed by tilting rotation.

He suggested that it was possible to interpret most ploblems of folding mechanism at the uplifting or sinking by tilting of the basement under the lateral compression. The author supports this idea principally, but on many problems such as the condition of lateral compression, natural evidences are still required.

The mechanism of these folds in the studied area is that the cover sediments which have initial wavy forms controled by the differential sinking movements of the basement at their depositional stage, is buckled and amplified by the secondary lateral compression due to the uplifting of the Saigawa Crushed Zone and the Central Zone of Uplifting (Chūō Uplifting Zone). Initial deflections such as the difference of the thickness and/or the surface irreguralities of the basement are acted as triggers of folding.

The cause of external force is the tilting of the basal blocks and it moves from the south to the north. The reasons as described above will be sumarized as follows.

(1) In the buckling folds, the amplitude-wavelength ratio and the mean shortening are expected to show the maximum value at the stratigraphic level of the competent layer within the stratigraphic sections and interlimb angle shows the minimum value at its level as shown in Figure 30. In the bending folds, the amplitude-wavelength ratio and the mean shortening are expected to be smaller and interlimb angle is larger toward the upper level as shown in Figure 29. In the Komiji Syncline and the Noma Anticline, the amplitude-wavelength ratio and the mean shortening have the maximum value, and the interlimb angle has the minimum value at the Ogawa and the Susobana Formations and at the Kido Member. These members are judged to be competent layers or competent units from their lithological facies.

Therefore, those morphological characters are to be consistent with those of buckling folds.

(2) According to the numerical experiments of bending folds by IKEDA and SHIMAMOTO (1974), the maximum compressive stress is vertical stress in the crest of the anticline, and nearly horizontal in the core of the anticline. But the distribution of the such horizontal compression is restricted and it disappears as the increase of the shortening. In the inner arcs of the Noma Anticline minor folds by buckling well-develope in spite of large shortening. Therefore, its stress-strain image is not that of bending folds but equal to that of buckling folds.

(3) In the west limb of the Komiji Syncline, the axes of minor folds which developed in the Aoki Formation along Aida River are not concordant with those developed in the upper part of the Bessho Formation, and in the lower part of the Aoki Formation along the route of Nagamine. That is, in the cross section, synclinal axis locates under the anticlinal axis and such disharmonic waves coexist in the same multi-layered sequence. Such disharmonic waves can be shown when competent layers of which the thickness are different are isolated each other moderately, that is, the distance between competent layers are more than one expected wavelength and the multi-layered sequence compressed lateraly (RAMBERG and STEPHANSSON, 1964; HARA, 1967; RAMBERG and STROMGRAID, 1971; KATO, 1975). Such disharmonic waves mean to be made by layer-parallel compression. In major folding area, well-developed minor folds indicate the dominated lateral compression at the time of minor folding at least. In other words, the minor folding area is the compression area. This idea supports that major folds are buckling folds.

(4) Slickensides like slips observed in the massive sandstone and conglomerate rocks of the Ogawa

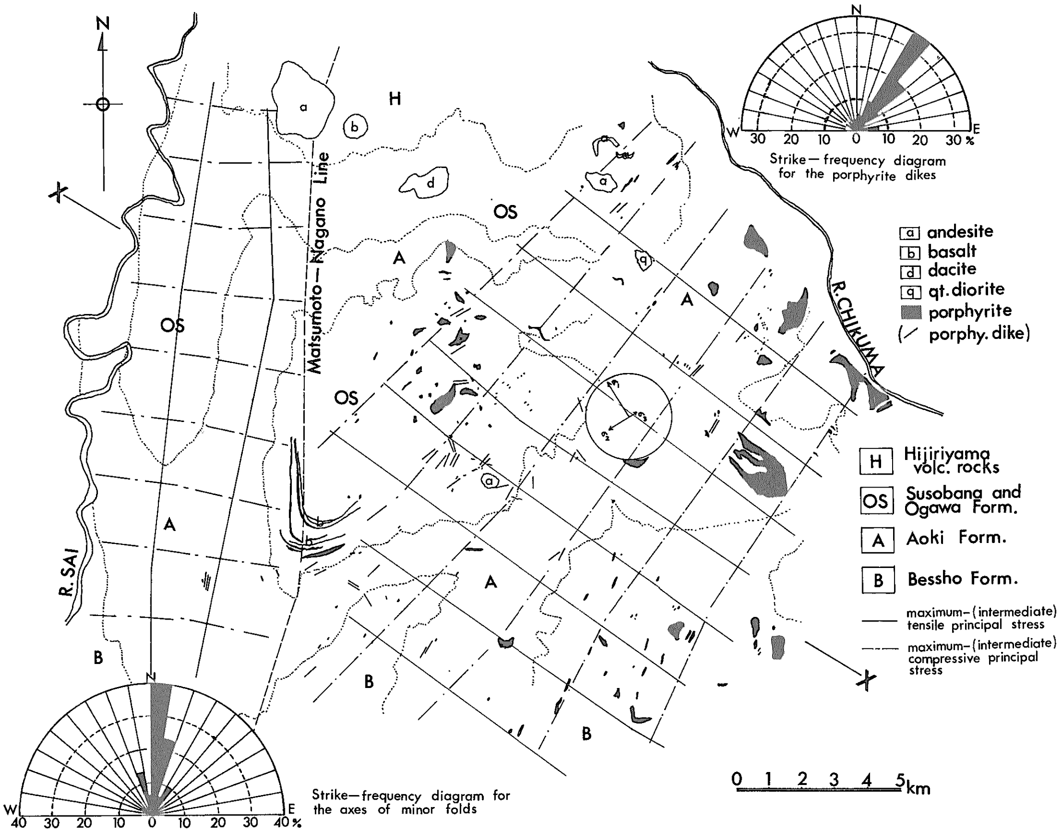

Fig. 42 The tectonic stress field in the studied area.

Formation along Omi River are flexural ones accompanied with folding as suggested by MIZUNO (1976). These slips are apt to be made in buckling process.

(5) If the Komiji Syncline and the Noma Anticline are buckled folds formed by the lateral compression, the tensional movements must be dominant in the outer area. The fact that minor reverse faults are restricted in the folding area satisfies at least the strain compatibility condition.

It will be considered the tectonic stress field in the studied area. The histogram of the axes trends of minor folds in the studied area in the west of the Matsumoto—Nagano Line is shown in Figure 42. Strike-frequency diagram for the axes of minor folds shows that the trends are mostly N–S, and that they are parallel to axes of major folds. When both major and minor folds are formed by buckling as described above, the plane made by the maximum tensile principal stress and the intermediate principal stress is parallel to the fold axes as shown by the solid line and the maximum compressive principal stress is perpendicular to them as shown by dotted line in Figure 42. This stress condition continued at least from middle Miocene to the uppermost Miocene. The histogram of strikes of porphyrite dikes distributed in the east of the Matsumoto—Nagano Line is also shown in Figure 42. They trend NE–SW. The plane made by the intermediate principal stress and the maximum compressive principal stress is parallel to the strike of dikes, and the maximum tensile principal stress is normal to them from the mechanism of the formation of volcanic dikes.

Though their intrusive stage is believed not to be only once, the stress condition described above

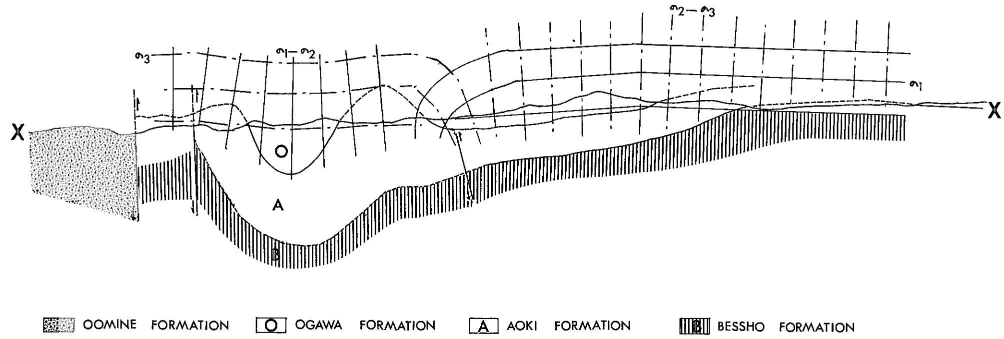

Fig. 43 The cross section of the tectonic stress field in the studied area.
shows the maximum tensile principal stress and/or the intermediate principal stress.
shows the maximum compressive principal stress and/or the intermediate principal stress.

continued at least from middle Miocene to upper Miocene as their strikes are constantly NE–SW. The stress condition derived from conjugate normal minor faults in this area is concordant with that from porphyrite dikes.

Figure 43 shows the cross section across the X-X in Figure 42.

The maximum compressive principal stress is horizontal in the folded area and the maximum tensile principal stress is horizontal in non-folded area. What condition does make this stress distribution possible? It will be discussed and compared with the result from numerical experiments by using finite element method and the result from geological investigation. The stress distribution in the cover layer when the block-shaped uplifting displacement is given at the basement, is got by using finite element method. In this numerical experiment by Kinugasa (1974), the following simulations are used. The experimental conditions are, nodal points of 172, cell numbers of 298, Young's modulus of 2.5×10^4 dyne/cm^2, density of 2.0 g/cm^3, Poisson's ratio of 0.5 and two dimension model of 3 km $\times$ 10 km.

Though Young's modulus is too smaller than the natural one, it is sufficient to show the stress distribution. The dotted line represents the tensile stress and the solid line shows the compressive stress, respectively (Fig. 44). This result is fairly concordant with taht of Figure 43. Therefore, at least, these folds can be interpreted to be buckling folds by the secondary lateral compression associated with the uplifting of basement blocks qualitatively. Though the quantitative investigation is very difficult at present time, it will be shown some possible interpretations as follows. In the western area of Chikuma River, the thickness of the Bessho Formation and the Aoki Formation, especially the Kido Member change remarkably along the Matsumoto—Nagano Line, and the axis of the Nishikibe Anticline (Figs. 4 and 7). The relations between the change in thickness and in axes of folds and the difference in thickness between both limbs are well known. It is also known that non-tectonic disturbance of the surface of the basement inferred from the cross bedding and other sedimentary structures acted as the trigger of folding initiation. These facts show that natural folds are not resulted from deformations of flat plates in the initial stage as most geologists assumed in their theoretical and experimental works, and that layers have initial deflections at the initiation. In the elastic model experiments (Kato, 1975), the initial wave occurs at the initial disturbance of silicon rubber sheet

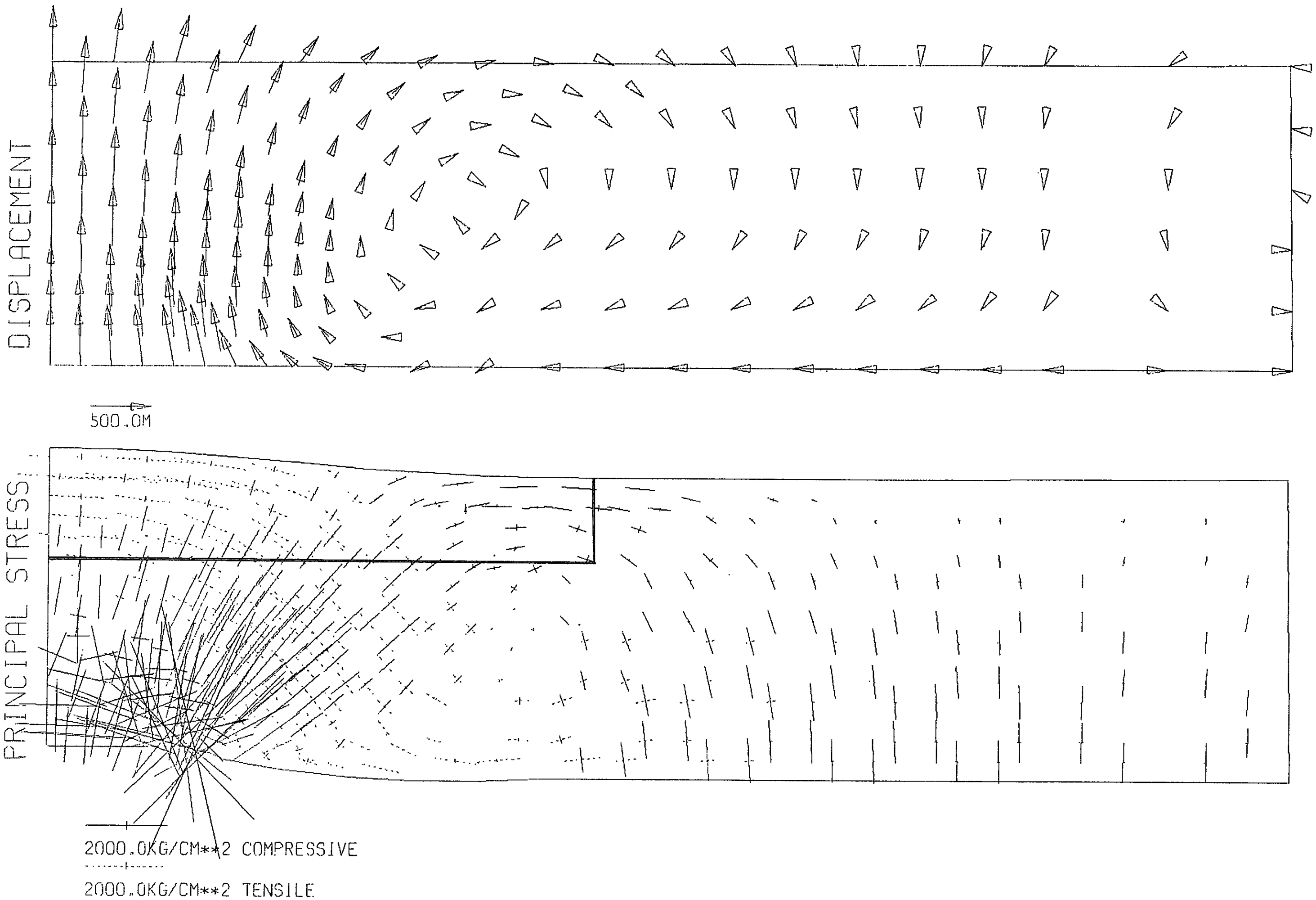

Fig. 44 An example of numerical experiment, which explains the stress distribution shown in Fig. 43 (After KINUGASA, 1974).

which is formed at the setting of the silicon rubber sheet into the gelatin matrix, and rapidly grows. The same fact has shown in Willis's and Cobbold's experiments as described previously. It is important in these experiments that large deformations are possible under the condition of small shortening (less than 10%), if layers have initial deflections. And such small lateral shortening may be possible by the causing uplift of basal blocks. Furthermore, by the Aida Fault and the Nanatsumatsu Fault, the eastern area of the Matsumoto—Nagano Line thrusts up to the west with high angles. This means that the western area (the folded area) is subjected to compression, and supports the idea described above.

5.3 Folding history

First, it will be considered about the pre-tectonic stage (that is, pre-folding stage), namely sedimentation of fold-forming strata and the features of sedimentary basins which controled the initial conditions of folding and the movements of the base.

The igneous activity of Greentuff volcanic rocks of the Uchimura Formation, which only distributed in the small part in the studied area, come to an end in middle Miocene and the maximum transgression of the sea which is represented by the sedimentation of the black shale of the Bessho Formation, began. The orientation of the sedimentary basin which controled the deposition of the Uchimura and the Bessho Formations is very important.

We have two different opinions for this. The one was proposed by Tomizawa (1953). He said that the boundary between the Uchimura and the Bessho Formations trends E–W and that its boundary is comparatively smooth, while the boundary between the Bessho and the Aoki Formations is much indented. The other opinion was proposed by Marui (1972) and/or Fujita (1973), and it is that the orientation of the basin trend N–S. Marui said that the Green tuff rocks are interfingered with the tuffaceous mudstone of the Uchimura Formation, that the sedimentary rocks dominates to the west, that the Bessho Formation increases its thickness to the west, and that folds in the Uchimura, Bessho and Aoki Formations plunge to N–E and do not affect the upper formation. Fujita said that folding axes trend N–S, that intrusive dikes trend N–S, too at the Green tuff movement, and that these facts suggest the orientation of fracturing at the initiation of the sedimentary basin. In order to determine the orientation of the basin, the isopack map must be drawn and compared with each distance from the thickest part, that is, the center of the basin to the margin of the basin.

Unfortunately, the Bessho Formation is mostly covered with the upper formations in the northern area. Therefore, the exact distribution of the thickness of the Bessho Formation in the northern area is not unknown to us, yet. In the E–W cross section in Figure 4, the thickness of the Bessho Formation decreases its thickness from Hofukuji to Chikuma River. In the N–S cross section in Figure 4, it increases its thickness to the south and near Matsushiro, that is, there are two basin centers.

This fact means that the relative uplift of the basement is at least more remarkable to the south, and that the sedimentary basin began to be differentiated by the uplifting belt which trends N–S, or NE–SW, at the time of the sedimentation of the Bessho Formation. This uplifting occured only in the local area and became to be remarkable at the later stage of the Bessho Formations sedimentation. This uplifting is a main factor caused clastic dikes and decided the shape of the uplifting basements looks like block. By this uplifting, a part of the area where the Bessho and the Uchimura Formations distributed turned to be the land and then was eroded. The evidences of this fact are that there are breccia and/or conglomerate of the Green tuff rocks derived from the Uchimura Formation, altered andesite, basalt and breccia of black shale derived from the Bessho Formation in the uppermost sandstone of the Bessho Formation and the Kido Member which is the basal part of the Aoki Formation. Furthermore, the igneous activity associated with this uplifting is known. Quartz-diorite gravels contained within the Kido Member are correlated to the quartz-diorite rocks in the Uchimura region according to IIJIMA and SAITO (1968). They considered that quartz-diorite had intruded before the sedimentation of the Aoki Formation with the uplifting area where the Green tuff distributed. KOBAYASHI *et al.* (1957) proposed "the Bessho Phase Movement". They considered that the most of porphyritic dikes penetrated into the Hongō Formation (a part of the Uchimura Formation) and the Bessho Formation during folding of the Nishikibe Anticline and so on, because these dikes concentrate in the axial areas of anticlines, and quartz-diorite intruded into there during the final stage of the sedimentation of the Bessho Formation in the process of the Green tuff movement from the reasons of the change in the sedimentary environments and the uplifting of the hinterland. The author does not always deny such movement shown by evidences such as the existences of the uplifting part, quartz-diorite gravels, clastic dikes, and many sorts of slumping structures, the distribution of black shale breccia derived from the Bessho Formation, the change in lithology and thicknesses in the uppermost part of the Bessho Formation and in the Kido Member, and the igneous intrusion during the development of the Nishikibe Anticline and the Kinokoyadani Syncline. But the author believes that this movement is rather local phenomenon, and that its activity is so small, because that the distribution of gravels derived from the Uchimura and the Bessho Formations is limited in very narrow area, quartz-diorite gravels are small in quantity, that slumping structures are less remarkable than the western area of the Matsumoto—Nagano Line, that igneous rocks had intruded after the sedimentation of the Bessho Formation but their exact stages are uncertain, and that the folding is very weak.

Next, it will be discussed about the studied area where the Bessho Formation distributes. TANAKA (1958) pointed out that the Nishikibe Anticline deformed from the Hongō Formation to the lowest part of the Aoki Formation, but that their deformation disappeared rapidly to the upper part of the Aoki Formation and that the basal conglomerate of the Aoki Formation included the Green tuff gravels. He considered that this anticline was made by the Bessho Phase movement. The author also believes that the Nishikibe Anticline and the Kinokoyadani Syncline are fundamentary buckling folds in the middle Miocene and that the competent unit is the Kido Member. These folds initiated earlier than those in the west area of the Matsumoto—Nagano Line. Minor folds in this area are considered to be made by the flowage of the muddy rock in the initial stage of the major folding of the Bessho Phase Movement from evidences such as their weak deformation, irregularities of their axes trends and the mechanical properties of rocks. The Saigawa Crushed Zone began to uplift from the southern part since the final stage of the sedimentation of the Bessho Formation from the distribution of clastic dikes, slump structures and black shale breccias. Though this area did not emerge above sea level, its affect to the sedimentary environments was remarkable after the later stage of the sedimentation of the Aoki Formation. Miocene sedimentary basin was divided into the east one and the west one by the Chūō Uplifting Zone in the period between the final stage of the Aoki Formation. The western sedimentary basin had developed in the later stage than the eastern area. And the western sedimentary basin is differentiated into some subbasins by the Matsumoto—Nagano Line and the Saigawa Crushed Zone. The Aoki Formation is composed of the alternation of sandstone and sandy mudstone, conglomerate, sandstone and mudstone with coal seams.

Namely, the composition of the Aoki Formation is coarser than that of the Bessho Formation. This fact means that the sedimentary environment of the Aoki Formation turned to the shallow sea and that the base of the basin lifted after the Bessho Formation deposited. Many sorts of slumping structures were formed under the above environments and the sinking in the basin differentiated still more. Thus, the thickness of the Aoki Formation changed in the horizontal direction. These irreguralities initiated not only minor folding but major folding as described in the previous section. The orientation of the sedimentary basin of the Aoki Formation will be considered from the change in thickness. The line of the maximum thickness parts of the Aoki Formation from the west of Aida to Kodaki, trends nearly N–S.

The differentiation in the western basin became to be remarkable after the late stage of the Aoki

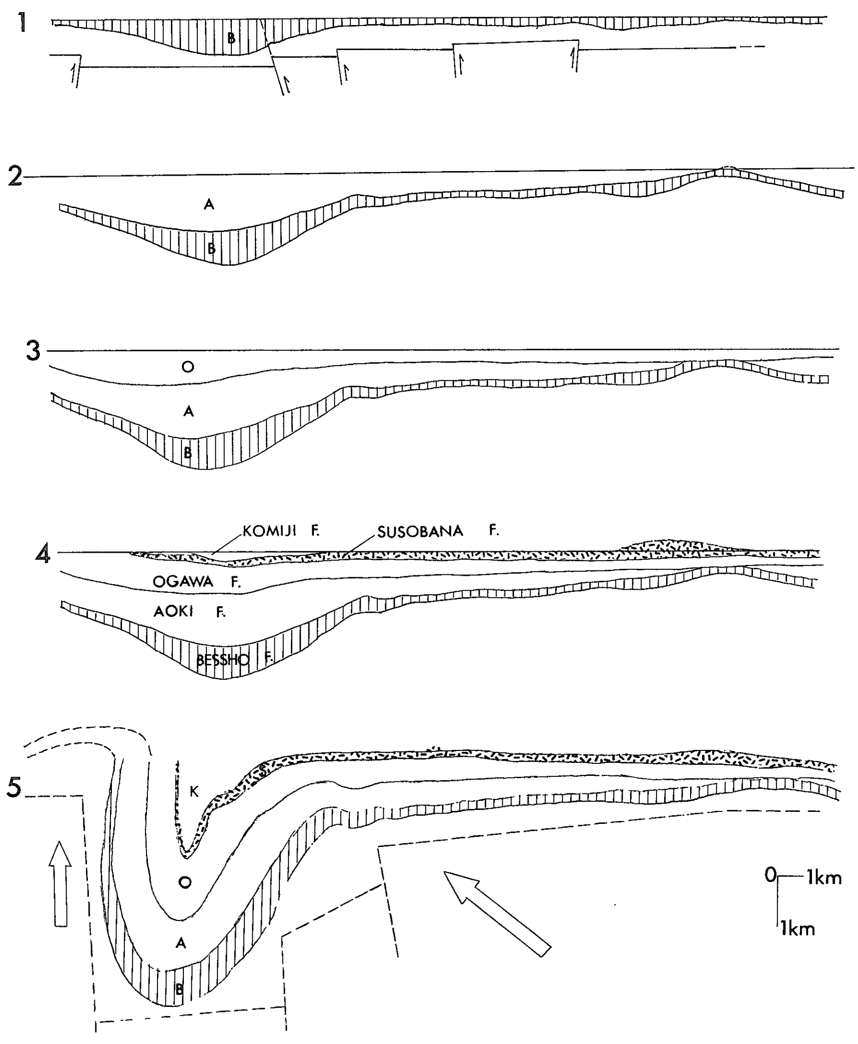

Fig. 45 Folding history.

Formation, and continued to the Ogawa Stage. In the Saigawa Area which is located near the western margin of the sedimentary basin of the Aoki Formation, there is also a boundary of the sedimentation which is equal to the Matsumoto—Nagano Line, that is, the Saigawa Disturbed Zon eproposed by SAIKAWA RESEARCH GROUP (1966). The Saigawa Crushed Zone is a part of this disturbed zone. The uplifting of this zone began from the final stage of the Bessho Formation when it initiates the Nodaira Anticline. As these upliftings cause the lateral secondary compression, some minor folds in the Aoki Formation have the possibility of initiation at the end of the Aoki Stage or at the beginning of the Ogawa Stage. Igneous activity is mostly restricted in the east area of the Matsumoto—Nagano Line. The Ogawa Formation is mostly composed of massive sandstone and conglomerate with *Ostrea* fossil beds, coal seams and some kinds of sedimentary structures frequently. Its lithofacies shows that the sedimentary environment of the Ogawa Formation becomes to be shallower than that of the Aoki Formation. The maximum thickness of the Ogawa Formation is more than 1,000 m near Sashikiri in the east limb of the Komiji Syncline, but it reaches 500 to 600 m in the east area of the Matsumoto—Nagano Line. The orientation of the sedimentary basin of the Ogawa Formation trends N–S as well as that of the Aoki Basin. And the Ogawa Basin is differentiated by the Matsumoto—Nagano Line. These differentiation continued from the Aoki Stage. The Saigawa Crushed Zone and the area between the axis of the Noma Anticline and the Matsumoto—Nagano Line turned to the remarkable raised parts. These raised parts and the maximum sinking parts emphasized the initial wavy shape of layers more and more. The sandstone in the late Ogawa Stage is tuffaceous and is partly intercalated with the Bōdaira Tuff Member. Furthermore, in the lower part of the Susobana Formation, acidic volcanic activity, for example, rhyolitic tuff and lava dominate.

The local center of this volcanic activity is near Mt. Kamuriki and andesitic volcanic activity also occurs there later. The main center of this eruption locates near Nagano City. As the welded tuff is found in the Susobana Formation around Mt. Kamuriki, a part of these eruption seems to have occured on the land surface.

The thickness of the Ogawa Formation is very thin in this area.

These facts suggest that there is the local unconformity in the Susobana Formation around Mt. Kamuriki, and that this area began to uplift locally from the late Ogawa Stage. Weak folds which folds trend nearly E–W develope around Mt. Kamuriki and along Omi River. In the axial part of the Komiji Syncline, the sinking of the basin in which the Komiji Formation deposited still continued. Before the eruption of Hijiriyama Volcanic Rocks and after the sedimentation of the Komiji Formation, that is, in the late Miocene, lateral compression was dominant directly at least in these folded area. As the layers had initial deflections as described in the previous sections, initial dips (may be less than 10 degrees) were emphasized by this compression and they took the present wavy form. This process as described above is roughly in Figure 45.

6. Conclusions

The purposes of this study have been to define the folding styles in the northern Fossa Magna Region, to analyze the deformation mechanism for those folding, to make clear the tectonic stress field of this region, and to discuss the folding history. The following conclusions are drawn from the field survey of the Higashi-Chikuma District, Nagano Prefecture, and the analytical studies of folding associated with the experiments.

(1) There is a good agreement between the experimental and theoretical results on buckling folds, and the field data analysis about natural folds with regard to the geometric characters, namely amplitude-wavelength ratio, mean shortening and interlimb angle.

(2) The strain distribution expected in the layers of buckling folds coinsides with that of natural folds, which is induced from the analysis of minor tectonic structures.

(3) Both major folds and most of minor folds of which wavelengths are larger than a few hundred meters are fundamentally formed by the buckling process. The Susobana and the Ogawa Formations and the Kido Member are estimated to be competent layers or units.

(4) Not only major folds but minor folds initiated at the irreguralities, namely the changing parts of the thickness and lithofacies, and the non-tectonic raised part at the deposition of layers, which are induced from the distribution of cross bedding and other slump structures.

(5) The Matsumoto—Nagano Line is also important tectonic line in relation to the folding mechanism. The eastern area of this line was in the tensile stress field and the western area was in the compressive field during middle-late Miocene. These are induced from many minor folds and other minor structures.

(6) The external force which caused the lateral compression which is buckling force, were originated from the tilting of basement blocks, namely the Chūō Uplifting Zone and the Saigawa Crushed Zone.

(7) The mechanism of folds in the studied area is that the cover sediments which had initial wavy forms controled by the differential sinking movements of the basement at deposition were buckled and emphasized by the secondary lateral compression caused by the uplifting of the Saigawa Crushed Zone and the Chūō Uplifting Zone.

(8) In minor folds, the lengths of axes are not always exactly proportional to the wavelengths, and the former is less than ten times as long as the latter.

7. Acknowledgement

Author's personal thanks are due to Dr. Y. FUJITA of Niigata University for his helpful and thoughtful suggestions and criticism of this manuscript.

I am especially grateful for the guidance and assistance of Dr. K. WATANABE of Tokyo University of Education.

Thanks are due to Dr. K. MATSUNO, Mr. T. KAKIMI, Mr. Y. KINUGASA and Dr. K. KODAMA of Geological Survey of Japan, Dr. F. TSUNODA of Saitama University and the members of the Tectonic Research Group and also the members of Geological and Mineralogical Institute of Tokyo University of Education.

I also thank Dr. S. IWAMURA very much for his suggestions and criticisms of this manuscript.

References

BELOUSSOV, V. V. (1954) *Basic ploblems in geotectonics*. Moscow, Gesgeolizdat. (japanese translation 1956, Tsukiji Shokan).

BIOT, M. A. (1961) Theory of folding of stratified viscoelastic media and its implication in tectonics and orogenesis. *Bull. Geol. Soc. Am.*, vol. 72, p. 1595–1632.

Cobbold, P. R. (1975) Fold propagation in single embedded layers. *Tectonophysics*, vol. 72, p. 333–351.

Currie, J. B., Patnode, H. W. and Trump, R. P. (1962) Development of folds in sedimentary strata. *Bull. Geol. Soc. Am.*, vol. 73, p. 655–674.

Dieterich, J. H. and Carter, N. L. (1969) Stress-history of folding. *Am. Jour. Sci.*, vol. 267, p. 129–154.

Fujimoto, H. *et al.* (1946) Geology of Nagano Oil Field. *Bull. Geol. Soc. Japan*, vol. 52, p. 48–55.

Fujita, Y. (1973) *The formation of Japanese Islands.—The Green-tuff Movement.* Tsukiji Shokan, Japan.

Fukazawa, M. (1972) Geology of Sakai Village in the Higashi-Chikuma District, Nagano Prefecture (MS.). Tokyo University of Education.

Hafner, W. (1951) Stress distribution and faulting. *Bull. Geol. Soc. Am.*, vol. 62, p. 373–398.

Hara, I. (1965) Movement pictures in confined competent layers in flexural folding, Deformation of heterogeneously layered rocks in flexural folding (I). *Jour. Geol. Soc. Japan*, vol. 72, p. 363–369.

——— (1966) Strain and movements in competent layers in flexural folding, Deformation of heterogeneously layered rocks in flexural folding (II). *Jour. Geol. Soc. Japan*, vol. 72, p. 413–425.

Hetenyi, M. (1946) Beams on elastic deformation. *Univ. Michigan Press*, Ann Arbor, Mich. p. 255.

Hirabayashi, T. (1969) About Matsumoto-Nagano Line and Otari Uplifting Belt in the nothern Fossa Magna. *Geol. Soc. Japan*, "Some ploblems about Greentuff", p. 117–122.

Honma, F. (1931) *Sinano-chūbu Chishitsushi.* Kokin Press.

Hudleston, P. J. (1973) An analysis of "single-layer" folds developed experimentally in viscous media. *Tectonophysics*, vol. 16, p. 189–214.

——— and Stephansson, O. (1973) Layer shortening and fold shape development in the buckling of single layers. *Tectonophysics*, vol. 17, p. 299–321.

Iijima, N. and Saito, Y. (1968) *Sarashina and Hanishina Chihō Chishitsushi.*

Ikeda, Y. and Shimamoto, T. (1974) Numerical experiments on the viscous bending folds. *Bull. Geol. Soc. Japan*, vol. 80, p. 65–74.

Ito, T. (1976) About the mechanism of the Nanakura Anticline near Futatsui, Akita Prefecture. Abstract of the 83th Geol. Soc. Japan, p. 137.

Itoi, M. (1972) About the Tertiary Formations in Shioda District in Ueda City, Nagano Prefecture (MS.). Tokyo University of Education.

Johnson, H. M. (1969) Development of folds within Carmel Formation, Arches National Monument, Utah. *Tectonophysics*, vol. 8, p. 31–77.

——— and Honea, E. (1975) A theory of concentric, kink and sinusoidal folding and of monoclinical flexuring of compressible elastic multilayers. *Tectonophysics*, vol. 27, p. 1–38.

Kasahara, C. (1973) The stratigraphy and the geological structures in the western area of Honjō Village in the Higashi-Chikuma District, Nagano Prefecture (MS.). Tokyo University of Education.

Kato, H. (1970) The late Miocene folds along the Omi and Kanakuma Rivers, Nagano Prefecture,—The analysis of folds, Part. 1. *Bull. Geol. Soc. Japan*, vol. 76, p. 579–590.

——— (1971) A morphological analusis of folds,—Result on the folds along the River Omi, Nagano Prefecture, Japan. *Bull. Geol. Soc. Japan*, vol. 77, p. 323–326.

——— (1973) Some considerations about fold models. *Bull. Geol. Soc. Japan*, vol. 79, p. 157–166.

——— (1975) Experimental study of the elastic buckling folds. *Bull. Geol. Soc. Japan*, vol. 81, p. 147–154.

Kawauchi, K. (1973) Geology of Omi and Sakakita Villages in the Higashi-Chikuma District, Nagano Prefecture (MS.). Tokyo University of Education.

Kikuchi, S. (1973) The Tertiary Formations near Aoki Village in the Chiisagata District, Nagano Prefecture in the northern Fossa Magna (MS.). Tokyo University of Education.

Kinugasa, Y. (1974) Photoelastic experiments of the transverse bending. *Rept. Geol. Surv. Japan*, no. 250–2, p. 159–174.

Kobayashi, K. (1957) The geologic development in Fossa Magna Region. *Chigaku Dantai Kenkyukai.*

Kobayashi, I. and Isomi, H. (1950) Geology of the Sarashina and Higashi-Chikuma District in Nagano Coal Field, Nagano Prefecture. *Rept. Geol. Surv. Japan*, no. 135, p. 1–26.

Kodama, K. *et al.* (1974) On the internal structure of box-shaped folds. *Rept. Geol. Surv. Japan*, no. 250–2, p. 121–143.

Komatsu, N. (1967) About the geological structures of Tertiary Formations in the margin of Matsumoto

Basin. *Earth Science*, vol. 21, p. 19–20.

KUTSUZAWA, A. and FUJITA, Y. (1967) Genesis of clastic dikes and planeless faults in the Miocene deposits of the Sendai district,—Studies on faults at the boundary of sedimentary basins (2). *Bull. Geol. Soc. Japan*, vol. 73, p. 19–34.

MERUI, S. (1972) Tertiary Formations in the eastern part of Shiga Village in the Higashi-Chikuma District, Nagano Prefecture (MS.). Tokyo University of Education.

MOODY, J. D. and HILL, M. J. (1956) Wrench fault tectonics. *Bull. Geol. Soc. Am.*, vol. 67, p. 1207–1246.

MORISHITA, A. *et al.* (1957) Geology of the southern part of Hijiri-yama, Nagano Prefecture,—On the stratigraphy of so-called "Tōchiku Facies" in the Ogawa Formation. *Bull. Geol. Soc. Japan*, vol. 63, p. 159–166.

NAGAHAMA, H. (1963) Cross beddings in the Tertiary Formation of Jōban Coal Field. *Bull. Geol. Surv. Japan*, vol. 14, p. 857–875.

NAGUMO, S. (1966) The dynamic theory of folding. *Bull. Geol. Soc. Japan*, vol. 72, p. 117–130.

NAKAMURA, K. (1969) Arrangement of parasitic cones as a possible key to regional stress field. *Bull. Volc.*, vol. 14, p. 8–20.

RAMBERG, H. and STEPHANSSON, O. (1964) Compression of floating elastic and viscous plates affected by gravity, A basis for discussing crustal buckling. *Tectonophysics*, vol. 1, p. 101–120.

SAIKAWA RESEARCH GROUP (1966) Geological structures of the Sai-kawa Fractured Zone.—Geology of the Sai-kawa Area, Nagano Prefecture, Central Japan (Part 4). *Monograph 12, Assoc. Geol. Collaboration Japan*, p. 94–102.

SAITO, Y. (1961a) A preliminary note on the structure-system of the Tertiary Formations in the northern part of the Fossa Magna. *Bull. Fac. Educ. Shinshu Univ.*, no. 12, p. 99–108.

——— (1961b) An interesting sole marking observed on overturned sandstone layers of the Aoki Formation (Neogene) in Ikusaka-mura, Higashi-Chikuma-gun, Nagano Prefecture, Japan. *Jour. Fac. Educ. Shinshu Univ.*, no. 12, p. 161–163.

SAKAI, M. (1976) Numerical analysis of viscous bending folds by the uplifting and/or downward movements of the basement (MS.). Shibaura Industrial University.

SANFORD, A. R. (1959) Analytical and experimental study of single geologic structures. *Bull. Geol. Soc. Am.*, vol. 70, p. 19–52.

SHIMAMOTO, T. and HARA, I. (1976) Geometery and strain distribution of single-layer folds. *Tectonophysics*, vol. 30, p. 1–34.

SKJERNAC, L. (1975) Experiments on superimposed buckle folding. *Tectonophysics*, vol. 27, p. 255–270.

SUZUKI, Y. and MITSUNASHI, T. (1974) Geotectonic division, geologic development and mechanisms of folding in the northern Fossa Magna region. *Rept. Geol. Surv. Japan*, no. 250–2, p. 79–91.

TAKEUCHI, A. and SAKAMOTO, M. (1976) Stratigraphy and geologic structure of the Neogene system in the midstream drainage of the River Sai-kawa, Nagano Prefecture, Central Japan. *Mem. Geol. Soc. Japan*, no. 13, p. 187–201.

TAKEUCHI, N. (1971) Geology in the west coast of Chikuma River in Hanishina-gun, Nagano Prefecture (MS.). Tokyo University of Education.

TANAKA, K. (1958) Geology in the upper stream of Aida River in the middle part of Nagano Prefecture. *Bull. Fac. Educ. Shinshū Univ.*, p. 267–276.

——— and SEKI, H. (1966) The Tertiary Formations in the north of Matsumoto City. *Bull. Fac. Educ. Shinshū Univ.*, no. 18, p. 139–159.

——— *et al.* (1973) Studies on the sedimentary structures observed in the Tertiary Formations in the northern part of Fossa Magna. *Bull. Fac. Educ. Shinshū Univ.*, no. 7, p. 49–88.

TOMIZAWA, T. (1953) On the stratigraphy and geological structure of the Susobana-kawa Region in the northern part of Nagano Prefecture. *Bull. Geol. Soc. Japan*, vol. 59, p. 552–560.

TSUNODA, F. (1973) Studies on folds of the Miocene Momonoki Subgroup in the Koma Massif, Central Japan. Science Report Tokyo Kyōiku Daigaku, Section C. (*Geogr. Geol. and Mineralogy*), vol. 11, p. 261–313.

UEMURA, T. (1971) About the geological structures in the Greentuff region. *Greentuff*, no. 3, p. 17–18.

——— and TAKAHASHI, A. (1974) Kinematic picture of basement rocks and folding of overlying layer,—An example of Kushigata Mountain Range, Niigata Prefecture, Japan. *Rept. Geol. Surv. Japan*,

no. 250–2, p. 1–21.
WILLIS, B. (1894) Mechanics of Appalachin structure. *U.S. Geol. Surv. 13th, Ann. Report*, p. 213–281.
YAMAGISHI, I. *et al.* (1963) The geology of Ueda-Chiisagata District, vol. 4, p. 5–252.

地名英和対応表

Agerō 上篭	Azumayasan 四阿屋山	Omi 麻積	Ōubayama 大姥山
Kamurikiyama 冠着山	Kōsō 高桑	Saigawa 犀川	Sashikiri 差切
Shige 重	Shijūhachimagaritōge 四十八曲峠	Shunaratōge 修那羅峠	Nishikibe 錦部
Bōdaira 坊平	Hofukuji 保福寺	Macchi 末地	Matsutome 松留
Yakyū 矢久	Yagoshi 矢越		

長野県東筑摩郡の中新世の褶曲について

加 藤 碵 一

本論文の目的は，北部フォッサマグナ地域に分布する新第三紀中新世層中に発達する褶曲の様式を決定し，その形成機構を明らかにして，当地域の構造発達史を論じようとするものである.

長野県東筑摩郡を中心に約 350km² におよぶ地域を野外調査し，その結果と室内での実験的研究から次のことを明らかにした.

1. 実験的研究から期待される座屈褶曲の形態特性，すなわち，振幅―波長比，平均短縮量や翼間角などの分布特性が，自然褶曲とくに込地向斜や野間背斜などのそれとよく一致する.

2. 実験的に得られた座屈褶曲の歪分布と，自然褶曲中に発達する各種の小構造の解析から得られた歪分布が少なくとも定性的に一致する.

3. 主褶曲群は，基本的には座屈褶曲とみなされ，裾花層・小川層や木戸部層がコンピーテント層に相当すると考えられる.

4. 小褶曲（波長が数 100m 以下）も座屈褶曲であり，コンピーテント層とみなされる砂岩・礫岩とインコンピーテント層とみなされる砂質泥岩とのコンピーテンシィ・コントラストは，きわめて小さく，このことは小褶曲形成時に層平行短縮のあったことを暗示する．また，小褶曲の軸長と波長は，厳密には必ずしも 1 対 1 の対応を示さないが有意な関係を持つ.

5. 主褶曲のみならず小褶曲も，層厚や層相の変化部や地層堆積時の隆起部など地層が形態的に不規則な場所に発生し，そこを頂部とする傾向が強い.

6. 松本―長野線は，褶曲形成に関して重要な構造線であり，この線を境として東西で造構運動・火成活動・堆積作用に顕著な差異が見られる．とくに褶曲形成期である中―後期中新世において東部地域は引張応力場にあり，西部地域は圧縮領域にあることが，小断層，小褶曲や岩脈の解析から推定される.

7. 座屈をおこした側圧は，基盤ブロックの傾動的隆起によるものと考えられる.

8. 結局，当地域の褶曲は，基盤の差別的沈降運動によってできた初期波形を持つ被覆堆積岩層が，犀川破砕帯以東の地域や中央隆起帯の傾動隆起に伴って発生した 2 次的水平圧縮力によって見かけ上大きく座屈し，初期波形が強調されて現在みられる形をとるに至ったものである.

(受付：1978年 3 月20日；受理：1978年 7 月 5 日)